JOURNAL OF CONDENSED MATTER NUCLEAR SCIENCE

Experiments and Methods in Cold Fusion

VOLUME 3, July 2010

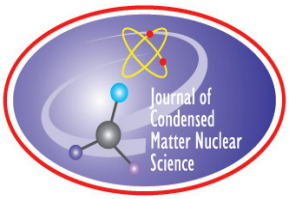

JOURNAL OF CONDENSED MATTER NUCLEAR SCIENCE

Experiments and Methods in Cold Fusion

JOURNAL OF CONDENSED MATTER NUCLEAR SCIENCE

Volume 3, July 2010

Orders, claims, author inquiries and journal inquiries

Please contact the Editor in Chief, CMNSEditor@iscmns.org or webmaster@iscmns.org

J. Condensed Matter Nucl. Sci. 3 (2010) 1–92

JOURNAL OF CONDENSED MATTER NUCLEAR SCIENCE

Volume 3 2010

CONTENTS

PREFACE

The "Journal of Condensed Matter Nuclear Science" is the only scientific peer-reviewed journal dealing with Cold Fusion. As the editor in chief, I wish to thank the authors of the papers included in this volume as well as the referees who did an excellent work in reviewing the papers.

In the first two volumes, the majority of papers are theoretical. I hope that in the future more experimentalists would publish their work. This journal is the place where even negative results could be shown. As an experimentalist, I know that I learn a lot with unsuccessful experiments, and personally I have performed a lot of these!

As our field is both new and without a proper theory to explain the effect, we work more or less in the dark, trying about anything we have both in our brain and also available in our laboratory. Edison has followed a similar approach to find the appropriate material for his light bulb. Scientists trying to raise the critical temperature of both low and high temperature superconductors faced the same difficulties.

Our field is extremely challenging since there are at the same time an enormous theoretical difficulty and great experimental difficulties. We are progressing on both fronts, but as of now, it is impossible to say when we will succeed. The rejection of the domain by mainstream science does not help us. It is difficult to get the financial and human resources that could speed up our progress.

Jean-Paul Biberian
July 2010

J. Condensed Matter Nucl. Sci. 3 (2010) 1–3

Letter to the Editor

Comments on Codeposition Electrolysis Results

Ludwik Kowalski *

Montclair State University, Montclair, NJ 07055, USA

Abstract

Results from SPAWAR-type experiments show that dominant pits, recorded with CR-39 detectors, are probably not due to alpha particles, as originally suspected. Two points of conflict, one experimental and another interpretational, remain to be resolved.

Keywords: Codeposition electrolysis, Cold fusion, CMNS, CR39, LENR, SPAWAR

1. Introduction

Can a chemical effect, such as electrolysis, trigger a nuclear effect? Numerous investigators, both theoreticians and experimentalists, have been trying to address this interesting question in different ways. This note is based on the most recent experimental contributions of US Navy Space and Naval Warfare System (SPAWAR) scientists [1,2]. Their initial results were reproducible, as illustrated by several researchers, including [3]. Subsequent control experiments, described in [1,2], rule out the possibility of several previously suspected artifacts. For example, nearly all tracks disappear when D_2O, used to make the electrolyte, is replaced by H_2O, or when $PdCl_2$, also used to make the electrolyte, is replaced by $CuCl_2$.

Accepting the SPAWAR interpretation, that dominant CR-39 pits are due to a new nuclear process, the author of [4] argued that the recorded projectiles were not alpha particles, as claimed in [5]. The argument was based on the observation that dominant SPAWAR type pits observed in [3] were significantly larger than pits due to alpha particles. The same conclusion can be reached on the basis of photographs shown in [1]. This article is based on another published report [6], which supports the same conclusion: dominant SPAWAR type CR-39 pits are probably not due to alpha particles with energies higher than 2 MeV.

2. Discussion

Experimental results described in [1,2] seem to be in conflict with results from a very similar experiment described in [6]. The authors of that paper discovered that at least 99.9% of dominant pits disappeared when a thin Mylar film was

*E-mail: kowalskiL@mail.montclair.edu

placed between the cathode and the CR-39 detector. The number of remaining pits –200, after 15 days of electrolysis– was significantly larger than in the control chips. In other words, most remaining pits were not due to cosmic rays or to natural radioactivity. The analyzed pits, however, were identified as due to protons, with energies close to 2.5 MeV, and not to alpha particles. The thickness of the Mylar film, 6 μm, would not have stopped alpha particles with energies above approximately 2 MeV.

Note that an electrolytic cell with a thin Mylar window, of the same thickness, was also used by the SPAWAR team, as described in [1]. The authors confirmed a significant reduction (approximately 90%) in the number of pits due to Mylar. This can be interpreted as an indication that about 90% of the pits observed without protecting the detector with Mylar were not due to alpha particles with energies higher than 2 MeV. Unfortunately, the most recent (2009) SPAWAR paper [1] does not refer to the earlier (2007) paper [6]. The difference between the "at least 99.9%" and "about 90%" is probably significant. The only obvious discrepancy between experimental conditions of the two teams was the presence of a strong magnetic field in [1] and its apparent absence in [6]. The effect of a magnetic field on the pit density is interesting; it seems to depend on the cathode material, according to [2].

Another interesting observation, reported in [1], has to do with the identification of tracks that were recorded when the CR-39 detector was separated from the cathode by the Mylar film. The authors wrote: "the majority of the particles formed as a result of Pd/D codeposition are 0.45–0.97 MeV protons, 0.55–1.25 MeV tritons, 1.40–3.15 MeV ^{3}He, and/or 1.45–3.30 MeV alphas." This can be interpreted as independently confirming (by a different method) that the contribution of alpha particles to production of dominant pits observed without Mylar is minimal.

Identifying particles listed above via tracks in CR-39 chips is difficult. Fortunately, this can be accomplished with commercially available surface-barrier silicon detectors. The SPAWAR electrolytic cell shown in [1] would be ideal for such a purpose. The guaranteed background noise of some commercially available detectors is one count per hour, provided the energy threshold is set up to 3 MeV. Furthermore "extensive care regarding detector and chamber cleanliness can result in background count levels as low as 0.05 counts/h/cm^2 of active area, corresponding to 6 counts/24 h, for a 450 mm^2 active area," at energies higher than about 2 MeV [7].

3. Conclusion

Independent researchers have reported emission of nuclear projectiles produced during the codeposition-type electrolysis. The pits created by the projectiles can be divided into two groups: (a) very numerous, detected without using a thin protective Mylar foil, and (b) much less numerous, detected when the foil is used. The controversy about the nature of the first group of pits was recognized and discussed in [3–5]. The controversy about the second group of pits was not even recognized in [1]; it remains to be discussed. Note, however, that any kind of nuclear projectiles, if independently confirmed, would validate the basic CMNS claim—reality of a nuclear process due to a chemical process. Progress in the field of codeposition electrolysis has been remarkable during the last three years. But points of conflict, both experimental and interpretational, remain.

To what extent are the above-mentioned discrepancies due to the "state of the art" limitations? That important question was asked by one of the referees. The author of this article was not able to provide an answer. His observations are based on the best information available, that is, on what has actually been published. Hopefully, the existing situation will provide impetus for better experiments.

References

[1] P.A. Mosier-Boss, S. Szpak, F.E. Gordon and L.P.G. Forsley, Characterization of tracks in CR-39 detectors obtained as a result of Pd/D Co-deposition, *Eur. Phys. J. Appl. Phys*. **46** (2009) 30901. The article can be downloaded for CMNS library as: http://lenr-canr.org/acrobat/MosierBosscharacteri.pdf

[2] P.A. Mosier-Boss, S. Szpak, F.E. Gordon, and L.P.G. Forsley, Reply to comment on 'The use of CR-39 in Pd/D co-deposition experiments': a response to Kowalski, *Eur. Phys. J. Appl. Phys.* **44** (2008) 291–295.
[3] L. Kowalski et al., Our Galileo Project March 2007 Report, *Winter Meeting of American Physical Society* (2007), Content of the presentation can be seen at http://pages.csam.montclair.edu/∼kowalski/cf/319galileo.html
[4] L. Kowalski, Use of CR-39 in Pd/D co-deposition experiments, *Eur. Phys. J. Appl. Phys.* **44** (2008) 287290. The article can be downloaded for CMNS library as: http://lenr-canr.org/acrobat/KowalskiLcommentson.pdf
[5] P.A. Mosier-Boss, S. Szpak, F.E. Gordon and L.P.G. Forsley, Use of CR-39 in Pd/D co-deposition experiments, *Eur. Phys. J. Appl. Phys.* **40** (2007) 293303.
[6] A.G. Lipson, A.S. Roussetski, E.I. Saunin, F. Tanzella, B. Earle and M. McKubre; Analysis of the CR-39 detectors from SRI's SPAWAR/Galileo type electrolysis experiments #7 and #5. Signature of possible neutron emission, *Proceedings of 8th International Workshop on Anomalies in Hydrogen/Deuterium Loaded Metals,* Catania, Italy, October 2007 (pp. 182203); edited by Jed Rothwell and Peter Mobberly.
[7] http://www.jlab.org/accel/inj_group/testcave/mott/ultra.htm also two telephone conversations with Mr. Kennedy from ORTEC (2007).

J. Condensed Matter Nucl. Sci. 3 (2010) 4–8

Letter to the Editor

Comments on Co-deposition Electrolysis Results: A Response to Kowalski

P.A. Mosier-Boss*
SPAWAR Systems Center Pacific, Code 71730, San Diego, CA 92152, USA

L.P.G. Forsley
JWK International Corp., Annandale, VA 22003, USA

F.E. Gordon
SPAWAR Systems Center Pacific (Retired), San Diego, CA 92122, USA

Abstract

In 2009, it was reported that the tracks observed on the front surface of CR-39 detectors as a result of co-deposition were due to 0.45–0.97 MeV protons, 0.55–1.25 MeV tritons, 1.40–3.15 MeV ^{3}He, and/or 1.45–3.30 MeV alphas. Recently those conclusions have been challenged. In this communication, additional experimental data and further analysis of our earlier results are provided that support our original conclusions.

Keywords: CR-39, Pd/D co-deposition

1. Introduction

In 2007, we reported the observation of tracks in CR-39 resulting from the co-deposition process [1]. The tracks were dark in color and primarily circular or oval in shape. When the microscope optics were focused inside the tracks, a bright spot was observed inside. This bright spot is due to the bottom of the track cone acting like a lens when the CR-39 detector is backlit. These features are diagnostic of a nuclear generated track. A series of control experiments were done to show that the tracks were not the result of radioactive contamination nor to mechanical damage. The most noteworthy of these control experiments was electrodeposition using $CuCl_2$ in place of $PdCl_2$. In both the $CuCl_2$ and

*Corresponding author. E-mail: pam.boss@navy.mil; Tel. +1-619-553-1603

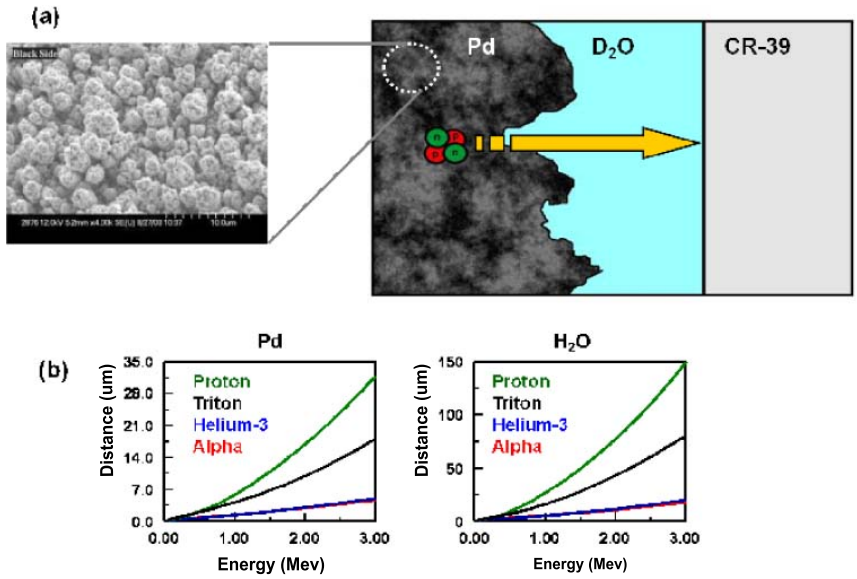

Figure 1. (a) Schematic describing the layers a charged particle has to negotiate before it impacts the CR-39 detector. After its birth, a charged particle has to exit the metal lattice and cross a thin water layer before it impacts the CR-39 detector. An SEM of the Pd deposit formed as the result of the co-deposition process is shown. The cauliflower morphology of the deposit traps pockets of water. (b) LET curves calculated for charged particles traversing through palladium and water.

$PdCl_2$ systems, the same electrochemical reactions are occurring. At the cathode, a metal is plating out in the presence of evolving deuterium gas while oxygen and chlorine gas evolution occurs at the anode. The only significant difference between the two systems is that Pd metal absorbs deuterium and Cu does not. While tracks were observed in the Pd/D system, none were observed in the Cu/D. These results indicate that the observed tracks in the Pd system were not due to chemical attack of the surface of the CR-39 by either D_2, O_2, or Cl_2 present in the electrolyte; nor to mechanical damage due to the impingement of D_2 gas bubbles on the surface of the detector; nor to damage caused by the metal dendrites piercing into the CR-39; nor to localized production of hydroxide ions that etch into the CR-39.

In 2009, experiments were conducted to characterize the Pd/D co-deposition generated tracks [2]. Specifically, an experiment was done in which a 6 μm thick Mylar film separated the CR-39 detector from the cathode. In addition track modeling was done using TRACK_TEST, a computer program developed by Nikezic and Yu [3]. Both the Mylar experiment and track modeling indicate that the energy of the particles are $\sim$1 MeV by the time they reach the CR-39 detector. To reach the detector, the particles have to traverse a thin water layer. Linear energy transfer (LET) curves, calculated using the SRIM-2003.26 code of Ziegler and Biersack [4], were used to evaluate the impact of water on the particle energies. Assuming water thicknesses varying between 0 and 10 μm, it is estimated that the majority of the particles formed as a result of Pd/D co-deposition are 0.45–0.97 MeV protons, 0.55–1.25 MeV tritons, 1.40–3.15 MeV ^{3}He, and/or 1.45–3.30 MeV alphas. However, Kowalski has questioned these conclusions. In particular, he has made the allegation that the tracks obtained on the CR-39 detectors are too large to be due to 1 MeV alphas. In this communication, we address the issues raised by Kowalski.

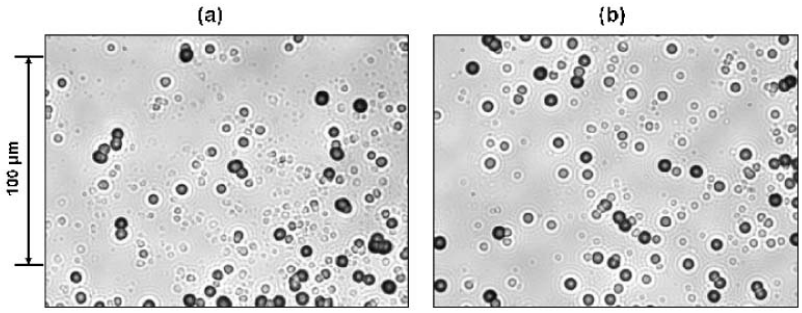

Figure 2. Photomicrographs obtained at 500× magnification for (a) Pd/D co-deposition tracks and (b) ∼1 MeV alpha tracks.

2. Discussion

In his introduction, Kowalski said that 'nearly all tracks disappear when $PdCl_2$ is replaced by $CuCl_2$.' The implication of this statement is that tracks were observed in the $CuCl_2$ electrolysis experiment. This is not true. As discussed in [1], no tracks above background were observed in the Cu deposition experiments. Also in his introduction, Kowalski stated that 'dominant SPAWAR type pits were significantly larger than pits due to alpha particles.' He further stated that photographs shown in [2] support his claim. However, he does not indicate which photographs in [2] support his claim. In [2], we examined the impact traversing through a water layer has on the energetics of the charged particles. Figure 1a describes the processes involved when an alpha particle impacts a CR-39 detector used in a Pd/D co-deposition experiment. An SEM of the Pd deposit is shown in Fig. 1a. The deposit has a cauliflower-like morphology that traps pockets of water. As shown in the schematic in Fig. 1a, after birth, the particles have to pass through the Pd lattice and the water layer before impinging the detector. Figure 1b shows LET curves calculated for protons, tritons, helium-3, and alpha particles in palladium and water. These LET curves are used to determine the magnitude of the effect of Pd and water on the energies of the particles. The LET curve for Pd indicates that, in order for particles to be detected by the CR-detector, the particles need to originate near the surface of the Pd. Particles formed deeper inside the deposit will simply not have enough energy to exit the lattice and travel through the deposit and water layer to reach the CR-39 detector.

The 6 μm Mylar experiment described in [2] resulted in a ∼90% reduction in the number of tracks. The LET curve for Mylar indicated that 6 μm thick Mylar blocks <0.45 MeV protons, <0.55 MeV tritons, <1.40 MeV helium-3, and <1.45 MeV alphas. The Mylar experiment indicates that, on average, the particles have energies on the order of 1 MeV when they reach the detector. Figure 2 shows a side-by-side comparison of Pd/D co-deposition tracks with ∼1 MeV alpha tracks formed by placing 24 μm of Mylar between an ^{241}Am alpha source and the CR-39 detector. The Pd/D and ∼1 MeV alpha tracks are indistinguishable. This was also discussed in [2]. The purpose of the experiment placing 24 μm of Mylar between the ^{241}Am source and the detector was to simulate the effect of water on the particles. One of the main criticisms raised about the tracks oberved in CR-39 detectors used in Pd/D co-deposition experiments is the sparsity of elliptical tracks. As shown in Fig. 2a, the observed tracks are primarily circular in shape. Likewise

the ∼1 MeV alpha tracks are primarily circular in shape, Fig. 2b. The results in Fig. 2 indicate that only particles with trajectories normal to the surface have sufficient energy to get through the water layer and Mylar to impact the detector. Particles traveling at oblique angles are deflected and do not reach the detector. It is worth noting that in his blog [5], Kowalski has stated 'Alpha particles of approximately 1 MeV can be used and their tracks can be compared with tracks produced during electrolysis. Suppose that the two kinds of tracks turn out to be very similar. That would reinforce the SPAWAR hypothesis.'

Kowalski has also indicated that the 6 μm thick Mylar experimental results reported in [2] conflict with the results of a similar experiment performed by SRI [6]. Specifically, we reported that we saw a ∼90% reduction of tracks in the Mylar experiment while Lipson et al. reported a 99.9% reduction. Our estimate is based upon the results of the automatic scanning we have done of our detectors. In experiments conducted with the CR-39 in direct contact with the cathode, we typically obtain 20,000–30,000 tracks. For the Mylar experiment, the automated scanner identified 2387 tracks, which is close to a 90% reduction in the number of tracks. We cannot comment on the SRI results. A number of experimental factors, such as the proximity of the wires to the Mylar film, surface area, etc. could explain the reported differences between the SRI and our results. Also different cathode substrates were used in the two experiments. The cathode substrate used in the SRI experiment was Ag while our experiment used Pt and Au wires in series. In [1], we showed that cathode substrate does affect the production of charged particles. For example, it was observed that, when Ni screen is used as the cathode substrate, tracks are only obtained in experiments conducted in the presence of either an external electric or magnetic field. However for Ag, Au, and Pt cathode substrates, tracks were obtained in both the presence and absence of an external field. The difference between the SRI and our results is not due to the presence or absence of a magnetic field as Kowalski suggests. The SRI, Mylar experiment, like ours, was conducted in the presence of a magnetic field [7].

Kowalski reports that the pits obtained in the SRI experiment [6] were identified as 2.5 MeV protons and not alpha particles. This is not correct. Lipson et al. have developed a sequential etching protocol to aide in identifying tracks [6]. Applying this methodology to the analysis of the tracks obtained in the SRI experiment, Lipson et al. attributed the tracks to proton recoils resulting from the interaction of the detector with fast neutrons. The energy of the neutrons responsible for these recoils was determined to be 2.5 MeV. The reason why the Lipson et al. [6] paper was not referenced in [2] is due to the fact that the Lipson et al. paper deals with neutrons, while our 2009 paper is concerned with charged particles.

Kowalski claims that identifying particles tracks in CR-39 is difficult. This is not the case. Lipson et al. [6,8] have shown that sequential etching and placing films between the cathode and detector can be used to identify particles and determine their energies. Astrophysicists have developed a LET spectrum analysis of passive detectors that enable them to both identify the charged particles and determine their energy distributions [9–11]. In our own experiments, we have successfully used track modeling to determine the energies of alpha particles. Kowalski suggests using a silicon barrier detector would be better. He also states the following: 'The guaranteed background noise of some commercially available detectors is one count per hour, provided *the energy threshold is set up to* 3 MeV. Furthermore "extensive care regarding detector and chamber cleanliness can result in background count levels as low as 0.05 counts/h/cm^2 of active area, corresponding to 6 counts/24 h, for a 450 mm^2 active area," *at energies higher than about* 2 MeV.' The CR-39 results indicate that the particle energies are on the order of 1 MeV by the time they traverse a water layer and impact the detector. The majority of the particles are well below the energies optimum for the silicon barrier detector.

In his conclusions, Kowalski claims that there is a controversy as to the identity of particles causing what he refers to as 'dominant SPAWAR pits'. We disagree with this assessment. Figure 2 shows that the Pd/D co-deposition tracks are very similar to ∼1 MeV alpha tracks. This conclusion is supported by the Mylar experiment and track modeling [2].

3. Conclusions

In this communication, we have addressed the issues raised by Kowalski. Specifically we show, yet again, that the Pd/D co-deposition tracks are consistent with those observed for ∼1 MeV alpha particles. This is supported by a side-by-side comparison of Pd/D co-deposition tracks with 1 MeV alpha tracks, Fig. 2; track modeling; the 6 μm Mylar experiment; and using LET curves to determine the magnitude of energy losses as the particles travel through the Pd deposit, water layer, and Mylar film.

Acknowledgements

This work was funded by the SPAWAR Systems Center San Diego S and T Initiatives Program, the Defense Threat Reduction Agency (DTRA), and JWK Corporation. The authors acknowledge the contributions of Dr. Stanislaw Szpak, retired from SPAWAR Systems Center Pacific, who pioneered the Pd/D co-deposition process.

References

[1] P.A. Mosier-Boss, S. Szpak. F.E. Gordon, L.P.G. Forsley, Use of CR-39 in Pd/D co-deposition experiments, *Eur. Phys. J. Appl. Phys*. **40** (2007) 293–303.
[2] P.A. Mosier-Boss, S. Szpak. F.E. Gordon, L.P.G. Forsley, Characterization of tracks in CR-39 detectors obtained as a result of Pd/D co-deposition, *Eur. Phys. J. Appl. Phys.* **46** (2009) 30901.
[3] D. Nikezic, K.N. Yu, Computer program TRACK_TEST for calculating parameters and plotting profiles for etch pits in nuclear track materials, *Comp.Phys. Commun.* **174** (2006) 160–165.
[4] J.F. Ziegler, J.P. Biersack, *The Stopping and Range of Ions in Solids*, Pergamon Press, New York (1985).
[5] http://pages.csam.montclair.edu/∼kowalski/cf/358summary.html
[6] A.G. Lipson, A.S. Roussetski, E.I. Saunin, F. Tanzella, B. Earle, M. McKubre, Analysis of the CR-39 detectors from SRI's SPAWAR/Galileo type electrolysis experiments #7 and #5. Signature of possible neutron emission, Proceedings of 8th International Workshop on Anomalies in Hydrogen/Deuterium Loaded Metals, J. Rothwell and P. Mobberley (Eds.), 2008, pp. 182–203.
[7] Fran Tanzella, personal communication.
[8] A.G. Lipson, A.S. Roussetski, G.H. Miley, C.H. Castano, In-siti charge particles and X-ray detection in Pd thin film-cathodes during electrolysis in Li_2SO_4 /H_2O, in 9th International Conference on Cold Fusion (2002).
[9] D.O' Sullivan, D. Zhou, W. Heinrich, S. Roesler, J. Donnelly, R. Keegan, E. Flood, L. Tommaino, Cosmic rays and dosimetry at aviation altitudes, *Radiat. Meas.* **31** (1999) 579–584.
[10] D. Zhou, D.O' Sullivan, E. Semones, N. Zapp, S. Johnson, M. Weyland, Radiation dosimetry for high LET particles in low earth orbit, *Acta Astronautica* **63** (2008) 855–864.
[11] D. Zhou, E. Semones, R. Gaza, M Weyland, Radiation measured with passive dosimeters in low earth orbit, *Adv. Space Res.* **40** (2007) 1575–1579.

J. Condensed Matter Nucl. Sci. 3 (2010) 9–30

Review Article

Judging the Validity of the Fleischmann–Pons Effect

E. K. Storms*
LANL (ret.), KivaLabs, Santa Fe, NM, USA

T.W. Grimshaw†
Lyndon B. Johnson School of Public Affairs, The University of Texas at Austin, TX, USA

Abstract

The Fleischmann–Pons Effect (FPE, aka cold fusion) was rejected as legitimate science within a year after its announcement in 1989. The growing need for a source of clean energy makes a re-examination of the initial rejection increasingly important. An effective way of assessing the status of the effect as legitimate science is to apply criteria that have been established by scientific skeptics. When 27 criteria set forth by Langmuir, Sagan and Shermer are applied, the requirements for scientific legitimacy appear to be met. In addition, a large and growing number of independent experiments are consistent with a nuclear mechanism being the cause of FPE.

Keywords: CMNS, Cold fusion, Critique, Nuclear energy, Review

1. Introduction

The phenomenon called cold fusion (CF), low-energy nuclear reaction (LENR), chemically assisted nuclear reaction (CANR), or condensed matter nuclear science (CMNS) was first demonstrated by Profs. Martin Fleischmann (former head of electrochemistry at the University of Southhampton) and Stanley Pons (then chairman of the Chemistry Department at the University of Utah) in papers starting in 1989 [1–26]. They claimed that a fusion reaction between deuterons could be initiated in palladium after it had acquired a high concentration of deuterium. Their claim was based mainly on production of too much heat energy to be explained any other way. This anomalous result is called "excess energy" or "excess power" in this paper and the general phenomenon is referred to as the Fleischmann–Pons Effect (FPE). Later, work showed that they had discovered a universal phenomenon that could be initiated several different

*E-mail: storms2@ix.netcom.com
†E-mail: thomaswgrimshaw@gmail.com

ways with similar results. Like most discoveries, theirs only revealed the tip of the iceberg. Eventually, the effect was found to result in helium-4, tritium, and various transmutation reactions, in addition to energy production. However, this paper is not a complete scientific review but rather an evaluation of criteria used by various skeptics to reject the claims. The reader is directed to the citations for more detail about what is known.

A combination of issues created a growing skepticism about the validity of the claims and experimental results. These issues included a significant difficulty in reproducing the claimed excess energy, conflicts with conventional theory, and the challenge that such a simple and low-cost source of energy could pose for the hot fusion program as well as for conventional sources of energy. Especially troubling was the absence of neutrons or other energetic radiation, all of which were expected based upon the nuclear products found using the plasma fusion method or when high-energy deuterium ions bombard a solid. Consequently, many influential scientists [27–34] became outspoken critics of the claim, only a small sample of which is cited here. The US Department of Energy (DOE) established the official policy of the US government in 1989 with a written report provided by the Energy Research Advisory Board (ERAB) [35]. A second review [36] was undertaken in 2004 and arrived at a similar, but less extreme negative opinion.

During the 20 years since the original claim, hundreds of successful replications have been published, and important understanding of the process has been achieved. Apparent reaction rates have been achieved starting at a few events per second to rates that exceed 10^{14} events per second, most well in excess of expected error. Nevertheless, a strong skeptical bias exists in the scientific profession even though many papers, reviews, and books have been published arguing that the phenomenon is real and important. Part of this bias is based on ignorance of what has been discovered. A vicious cycle has apparently developed: because of this bias many respected scientific journals will not publish information on the subject. As a result, information does not reach the professional public and potential reviewers of submitted papers then reject the work as being poor science.

Physical science has adopted criteria that can be used to evaluate the reality of claims. Variations on these criteria have been proposed by several respected scientists including Irving Langmuir, Carl Sagan, and Michael Shermer. These criteria can be stated as questions that this paper will use to answer the basic question: "Is cold fusion science or pseudoscience?" This question has become increasingly important because the skeptical bias continues even though the need for the kind of energy promised by this effect becomes more critical and as evidence supporting the claims mounts.

Using the information provided here, the reader can decide in an objective way whether the claims meet the criteria required of good science and whether further study of the evidence is warranted. For brevity, only a fraction of the available papers and published observations are cited or discussed. A complete list of citations to the evidence exceeding 1000 publications can be found in books [37–44] and on websites [45–47].

2. Summary of evidence for the Fleischmann–Pons effect

FPE research has continued vigorously during the 19 years following its rejection early in 1990 by many people. The FPE effect has been achieved by four different methods – electrolysis, exposure to ambient gas, gas discharge, and sonic implantation. Sufficient evidence is now available to evaluate the effect with respect to experimental results, theory development, methods employed, and the number of people doing the research. Before addressing the criteria required of good science, a brief general summary of the evidence is provided based mainly on the electrolytic method for which the greatest number of replications exist.

2.1. Results of investigations

The five claimed experimental indicators (signatures) of FPE reactions are energy production in excess of any known chemical reaction, production of helium and tritium, radiation characteristic of nuclear reactions, and transmutation of

one element into another. Of these, helium and energy production have been shown to have a quantitative relationship to each other. In addition, a few experimental variables, including current applied to an electrolytic cell, deuterium concentration in a palladium cathode, and the nature of the materials, have been shown to clearly influence production of excess energy. Additional variables are actively being explored and are frequently found to influence the process. The important variables are still not well enough understood to make the process occur with a frequency sufficient to allow efficient exploration of the mechanism. Although many attempts have been made to explain the observations, none has been fully successful and is generally accepted. Clearly, much more effort has to be invested before these problems can be solved. This paper explores some reasons why this effort is not being applied and why it should be.

2.1.1. *Experimental indications*

Storms [37] has listed over 380 reports of successful experiments for the four FPE signatures as shown in Table 1. This list contains only those reports that could be described in a quantitative way. Hence, many more successful observations that are non-quantitative were actually made. Furthermore, more than one successful test was frequently reported in the cited publication but not counted in this list. Consequently, this is a minimum number of known successful results as of 2007. Many more have been reported since then. Of course, many more failures, both reported and unreported, exist. The number of failures is not important in evaluating the claims because many conditions, both known and unknown, can prevent the effect from occurring. Some of these are addressed.

Table 1. Reported successful FPE experiments (Table number and page numbers are those in the book by Storms [37]).

	Table No., pages	Number of successes
Excess heat	2, 53–61	184
Tritium production	6, 79-81	61
Helium	Not in table form	6
Transmutation	8, 93–95	80
Radiation	11, 101–104	55
	Total	386

Most of the effects are large and easily detected when they occur at all. Heat, helium, tritium, and energetic particle radiation have been detected at levels well above the expected uncertainty of each measurement. However, neutron emission is detected only at low levels near the detection limit even though many attempts have been made to find this anticipated emission. Four of the signatures are described below.

(A) *Excess Energy* has been measured by four different types of calorimeters – single wall isoperibolic, double-wall isoperibolic, flow-type, and Seebeck. Excess heat has been detected over a wide range as shown as a histogram in Figs. 1 and 2 of reported success vs reported power. The compared measurements are selected from the complete list on the basis of an acceptable expected uncertainty. The range of excess energy is from 0.005 to 183 W, depending on sample size, applied current, and amount of nuclear-active material present on the cathode, which has been shown to be the source of the extra energy. Clearly, the effect is not always small and is usually well in excess of expected error for the method used.

If excess energy results from a nuclear reaction, nuclear products and radiation should be detected. This necessary requirement has been satisfied. Tritium has been created several different ways, but not enough to explain the excess energy. On the other hand, the amount of helium detected is consistent with the amount of excess energy. When suitable detectors are applied, energetic radiation is also detected, but not the type and energy expected based on the behavior during hot fusion. Failure to find the same products as produced by hot fusion has been a major reason for rejection.

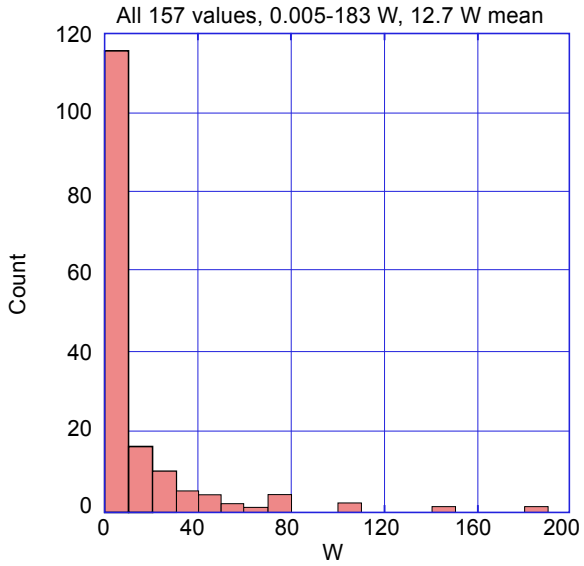

Figure 1. Histograms of reported excess energy [37]. All 157 values, with a range of 0.005–183 W.

(B) *Tritium* is easy to measure because it is radioactive. However, because D_2O always contains a small amount of tritium, the amount made by a claimed fusion process is the amount found in the cell above this background value. Sixty-one [37] independent reports have been identified using electrolyte cells containing D_2O as well as during

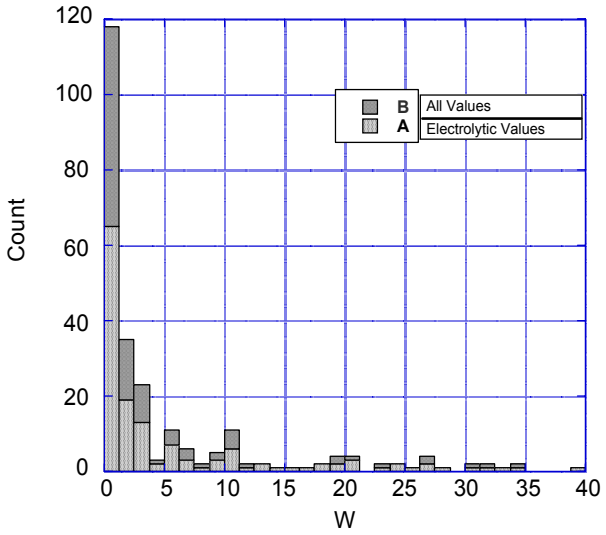

Figure 2. Histograms of reported excess energy [37]. Experiments producing power up to 40 W. Values are shown for all experiments and experiments using electrolytic cells.

low-voltage gas discharge using deuterium gas. Because most researchers do not have access to equipment required to measure tritium, the number of successes might be greater. The amount has been reported as high as 2×10^5times background [48] and as many as 2×10^{16} atoms have been produced in one study [49]. The neutron/tritium ratio is always small with a value between 10^{-4} and 10^9 based on 14 studies. This small neutron/tritium ratio is in sharp contrast to a value of unity found under hot fusion (plasma) conditions.

(C) *Helium* is the main nuclear product of FPE, but it is a challenge to measure accurately because the natural concentration of helium in ambient air is about 5.2 ppm. Helium from the air can enter a cell through a leak or by diffusion through the walls, thereby adding uncertainty to the small signal. In addition, the mass of helium and deuterium are sufficiently similar that great care is required to distinguish between the two species in a mass spectrometer. Nevertheless, studies have shown a relationship between the amount of heat produced and the amount of helium detected [50–59].

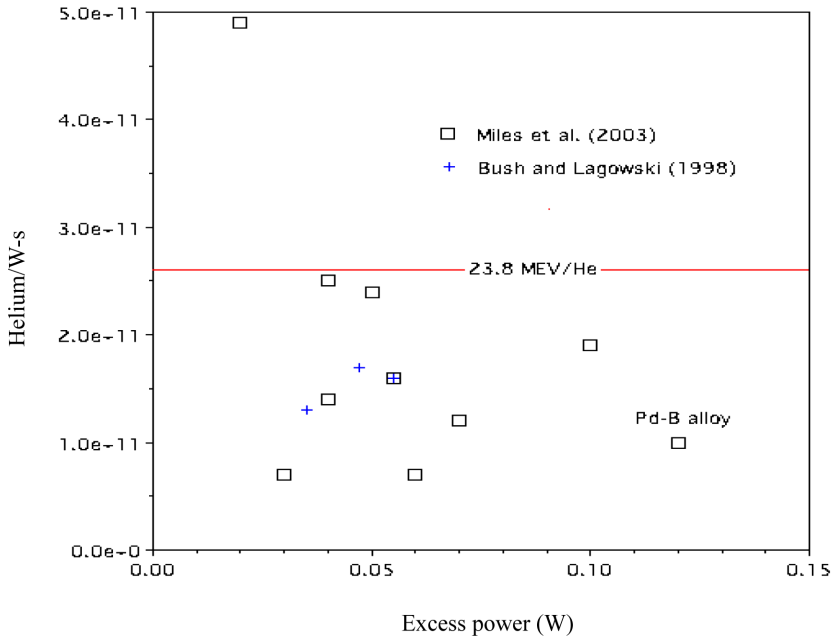

Figure 3. Comparison between several measurements of amount of helium released by the cathode divided by the energy measured as a function of excess power [37] The expected ratio is shown by the horizontal line at 23.8 MeV/He. The cathode is palladium except in the one case when a Pd + B alloy is used, as indicated on the figure.

Figure 3 compares the results from two independent studies using different palladium samples as the cathode and different calorimeter types. All but one of the points fall below the expected ratio (horizontal line) because at least half of the generated helium is usually retained in the cathode, which prevents it from being detected in the generated gas. The data reported by Bush and Lagowski [56] has less scatter than the study reported by Miles et al. because a Seebeck calorimeter was used instead of a double-walled isoperibolic type [58,60]. A similar relationship between heat and helium generation is indicated in both studies. Excess energy along with helium, apparently from FPE, has also been produced [61–65] and replicated [66] simply by exposing special materials to deuterium gas.

(D) *Radiation* of various kinds is expected when a nuclear reaction occurs. For example, helium production from fusion is expected to be accompanied by gamma radiation. Other fusion reactions are expected to emit energetic charged particles, X-rays can be produced by Bremsstrahlung, and neutrons might be produced by energetic alpha particles interacting with various light elements. If the process is similar to hot fusion, emission of energetic tritons, protons, and neutrons will occur.

One of the unexpected behaviors of the FPE is the absence of significant energetic radiation. Occasionally, energetic electromagnetic radiation is found using X-ray film [67–74], and gamma ray detectors. Energetic particle emission is detected using CR-39 [75–81], silicon barrier detectors and Geiger–Mueller detectors. However, the intensity of the radiation does not appear to be consistent with the amount of excess energy. Once again, anomalous behavior associated with nuclear activity is clearly observed during FPE, but it is not consistent with conventional expectations.

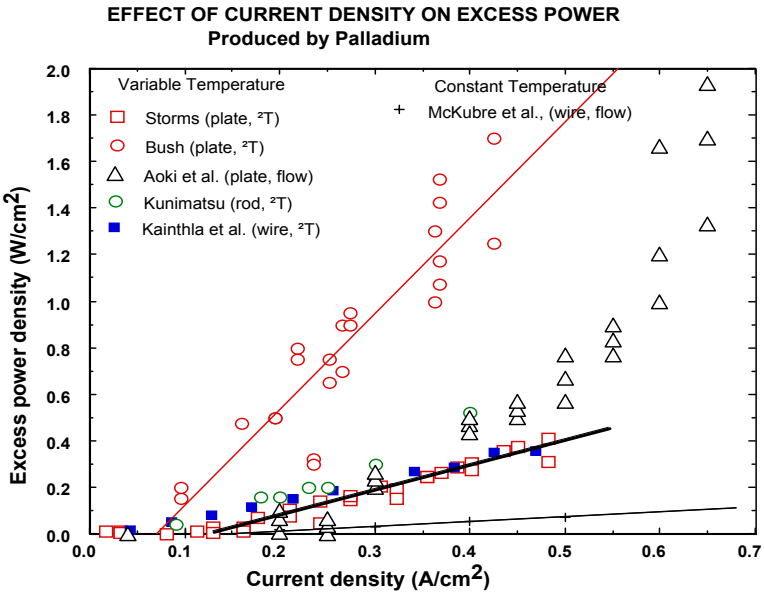

Figure 4. Examples of the effect of applied current on excess power using bulk palladium as the cathode in electrolytic cells [37]. This relationship has been found in all studies of bulk palladium when the values are measured.

2.1.2. *Correlation of cause and effect*

The amount of excess power has been related to applied current (Fig. 4), D/Pd ratio (Fig. 5), and the source of cathode materials. Some batches of palladium are more successful than others regardless of the method used to initiate the anomalous effects. Recently, laser stimulation has been found to enhance the effect [82–94]. More is said about the effect of variables in Section 2.4

2.1.3. *Possible prosaic explanations of heat and tritium observations*

Experimental observations of FPE have been questioned as being the result of error, contamination, or other common sources. The most significant are questions about heat and tritium production. FPE can be accepted only after such

processes are ruled out. The questions are discussed in detail because different types of evidence may have several different simple explanations. As expected, many prosaic explanations have been proposed. Only the most plausible are discussed here.

(A) *Heat:* Several different types of calorimeters and cell design, each with its own source of error, have been used and allow the influence of some processes to be evaluated.

Calorimeter: The popular isoperibolic type of calorimeter uses a temperature difference between the electrolyte fluid and the outside of the cell to determine the rate at which heat flows through the wall of the cell. Any temperature gradient within the liquid, caused by convection currents, can introduce an error. The original work of F–P was criticized for having this error [103,104].

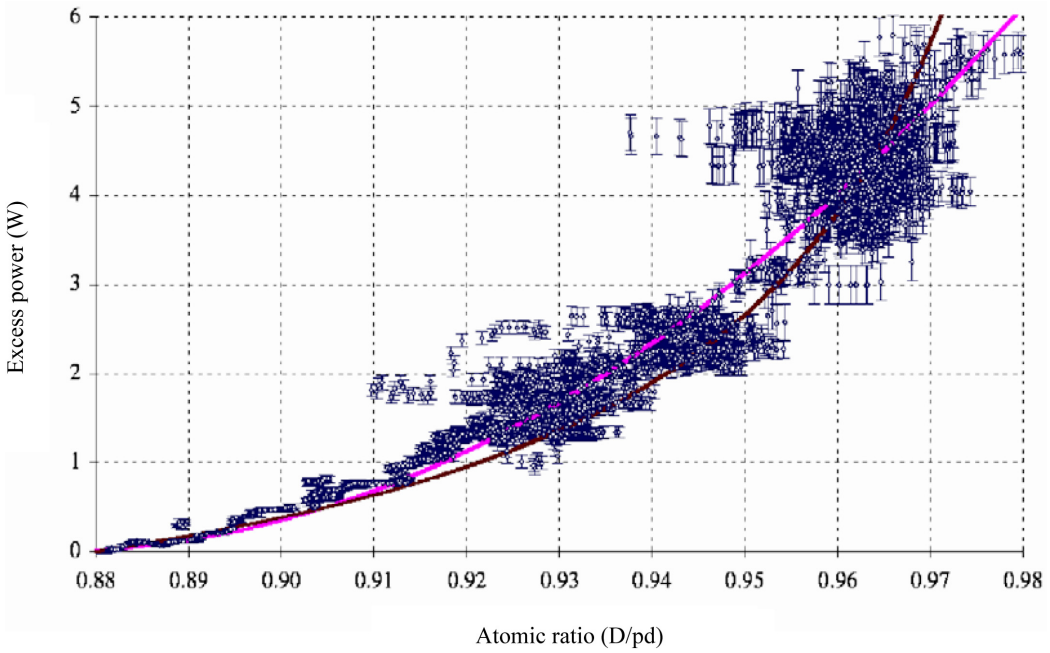

Figure 5. Examples of the effect of average D/Pd ratio of a Pd cathode during electrolysis [51,95]. Only samples of bulk palladium with a D/Pd above a critical value are found to produce excess energy.

This error is eliminated by using calorimeters that do not require measurement of temperature within the cell, such as the flow-type, Seebeck-type, and the double wall isoperibolic-type calorimeter. Production of excess heat energy has been observed numerous times using these types of calorimeter as has been tabulated by Storms [37]. Consequently, calorimeter error based on temperature gradients is no longer a rational explanation of excess energy in many studies.

Cell Design: Electrolysis releases D_2 and O_2 from the D_2O in the electrolyte. If these gases are allowed to leave the cell, as occurs when the so-called open cell is used, energy is lost and a correction needs to be made. This correction can be in error if an unknown amount of this gas recombines to form D_2O within the cell. Again, the original work of F–P was criticized for having this error even though they were fully aware of and took pains to eliminate the error [105].

This error can be eliminated by measuring the amount of electrolyte missing from the cell, as Fleischmann and Pons did. Such a measurement provides the exact amount of gas that exited the cell for which a correction can be made. Alternatively, a catalyst can be placed in the cell that recombines all the D_2 and O_2 back to D_2O, thereby eliminating any gas that might leave the cell and allowing the cell to be closed to any entry or loss of gas. Excess heat energy has been observed when such closed cells have been used as well as when the amount of missing D_2O is measured. Consequently, an error based on unknown recombination within the cell is no longer a rational explanation for excess energy in many studies.

Energy Storage: Energy might be stored in the cell if electrolysis lasts for a long time before excess heat is detected, which could be released later and misidentified as excess energy. This potential source of extra heat has been addressed in two ways. First, all chemical reactions that might take place in such a cell have been examined [106] and found to be too small to account for most of the observed excess power. Second, the excess power is found on many occasions to start soon after electrolytic power is applied, especially after the material has been activated by previous electrolysis or after application of an active layer. Consequently, very little energy has been added to the cell before excess energy is detected. In addition, excess power produced by direct reaction between special materials and deuterium gas provides no opportunity for energy storage. Therefore, many observations attributed to FPE exist that cannot be explained by energy storage.

If such a chemically simple system having such a small mass could store the amount of energy occasionally produced, the process would be thousands of times more potent than the best batteries and could produce the most powerful explosive or chemical fuel known. If energy is actually being stored and then released, this ability should demand intense examination, rather than being cited as a reason to reject or ignore the claims.

(B) *Tritium:* The claimed extra tritium has been proposed to result from contamination of the palladium metal, from ambient tritium in the environment leaking into the cell, or by enrichment of the tritium initially present in the D_2O. Each of these potential sources of tritium has been evaluated. Cedzynska et al. [107–109] analyzed ninety samples of palladium obtained from various commercial sources and found no tritium contamination. In fact, the process of refining commercial palladium would remove all trace of hydrogen. In addition, many studies used palladium that had been purposely subjected to a treatment that is known to remove all dissolved tritium. On the other hand, Storms and Talcott-Storms [110] showed that when any tritium dissolved in palladium is removed during electrolysis, it always is found in the gas, not in the electrolyte where anomalous tritium is always found. Consequently, tritium contamination of palladium as an explanation is not supported by observation.

Tritium entering from the environment would accumulate in the cell immediately, in contrast to the delay that is frequently observed. Besides, the concentration of tritium in the environment is much smaller than the concentration of tritium created in many cells. Extra tritium caused by enrichment within an electrolytic cell has been eliminated in numerous cases by using a sealed cell or by applying corrections. When these factors are taken into account, the amount of tritium detected in many studies is far in excess of any rational explanation based on contamination.

In addition to tritium being occasionally observed in electrolytic cells, it has also been produced in sealed cells subjected to gas discharge of deuterium at voltages too low to produce conventional fusion [111–113]. This tritium has been shown not to result from contamination and it has been measured using two different methods that give consistent result. Success is related to the metal alloy used as the cathode.

2.1.4. *Conditions for experimental success*

Certain conditions are now known to be required for results consistent with FPE to be produced [96,97]. When these conditions are not met, the required behavior will not be observed and the experiment cannot be used to evaluate the reality of the basic claim. Failure to achieve these conditions is the major reason replication has been difficult. Six necessary conditions for the electrolytic method are described below. The other methods have their own set of conditions

that would not be discussed here.

No. 1. The D/Pd ratio in the bulk palladium cathode should be in excess of a critical value.

Compositions in excess of a critical value are required in order to support the critical higher composition on the surface. This critical minimum is difficult to achieve and it is variable because it depends on the nature of the active surface. The surface composition can be determined using the open-circuit-voltage [98,99] when the electrolytic method is used.

No. 2. The palladium must be free of cracks

Stress produced during loading of deuterium into the palladium lattice, combined with impurities in the palladium, can produce cracks. These allow deuterium to leave the metal and prevent the critical D/Pd ratio from being achieved at the surface. Initial reaction with deuterium needs to be done slowly at low current density to reduce the formation of these stress fractures [100]. The crack density can be determined by comparing the measured volume to the expected volume based on the D/Pd ratio [101].

No. 3. Except for thin coatings of palladium on platinum, the applied current density has to be above a critical value near 100 mA/cm^2 before detectable heat will be produced

The current must be sufficient to compensate for the loss of deuterium from the cathode in order to achieve the critical surface composition (see Fig. 4) The value depends on the shape of the cathode [102]. A thin coating of palladium plated on platinum does not show a need for a critical current because the loss is much less than from a bulk sample.

No. 4. The D_2O used in the electrolyte must be as free of H_2O as possible.

The presence of H_2O even at the one atomic percent level in D_2O will add enough H^+ to the palladium to stop the heat producing process. Many early studies did not take care to keep the D_2O free of H_2O. The H_2O content can be determined using NMR. However, under certain conditions, cells containing only H_2O have been found to produce excess energy, occasionally by what is proposed to be a nuclear process. Therefore, this electrolyte does not necessarily constitute a blank that can be used to test a calorimeter, as was required of Fleischmann and Pons by various skeptics.

No. 5. Certain impurities in the D_2O electrolyte are known to help and others are known to hinder the process. Therefore, care must be used to insure that the D_2O remains pure

Successful cathodes are frequently found to have silicon dioxide and other stable oxides on their surface. Addition of aluminum or arsenic to the electrolyte has also been found to help achieve the required high deuterium content. However, exposure of copper, such as from unprotected connecting wires, to the electrolyte can result in copper being deposited on the cathode and a failed experiment. A complex assortment of elements is normally found on cathodes after a long study, the role of which is gradually being understood. Some can be beneficial and other might be harmful, which can account for the unpredictable success or failure.

No. 6. Application of additional energy may help initiate the effect

Other conditions are now known to help the process such as application of non-equilibrium conditions and extra energy such as by using a laser, applying RF, or heating the cell to a higher temperature.

Many experiments undertaken early in FPE history did not meet the conditions listed above and could not have succeeded, but were nevertheless cited as evidence that Fleischmann and Pons were wrong. Because all required conditions are still not known, an experiment can nevertheless fail even when the above conditions have been satisfied.

2.2. Theory development

An adequate theoretical underpinning of FPE experimental observations has not yet been achieved. Nevertheless, a number of novel theories have been proposed. The challenge is to account for the very different environments in which hot (plasma) fusion and cold fusion operate. The high concentration of electrons combined with a regular arrangement of atoms in a crystal lattice may allow mechanisms to surmount

the Coulomb barrier that do not exist in gaseous plasma, thus providing a way to solve the apparent conflict between observation and expectation.

Theoreticians have taken several different paths. One group proposes that the nuclear reactions result when neutrons are added to various nuclei. These neutrons are proposed to be in the material as a stable cluster that is occasionally made reactive. Or the neutrons are created in the material by a process unique to each theory. Because neutrons have no charge, the Coulomb barrier is not a factor. However, the proposed source of the neutrons requires several novel processes to operate and most of the nuclear products are not consistent with neutrons being involved because many such reactions produce radioactive isotopes that are not found.

Another general approach is based on overcoming the Coulomb barrier in various ways. Various processes are proposed to force the deuterons close enough to cause a detectable reaction or to partially neutralize the positive charge so that the distance is more easily reduced. Some of these mechanisms involve resonance to concentrate energy in certain locations where a high concentration of deuterium is located. Ideas based on particle–wave conversion also have been explored. Even the involvement of unique particles, either from outer space or created in the sample have been suggested. All theories have serious difficulty in being reconciled with accepted nuclear theory or with the known behavior of the process. Nevertheless, many creative ideas are being explored and tested in the laboratory.

A particular theory is not advocated here, although several general characteristics are thought to be required. A theory must describe a process that does not violate the conservation of energy or momentum. In addition, it must be clearly related to the chemical and physical properties of real materials. Unlike the need to apply extra energy as required by hot fusion, the FPE nuclear reactions occur spontaneously only after the required chemical environment has formed, largely by chance at the present time. This behavior forces an explanation to consider materials science rather than just the type of nuclear physics applied to hot fusion. This situation is not unlike the materials problems that plagued early transistors and required investment of billions of dollars to discover that a few parts per billion of certain impurity atoms were important to achieve reliable behavior in spite of the physical process being understood.

In spite of these present limitations, a good understanding is required before acceptance of the effect can be complete and it is essential before practical application is possible. However, such understanding is not required to justify further study.

2.3. Research methods and investigators

Conventional methods are universally employed in FPE research, in many cases at major laboratories using commercially available equipment. FPE research is conducted at the present time by well-respected scientists in many countries, including the US, Italy, Japan, Russia, China, Israel, and France.

The FPE community consists of at least 200 active researchers as well as many other experts and interested parties. Table 2 lists a sample of 57 people who have made recent contributions to the subject by being the main author on recent published papers. Many researchers who are listed under the experimental category are also contributing to development of theory. This rather small effect is largely dictated by the widespread skeptical attitude toward the subject, not by failure to achieve successful replication of the claims.

FPE investigators have developed a research setting that is outside of, but in many ways parallel to mainstream science. For example, a professional organization has emerged as the International Society of Condensed Matter Nuclear Science (ISCMNS). Conferences are held about every 16–18 months with the most recent being the 15th ICCF Conference, held in Rome, Italy with over 150 attendees. Publications of the proceedings for the last three conferences are available at www.WorldScientific.com.

Papers are regularly given at periodic American Chemical Society (ACS) and American Physical Society (APS) meetings. Local conferences on the subject are regularly held in Japan[a] and Russia[b].

An open source journal for cold fusion papers (*J. Condensed Matter Nucl. Sci.*) has been initiated. At least two websites have been developed that include most of the papers published in CF research since the beginning; one of the sites (www.LENR.org) includes more than 500 papers and a bibliography of over 3,000 journal articles and books. Newsworthy CF events are covered on The New Energy Times website. Technical and sociological dialogue takes place on a Google Group private mailing list, named Condensed Matter Nuclear Science (CMNS), which can be joined by invitation from a current participant. The site has been active for about 4 years and has experienced over 10,000 postings, with an average of about 180 postings per month[c] Currently there are about 210 participants.

Interest remains at a significant level after a rapid drop during the first few years following the initial strong rejection[d]. Downloads of full text papers from LENR-CANR.org has remained steady over the last few years at 40,000/month, as shown in Fig. 6. The average monthly downloads of full-text papers is now slowly increasing with spikes in interest when the media focuses attention on the subject. Clearly, significant interest in the subject continues, although it remains relatively low.

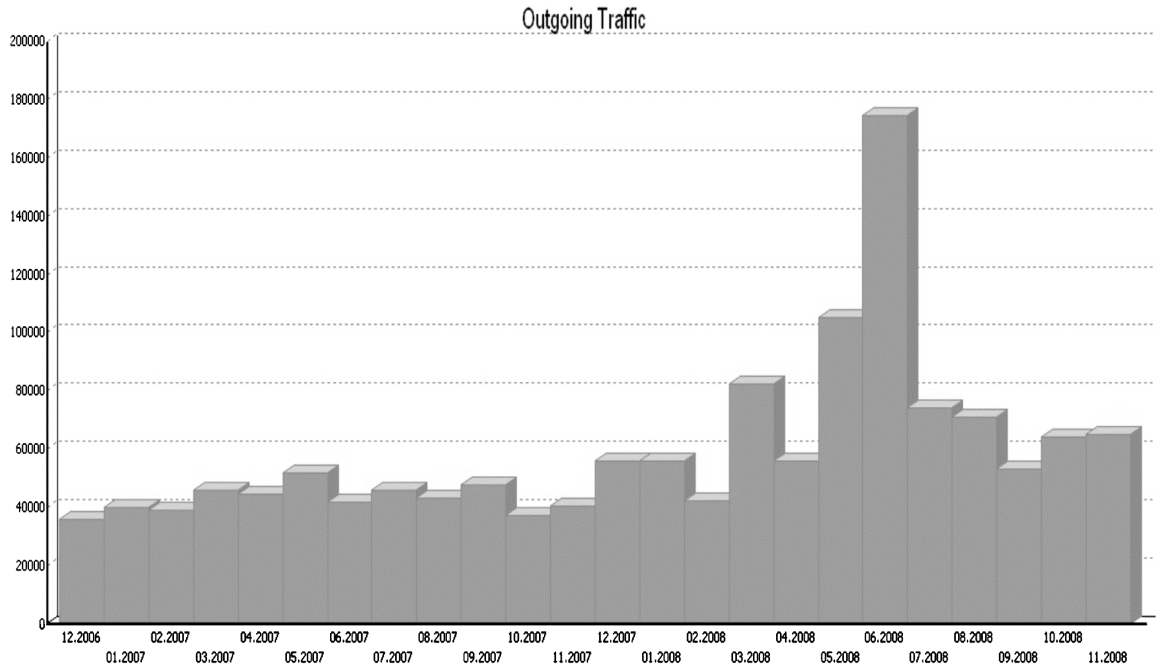

Figure 6. Monthly downloads of full text papers for 2007 and 2008 from LENR-CANR.org.

[a]Nineth annual meeting of Japan CF-Research Society, 28–29 March 2009, Shizuoka, Japan.
[b]Sixteenth Russian Conference on Cold Nuclear Transmutation & Ball Lightning (RCCNT&DL-16).
[c]Personal communication, Heiko Leitz, Group Sponsor, January 2009.
[d]See http://www.google.com/insights/search/#cat=174&q=cold%20fusion&cmpt=q for detailed information.

3. Application of skeptics' criteria

Langmuir, Sagan and Shermer have proposed three somewhat overlapping sets of criteria for distinguishing science from pseudoscience. Some of these criteria have been used in the past to discredit the Fleischmann–Pons claims. Now that additional information is available, these criteria may be more objectively applied. The criteria are stated here as 27 questions that must be answered in order for FPE to qualify as legitimate science. The responses provided here are based on the observations briefly described in Section 2 and on the cited literature.

3.1. Irving Langmuir's symptoms of pathological science

Irving Langmuir conducted research over a forty-year career until he retired in 1950. He won the Nobel Price in Chemistry in 1932. Langmuir was also interested in scientific boundary work – in defining what he called "pathological science." Although he did not formally publish his work in this area, he held a colloquium in 1953 that was subsequently transcribed. The highlights were subsequently published [114] and are shown in Fig. 7. Many papers and books have used the Langmuir criteria to conclude that FPE is a pathological science. Consequently, test of the claims using these criteria is important. Table 2. Sample of 57 recent contributors to FPE Research

(IL1) Is the maximum effect that is observed produced by a causative agent of more than barely detectable intensity?

The causative agent for the nuclear reactions is unknown, but it can be created on occasion. When it is created, most of the effects are large and easily detected. Heat, helium, tritium, and energetic particle radiation have been detected well above the expected uncertainties of each measurement. Only the expected neutron emission is detected at low levels near the detection limit (see Section 3.1.1.)

(IL2) Is the magnitude of the effect substantially dependent on (not independent of) the intensity of the cause?

The magnitude is increased by various changes in experimental conditions. For example, applied current (Fig. 4), D/Pd ratio (Fig. 5), and source of materials all affect the magnitude of the FPE signatures. Some batches of palladium

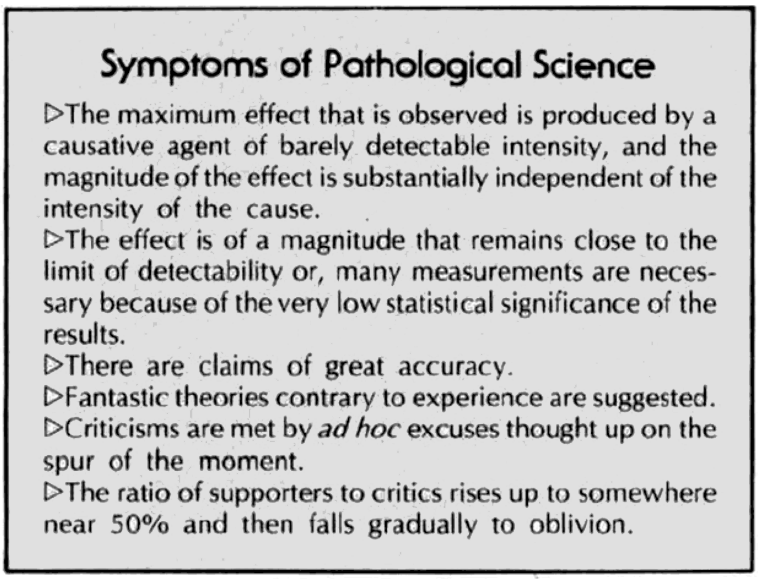

Figure 7. Monthly downloads of full text papers for 2007 and 2008 from LENR-CANR.org.

Table 2. Sample of 57 recent contributors to FPE Research

Author	Institution/Location
Theory	
Bass, R.	USA
Bazhutov, Y.	Inst. Terrestrial Magnet, Russia
Chubb, S.	Research Systems Inc., USA
Chubb, T.	NRL (ret.) USA
Collis, W.	ISCMNS, Italy
Fisher, J.	USA
Hagelstein, P.	MIT, USA
Kim, Y.	Purdue University, USA
Kozima, H.	Cold Fusion Research Lab., Japan
Nagel, D.	The George Washington Univ. USA
Srivastava, Y.	Univ. Studi di Perugia, Italy
Takahashi, A.	Osaka Univ., Japan
Widom, A.	Norhteastern Univ., USA
Experimental	
Arata, Y.	Osaka Univ. Japan
Biberian, J-P.	Univ. Marseilles Luminy, France
Bockris, J.	Texas A&M, (ret.)USA
Campari, E.	Univ. di Bologna, Italy
Cantwell, R.	Coolesence LLC, USA
Celani, F.	INFN, Italy
Claytor, T.	LANL, USA
Cravens, D.	Private Lab., USA
Dardik, I.	Energetics LLC, Israel
Dash, J.	Portland State Univ. (ret.)USA
De Ninno, A.	ENEA, Italy
Dufour, J.	CNAM, France
Fleischmann, M.	Univ. Southampton (ret.), UK
Iwamura, Y.	Mitsubishi Heavy Industries, Japan
Jones, S.	BYU (ret.) USA
Karabut, A. B.	FSUE "LUCH", Russia
Kasagi, J.	Tohoku Univ, Japan
Ken-ichiro, O.	National Univ, Japan
Koldamasov, A.	Sci Ctr of Syst Res & Technol, Russia
Kowalski, L.	Montclair State Univ. (ret.), USA
Letts, D.	Private Lab., USA
Li, X. Z.	Tsinghau Univ., China
Lipson, A.	The Russian Acad. Sci., Russia
Liu, B.	Tsinghua Univ., China
McKubre, M.	SRI International, USA
Miley, G.	Univ. of Illinois (ret.) USA
Mills, M.	USA
Mizuno, T.	Hokkaido Univ. Japan
Mosier-Boss, P.	US Navy, SPAWAR, USA
Oriani, R.	Univ. Minnesota, USA
Passell, T.	EPRI (ret.), USA
Savvatimova, I.	FSUE, "LUCH", Russia
Srinavasan, M.	BARC (ret.), India

Author	Institution/Location
Experimental (continued)	
Storms, E.	LANL (ret.), KivaLabs, USA
Stringham, R.	First Gate Energies, USA
Swartz, M.	JET Technol., USA
Szpak, S.	US Navy, SPAWAR (ret.), USA
Tian, J.	Changchun Univ,. China
Violante, V.	EURATOM-ENEA, Italy
Vysotskii, V.	Kiev Na'l Shevchenko Univ., Ukraine
Wei, Q. M.	Tsinghua Univ., China
Yamada, H.	Iwate Univ., Japan
Yamaguchi, T.	Kobe Univ., Japan
Zhong, X.	Tsinghua Univ., China

or other active material are more successful than others. Recently, laser stimulation has been found to enhance the effect [82–94]. How these conditions relate to the cause is unknown.

(IL3) Is the effect well above (not close to) the limit of detectability?

The signatures of FPE are detected well above the expected uncertainty for each. Note Figs. 1 and 2 as an example of the magnitude of heat production typically reported.

(IL4) Is the statistical significance of the results high, so that an excessive number of measurements are unnecessary?

The effect is robust and unambiguous when it occurs (see Section 2.1). For example, tritium measurements in successful experiments have been reported as high as 2×10^5 times background and excess power production is frequently over 100 times the expected uncertainty.

(IL5) Is there an absence of claims of great accuracy?

The claims for accuracy are typical of what is normally experienced and reported using the conventional experimental methods applied to FPE studies. For example, calorimeters that are used to measure excess heat in electrolytic cell investigations are well understood and have an uncertainty less than 0.1 W.

(IL6) Is there an absence of fantastic theories contrary to experience? Many theories have been advanced to explain FPE phenomena mostly in the context of what is already known about nuclear physics. The theories have a wide range of acceptability, but each attempts to explain some part of the observations. The theories that remain in serious contention in the FPE research community are generally grounded in currently accepted understanding. However, fantastic theories are occasionally suggested and may actually be required before the effect is understood (see Section 2.2).

(IL7) Are ad hoc excuses thought up on the spur of the moment when criticism is received?

The explanations have been well thought out and published. Several Google discussion groups are active in the critique of proposed theories (see Section 2.3).

(IL8) Has there been a rise of the ratio of supporters up to somewhere near 50% and then a gradual fall to oblivion?

The number of supporters has fallen after the initial rejection, but remains relative constant since then as can be seen in Fig. 6 (see Section 2.4). With a present research community of well over 200 scientists, a fall to oblivion has not occurred.

3.1.1. *Carl Sagan's baloney detection kit*

Carl Sagan was a scientist and science popularizer of considerable note. One of his most influential works was "The Demon-Haunted World"[e], an exposition of the role of science in promoting human welfare. Sagan also advocated the role of healthy skepticism in protecting the public welfare, particularly in Chapter 13, "The Fine Art of Baloney Detection." The scientific method and skeptical thinking are described as follows (pp. 209–210).

'In science we may start with experimental results, data, observations, measurements, "facts." We invent, if we can, a rich array of possible explanations and systematically confront each explanation with the facts. In the course of their training, scientists are equipped with a baloney detection kit. The kit is brought out as a matter of course whenever new ideas are offered for consideration. If the new idea survives examination by the tools in our kit, we grant it warm, although tentative, acceptance. If you're so inclined, if you don't want to buy baloney even when it's reassuring to do so, there are precautions that can be taken; there's a tried-and-true, consumer-tested method. What's in the kit? Tools for skeptical thinking. What skeptical thinking boils down to is the means to construct, and to understand, a reasoned argument and—especially important— to recognize a fallacious or fraudulent argument. The question is not whether we like the conclusion that emerges out of a train of reasoning, but whether the conclusion follows from the premise or starting point and whether that premise is true." (pp. 210–212)

The criteria in Sagan's baloney detection kit can be posed as questions shown below.

(CS1) Has there been independent confirmation of the "facts"?

The "facts" are obtained from measurement of the four principal FPE signatures. Table 1 provides a summary of 386 confirmations of these signatures. The measurements of the signatures have been replicated numerous times (see Section 2.1).

(CS2) Has there been substantive debate on the evidence by knowledgeable proponents of all points of view?

Extensive debate has taken place among the more than 200 scientists engaged in FPE research, using published papers, conference presentations, internet chat rooms, and personal contact (see Section 2.3).

(CS3) Have assertions been free from "argument from authority?

Because no recognized authority yet exists for FPE, assertions are based on experimental observations. Many of the more than 200 authors are experts in the methods they use to study the effect, such as calorimeters and mass spectrometers. Credible authority is therefore applied to the interpretation of the FPE observations in a manner similar to other fields of study.

On the other side of the coin, there appears to be evidence of argument from authority against public support for FPE research in the early days after its announcement. In April 1989 Glenn Seaborg advised President Bush against support based primarily on his own opinion and authority, when little experimental evidence had yet been developed[f]. Even today, this approach is occasionally used to reject the observations.

(CS4) Has more than one hypothesis been considered (e.g., "multiple working hypotheses"?)

Many theories have been advanced with varying degrees of merit that are frequently subjected to examination, debate, and refinement. A consensus has not yet emerged (see Sections 2.2 and 2.3).

(CS5) Have the hypotheses been free of personal attachment or bias?

While the ideal scientist is expected to be free of personal bias, this is seldom achieved. The only realistic criteria involve the degree of bias and whether the scientist is able to achieve a suitable objective consideration of evidence that runs counter to personal bias. This statement applies to a bias both for and against a claim. The real issue is whether skeptics can be sufficiently free from personal bias to examine the case with an open mind.

---

[e] Sagan, Carl. *The Demon-Haunted World – Science as a Candle in the Dark*. New York, Random House, 1995.

[f] Seaborg, Glenn. "FDR to Bush – Fifty Years of Advising the Presidents". Presentation made at Lawrence Berkeley National Laboratory, October 28, 1995. Online. Available: http://video.google.com/videoplay?docid=-6144236233611516224&hl=en.

(CS6) Has a rigorous attempt been made to quantify the assertion or experiment?

Work on FPE has continued for 20 years in at least 12 countries involving hundreds of scientists, which produced over 380 clear indications that the assertion is real. The assertions have been debated both with skeptics and among supporters in print and in private. All of this information is easily available to interested scholars in books and on websites (see Section 2.3). Various methods and equipment are used in the different approaches for achieving FPE. The different signatures – excess heat, helium, tritium and radiation – are measured by different instruments or techniques, which frequently yield consistent results.

(CS7) If there is a chain of argument and is every link in the chain valid?

The theory is still being developed. Consequently, the chain of argument is constantly changing. Nevertheless, the links are constantly being examined for validity. The experimental support is described in Sections 2.1–2.3.

(**CS8**) If more than one hypothesis is applicable, has the simplest one been selected (Occam's razor)?

Evaluation of the explanations is still underway. Simplicity is one of several criteria that are actively applied as theories are compared. Selection of the most straightforward hypothesis can only take place after complete explanations have been developed. At the present time, no theory can explain all observations.

(CS9) Can the hypothesis, at least in principle, be falsified?

The basic hypothesis that nuclear reactions can be initiated in special solids at ambient temperatures has been supported by the observation of concurrent nuclear products, radiation, and excess energy. This conclusion can only be falsified by finding prosaic explanations for each of the hundreds of observations. Use of trivial processes to account for FPE has not been successful so far (see Section 2.1.3). On the other hand, experimental failures were used to reject the effect. Most failures are caused by not using conditions required to achieve success, hence are not a true falsification.

3.1.2. *Michael Shermer's boundary detection kit*

Michael Shermer is a science historian who also specializes in the boundary work of skepticism. He has written a number of books on pseudoscience, superstition, skepticism and the border between what is rational and what is not. He founded the Skeptics Society, which has over 50,000 members, and he also writes a monthly column, "Skeptic", for the popular science magazine, "Scientific American". In addition, he has been an outspoken skeptic of FPE. In one of his main works, "Borderlands" [115], Shermer sets forth a "Boundary Detection Kit", which he describes (pp. 17,18) as follows:

"The Boundary Detection Kit"

Like any kit to be properly built and used, one must read the instructions carefully to receive the full benefit of the product. The Boundary Detection Kit requires the user to examine each claim in great detail, and to get to know the subject deeply enough to have a good feel for how to answer these questions. in so doing there is an implicit commitment to be honest and fair, and to not go into the investigation with a prearranged verdict in mind. This is difficult to do, of course, since none of us comes to the data with unvarnished thoughts free of theory. Science is theory laden. We all bring to the table a set of preconceptions born from the paradigms in which we were trained or raised. Nevertheless, we can rise above our biases, if not to an Archimedean point of unsullied objectivity, at least to a level at which the claimant under investigation might feel he or she got a fair shake. In fact, a principle of fairness in our Boundary Detection Kit might be to ask this question—what I call the fairness question — before all others: *If I were to ask the holders of the claim if they felt that they and their beliefs were fairly treated, how would they respond?* Where possible, in fact, why not ask them? I have done so on a number of occasions and to my considerable surprise I discovered that I had not been fair in my analysis, particularly in truncating someone's beliefs to a handful of simplified tenets that could be more easily analyzed (and, usually, debunked). This is sometimes called the "straw man" fallacy in logic, where one sets up a straw man that can be easily toppled but does not represent anyone's actual position. I find that I learn a lot more in the process when I bear in mind the fairness question. In many cases questioning the belief holder is not practical, but

the fairness question still works as a hypothetical standard toward which to aim." Shermer lists "ten useful questions to ask in determining validity of a claim. These ten questions were also published by Shermer in a series of two articles in his "Skeptic" column in Scientific American in 2001. The version in the Skeptic column was renamed "baloney detection" and had a set of annotations accompanying the questions that differed from those in the boundary detection kit. The ten questions are provided below with responses for the FPE case.

(MS1) How reliable is the source of the claim?

Most researchers in the FPE are competent scientists who have successful or even distinguished careers in other fields. In fact, Profs. Bockris and Fleischmann are pioneers in the field of electrochemistry and acknowledged leaders in their profession. Many other scientists still conduct research in "mainstream" science simultaneously with their FPE investigations. Given the large number and excellent credentials of the FPE research community, reliability of the source appears to be one of the main strengths of the FPE case (see Section 2.3)

(MS2) Does this source often make similar claims?

These sources have not made similar claims beyond their published work on the subject.

(MS3) Have the claims been verified by another source?

Numerous investigators have repeatedly verified the claims by during the past 20 years. Verifications have included more than 380 documented experimental successes (see Section 2.1).

(MS4) How does the claim fit with what we know about how the world works?

The effect is not consistent with how we "know" the world works, which is characteristic of all new discoveries. This is the reason the effect has been largely rejected in the past. Efforts are being made to expand nuclear theory to account for the FPE observations (see Section 2.2).

(MS5) Has anyone gone out of the way to disprove the claim, or has only supportive evidence been sought?

An experiment either produces excess heat, nuclear products and/or radiation, or it does not. Most attempts have failed to produce the anomalous FPE results. The question is whether the failures were caused by non-existence of FPE or because the experiment was not properly performed. This issue has been given a lot of attention as described above because it is the main reason used to reject the observations (see Section 2.1.3).

(MS6) Does the preponderance of evidence point to the claimant's conclusion or to a different one?

Occurrence of nuclear reactions is the only conclusion that is consistent with observed products. However, several different conclusions can be suggested about the process and mechanism. These conclusions are being debated and additional studies are underway to form an exact opinion.

(MS7) Is the claimant employing the accepted rules of reason and tools of research, or have these been abandoned in favor of others that lead to the desired conclusion?

The researchers and theoreticians who are active in the field regularly employ accepted rules of reason and conventional tools of research as described in Section 2. For example, the possible prosaic explanations have been well investigated and found to be insufficient to account for the observations of excess heat and production of helium. As another example, well-developed calorimeters with acceptable levels of uncertainty ($<$0.1 W) are routinely used to measure excess heat. Radiation is being measured using a variety of well-accepted methods.

(MS8) Is the claimant providing an explanation for the observed phenomena or merely denying the existing explanation?

Efforts are being made at the present time in laboratories located in eight countries to extend conventional theory in order to explain the anomalous FPE observations. The existing explanation, which is applicable to conventional "hot" fusion, clearly is inconsistent with the observations attributed to FPE. One possible explanation, noted in Section 2.2, is based on the high concentration of electrons and the regular arrangement of atoms in the metal lattice in the FPE environment. These conditions are much different from gaseous plasma and may provide mechanisms to surmount the Coulomb barrier that are not yet understood. In addition, evidence is growing that the physical environment can affect many other nuclear processes, in contrast to what conventional theory would predict.

(MS9) If the claimant proffers a new explanation, does it account for as many phenomena as the old explanation did?

The "old" explanation describes a different environment and a different range of applied energy. It does not address the effects that might occur in a solid. On the other hand, any new explanation based on a solid environment cannot be applied to conventional plasma. The conditions within the two environments are just too different. Acceptance of a new theory depends on whether the reader will consider that the environment in a solid might play a role in initiating nuclear reactions at low energy.

(MS10) Do the claimant's personal beliefs and biases drive the conclusions, or vice versa?

The researchers who support the claim of FPE are expected to be influenced by their personal beliefs and biases in the same manner as any other scientist. However, given the size, diversity, and quality of the research community, and the conventional methods they use, it is unlikely that bias is greater for investigators of FPE than it is for researchers in any other field of science.

4. Conclusions

FPE, unlike most other rejected scientific claims, has not faded into oblivion. Continued research in the field has yielded many confirmations of the principal signatures of FPE reactions. Prosaic explanations for most observations no longer apply. Contrary to common belief, evidence of FPE has grown in magnitude and become more consistent as better understanding has been achieved. Many critical variables have been identified that make the effect easier to replicate.

Theory development and experimental methods are consistent with the practices of mainstream science. The community of active FPE researchers consists of conventional scientists who, in most cases, are actively engaged in conventional areas of investigation independent of FPE. Borrowing from the legal field, there appears to be a preponderance of evidence that FPE is a "real" phenomenon based on experimental verification and the credentials of the scientists making the FPE claims.

The phenomenon cannot always be produced on demand, and no satisfactory theory explains the process or describes all of the required conditions. Despite this lack of understanding, anomalous behaviors are clearly evident under conditions that would normally produce no nuclear reactions and no energy at the levels being observed. These limitations demonstrate that more work is required to achieve success rather than, as the antagonists argue, being further evidence for bad science.

The original claims made by Profs. Fleischmann and Pons stand and are now supported by a well documented body of work. When the criteria for science versus pseudoscience are applied to FPE, all of the criteria appear to be met. It is therefore concluded that FPE, and the research into its causes and conditions, are legitimate science rather than pseudoscience.

Regardless of the explanation or the history of the claims, it is important for the reader to decide whether this phenomenon is now worthy of unrestrained investigation. The need for a potential source of energy, such as this phenomenon promises, is too important to reject the claims for trivial reasons.

Acknowledgement

The authors are grateful to Jed Rothwell for his editorial suggestions and to Christy Fraser and the New Energy Foundation for financial support that made this paper possible.

References

[1] Fleischmann, M., Pons, S., Hawkins, M., Electrochemically induced nuclear fusion of deuterium, *J. Electroanal. Chem.* 261, 301 and errata in Vol. 263 (1989).

[2] Fleischmann, M., Pons, S., Hawkins, M., Hoffman, R. J., Measurements of gamma-rays from cold fusion, *Nature*, London **339** (1989) 667.

[3] Fleischmann, M., in *The First Annual Conference on Cold Fusion* (ed. Will, F.), p. 344 (National Cold Fusion Institute, University of Utah Research Park, Salt Lake City, Utah, 1990).

[4] Pons, S. , Fleischmann, M., in *The First Annual Conference on Cold Fusion* (ed. Will, F. G.), p. 1 (National Cold Fusion Institute, University of Utah Research Park, Salt Lake City, Utah, 1990).

[5] Pons, S., Fleischmann, M., Walling, C. T., Simons, J. P. (WO 90/10935,1990, 1990).

[6] Fleischmann, M., Pons, S., Anderson, M. W., Li, L. J., Hawkins, M., Calorimetry of the palladium–deuterium–heavy water system, *J. Electroanal. Chem.* **287** (1990) 293.

[7] Pons, S. , Fleischmann, M., Calorimetric measurements of the palladium/deuterium system: fact and fiction, *Fusion Technol.* **17** (1990) 669.

[8] Fleischmann, M., in *Second Annual Conference on Cold Fusion, "The Science of Cold Fusion"* (eds. Bressani, T., Del Giudice, E. , Preparata, G.), p. 475 (Societa Italiana di Fisica, Bologna, Italy, Como, Italy, 1991).

[9] Pons, S. , Fleischmann, M., in *Second Annual Conference on Cold Fusion, "The Science of Cold Fusion"* (eds. Bressani, T., Del Giudice, E. , Preparata, G.), p. 349 (Societa Italiana di Fisica, Bologna, Italy, Como, Italy, 1991).

[10] Fleischmann, M. , Pons, S., Some comments on the paper "Analysis of experiments on the calorimetry of LiOD-D_2O electrochemical cells", R.H. Wilson et al., J. Electroanal. Chem. 332 [1992] 1. *J. Electroanal. Chem.* **332**(1992) 33.

[11] Fleischmann, M. , Pons, S., in *Third International Conference on Cold Fusion, "Frontiers of Cold Fusion"* (ed. Ikegami, H.), p. 47 (Universal Academy Press Inc., Tokyo, Japan, Nagoya Japan, 1992).

[12] Pons, S. , Fleischmann, M., Concerning the detection of neutron and gamma-rays from cells containing palladium cathodes polarized in heavy water, *Nuovo Cimento Soc. Ital. Fis. A* **105A**(1992) 763 .

[13] Fleischmann, M., Pons, S., Le Roux, M. , Roulette, J. in *Fourth International Conference on Cold Fusion* (ed. Passell, T. O.), p. 1 (Electric Power Research Institute 3412 Hillview Ave., Palo Alto, CA 94304, Lahaina, Maui, 1993).

[14] Fleischmann, M. , Pons, S. Calorimetry of the Pd-D_2O system: from simplicity via complications to simplicity, *Phys. Lett. A* **176**(1993) 118 .

[15] Pons, S. , Fleischmann, M. , in *Fourth International Conference on Cold Fusion* (ed. Passell, T. O.), p. 8 (Electric Power Research Institute 3412 Hillview Ave., Palo Alto, CA 94304, Lahaina, Maui, 1993).

[16] Fleischmann, M., Pons, S. , Preparata, G., Possible theories of cold fusion, *IL Nuovo Cimento* **107A**(1994) 143. .

[17] Fleischmann, M. , Pons, S., Reply to the critique by Morrison entitled 'Comments on claims of excess enthalpy by FLeischmann and Pons using simple cells made to boil, *Phys. Lett. A* **187**(1994) 276 .

[18] Fleischmann, M., Pons, S., Le Roux, M. , Roulette, J., Calorimetry of the Pd–D_2O system: The search for simplicity and accuracy, *Trans. Fusion Technol.* **26**(1994) 323 .

[19] Pons, S. , Fleischmann, M., Heat after death, *Trans. Fusion Technol.* **26**(1994) 97 .

[20] Fleischmann, M. , in *5th International Conference on Cold Fusion* (ed. Pons, S.), p. 152 (IMRA Europe, Sophia Antipolis Cedex, France, Monte-Carlo, Monaco, 1995).

[21] Fleischmann, M., in *5th International Conference on Cold Fusion* (ed. Pons, S.), p. 140 (IMRA Europe, Sophia Antipolis Cedex, France, Monte-Carlo, Monaco, 1995).

[22] Pons, S. , Fleischmann, M., Etalonnage du systeme Pd–D_2O: effets de protocole et feed-back positif. ["Calibration of the Pd–D_2O system: protocol and positive feed-back effects"], *J. Chim. Phys.* **93**(1996) 711 (in French) .

[23] Fleischmann, M., in *The Seventh International Conference on Cold Fusion* (ed. Jaeger, F.), p. 119 (ENECO Inc., Salt Lake City, UT., Vancouver, Canada, 1998).

[24] Fleischmann, M., in *8th International Conference on Cold Fusion* (ed. Scaramuzzi, F.), p. XXIII (Italian Physical Society, Bologna, Italy, Lerici (La Spezia), Italy, 2000).

[25] Miles, M. H., Imam, M. A. , Fleischmann, M., in *8th International Conference on Cold Fusion* (ed. Scaramuzzi, F.), p. 105 (Italian Physical Society, Bologna, Italy, Lerici (La Spezia), Italy, 2000).

[26] Fleischmann, M., Reflections on the sociology of science and social responsibility in science, in relationship to cold fusion, *Accountability Res.* **8**(2000) 19 .

[27] Close, F., *Too hot to handle. The race for cold fusion* (Penguin, paperback, New York, 1992).

[28] Close, F., Cold fusion I: The discovery that never was, *New Scientist* **1752**(1991) 46 .

[29] Huizenga, J. R., *Cold fusion: The scientific fiasco of the century* (Oxford University Press, New York, 1993).

[30] Goodstein, D., Pariah science. Whatever happened to cold fusion? ,*The American Scholar* **63**(1994) 527 .

[31] Morrison, D. R. O., Review of progress in cold fusion, *Trans. Fusion Technol.* **26**(1994) 48 .
[32] Jones, S. E., Current issues in cold fusion research: heat, helium, tritium, and energetic particles, *Surf. Coatings Technol.* **51**(1992) 283 .
[33] Park, R. L., The cold fusion story has been an object lesson on why science flourishes only in the open, *The Chronicle of Higher Education*, A44 (1989).
[34] Park, R., *Voodoo science* (Oxford University Press, New York, NY, 2000).
[35] ERAB (Department of Energy, DOE/S-0073, Washington, DC, 1989).
[36] DoE. in, *Review of Low Energy Nuclear Reactions* (Department of Energy, Office of Science, Washington, DC, 2004).
[37] Storms, E. K. , *The science of low energy nuclear reaction* (World Scientific, Singapore, 2007).
[38] Rothwell, J., *Cold fusion and the future* , www.LENR.org, 2007.
[39] Kozima, H., *The science of the cold fusion phenomenon* (Elsevier Science, Amsterdam, 2006).
[40] Krivit, S. B. , Winocur, N., *The rebirth of cold fusion; Real science, real hope, real energy* (Pacific Oaks Press, Los Angeles, CA, 2004).
[41] Simon, B., *Undead science: Science studies and the afterlife of cold fusion* (Rutgers University Press, New Brunswick, NJ, 2002).
[42] Beaudette, C. G., *Excess heat. Why cold fusion research prevailed* (Oak Grove Press (Infinite Energy, Distributor), Concord, NH, 2000).
[43] Mizuno, T. ,*Nuclear transmutation: The reality of cold fusion* (Infinite Energy Press, Concord, NH, 1998).
[44] Mallove, E., *Fire from ice* (John Wiley, NY, 1991).
[45] , www.LENR.org.
[46] Britz, D. , http://www.kemi.aau.dk/∼britz/fusion.
[47] Japan CF Society, http://dragon.elc.iwate-u.ac.jp/jcf/indexe.html.
[48] Romodanov, V. A., in *Tenth International Conference on Cold Fusion* (eds. Hagelstein, P. L. , Chubb, S. R.), p. 325 (World Scientific, Cambridge, MA, 2003).
[49] Kaushik, T. C. et al. , Preliminary report on direct measurement of tritium in liquid nitrogen treated TiDx chips, *Indian J. Technol.* **28**(1990) 667 .
[50] Miles, M., in *Tenth International Conference on Cold Fusion* (eds. Hagelstein, P. L. , Chubb, S. R.), p. 123 (World Scientific, Cambridge, MA, 2003).
[51] McKubre, M. C. H., in *Tenth International Conference on Cold Fusion* (eds. Hagelstein, P. L. , Chubb, S. R.) (World Scientific, Cambridge, MA, 2003).
[52] De Ninno, A., Frattolillo, A., Rizzo, A. , Del Gindice, E., in *Tenth International Conference on Cold Fusion* (eds. Hagelstein, P. L. , Chubb, S. R.), p. 133 (World Scientific, Cambridge, MA, 2003).
[53] Arata, Y. , Zhang, Y.-C. , The basics of nuclear fusion reactor using solid pycnodeuterium as nuclear fuel, *High Temp. Soc, Japan* **29**(2003) 1 .
[54] Miles, M., Imam, M. A. , Fleischmann, M. ,Excess heat and helium production in the palladium-boron system, *Trans. Am. Nucl. Soc.* **83**(2000) 371 .
[55] Gozzi, D. et al., Erratum to "X-ray, heat excess and ^{4}He in the D/Pd system", *J. Electroanal. Chem.* **452**(1998) 251 .
[56] Bush, B. F. , Lagowski, J. J., in *The Seventh International Conference on Cold Fusion* (ed. Jaeger, F.), p. 38 (ENECO Inc., Salt Lake City, UT., Vancouver, Canada, 1998).
[57] Miles, M. H. , Bush, B. F. ,Heat and helium measurements in deuterated palladium, *Trans. Fusion Technol.* **26**(1994) 156 .
[58] Miles, M. H., Hollins, R. A., Bush, B. F., Lagowski, J. J. , Miles, R. E., Correlation of excess power and helium production during D_2O and H_2O electrolysis using palladium cathodes, *J. Electroanal. Chem.* **346**(1993) 99 .
[59] Bush, B. F., Lagowski, J. J., Miles, M. H. , Ostrom, G. S., Helium production during the electrolysis of D_2O in cold fusion experiments, *J. Electroanal. Chem.* **304**(1991) 271.
[60] Miles, M., Bush, B. F. , Lagowski, J. J., Anomalous effects involving excess power, radiation, and helium production during D_2O electrolysis using palladium cathodes, *Fusion Technol.* **25**(1994)478 .
[61] Arata, Y. , Zhang, Y. C. , in *The 9th International Conference on Cold Fusion, Condensed Matter Nuclear Science* (ed. Li, X. Z.), p. 5 (Tsinghua Univ. Press, Tsinghua Univ., Beijing, China, 2002).
[62] Arata, Y. , Zhang, Y. C., Definitive difference between [DS-D_2O] and [Bulk-D_2O] cells in 'deuterium-reaction'. *Proc. Jpn.*

Acad., Ser. B 75 Ser. B, 71 (1999).
[63] Arata, Y. , Zhang, Y. C. , Observation of anomalous heat release and helium-4 production from highly deuterated fine particles, *Jpn. J. Appl. Phys. Part 2* **38**(1999) L774 .
[64] Arata, Y. , Zhang, Y. C., in *8th International Conference on Cold Fusion*, (ed. Scaramuzzi, F.),p. 11 (Italian Physical Society, Bologna, Italy, Lerici (La Spezia), Italy, 2000).
[65] Arata, Y. , Zhang, Y. C., Formation of condensed metallic deuterium lattice and nuclear fusion, *Proc. Jpn. Acad., Ser. B* **78**(2002) 57 .
[66] McKubre, M. C. H., Tanzella, F. L., Tripodi, P. , Hagelstein, P. L. ,in *8th International Conference on Cold Fusion* (ed. Scaramuzzi, F.), p. 3 (Italian Physical Society, Bologna, Italy, Lerici (La Spezia), Italy, 2000).
[67] Iyengar, P. K. , Srinivasan, M. , in *The First Annual Conference on Cold Fusion* (ed. Will, F.), p. 62 (National Cold Fusion Institute, University of Utah Research Park, Salt Lake City, Utah, 1990).
[68] McKubre, M. C. H. et al., in *The First Annual Conference on Cold Fusion* (ed. Will, F. G.), p. 20 (National Cold Fusion Institute, University of Utah Research Park, Salt Lake City, Utah, 1990).
[69] Rout, R. K., Shyam, A., Srinivasan, M. , Bansal, A., Copious low energy emissions from palladium loaded with hydrogen or deuterium, *Indian J. Technol.* **29**(1991) 571 .
[70] Rout, R. K., Shyam, A., Srinivasan, M., Garg, A. B. , Shrikhande, V. K., Reproducible, anomalous emissions from palladium deuteride/hydride, *Fusion Technol.* **30**(1996) 273 .
[71] Savvatimova, I. B. , Karabut, A. B., Radioactivity of palladium cathodes after irradiation in a glow discharge, *Poverkhnost (Surface)*, 76 (in Russian) (1996).
[72] Violante, V. et al., in *The 9th International Conference on Cold Fusion, Condensed Matter Nuclear Science* (ed. Li, X. Z.), p. 376 (Tsinghua Univ. Press, Tsinghua Univ., Beijing, China, 2002).
[73] Szpak, S., Mosier-Boss, P. A. , Smith, J. J., On the behavior of Pd deposited in the presence of evolving deuterium, *J. Electroanal. Chem.* **302**(1991) 255 .
[74] Matsumoto, T. , Observation of new particles emitted during cold fusion, *Fusion Technol.* **18**(1990) 356 .
[75] Fisher, J. C., in *8th International Workshop on Anomalies in Hydrogen/Deuterium Loaded Metals* (eds. Rothwell, J. , Mobberley, P.), p. 62 (The International Society for Condensed Matter Science, Catania, Sicily, Italy, 2007).
[76] Kowalski, L., Jones, S., Letts, D. , Cravens, D., in *11th International Conference on Cold Fusion* (ed. Biberian, J.-P.), p. 269 (World Scientific, Marseille, France, 2004).
[77] Lipson, A. G., Lyakhov, B. F., Rousstesky, A. S. , Asami, N. in, *8th International Conference on Cold Fusion* (ed. Scaramuzzi, F.), p. 231 (Italian Physical Society, Bologna, Italy, Lerici (La Spezia), Italy, 2000).
[78] Mosier-Boss, P. A., Szpak, S., Gordon, F. E. , Forsley, L. P. G., Use of CR-39 in Pd/D co-deposition experiments, *Eur. Phys. J. Appl. Phys.* **40**(2007) 293–303 .
[79] Oriani, R. A. , Fisher, J. C., in *11th International Conference on Cold Fusion* (ed. Biberian, J.-P.), p. 295 (World Scientific, Marseilles, France, 2004).
[80] Qiao, G. S. et al., in *The 7th International Conference on Cold Fusion* (ed. Jaeger, F. G.), p. 314 (Vancouver, Canada, 1998).
[81] Roussetski, A. S., in *11th International Conference on Cold Fusion* (ed. Biberian, J.-P.), p. 274 (World Scientific, Marseilles, France, 2004).
[82] Tian, J., Jin, L. H., Shen, B. J., Weng, Z. K. , Lu, X., in *ICCF-14 International Conference on Condensed Matter Nuclear Science* (ed. Rothwell, J.) www.LENR.org, Washington, DC, 2008).
[83] Letts, D., Cravens, D. , Hagelstein, P. I., in *ACS Symposium Series 998, Low-Energy Nuclear Reactions Sourcebook*, (eds. Marwan, J. , Krivit, S. B.), p. 337 (American Chemical Society, Washington, DC, 2008).
[84] Letts, D. , Hagelstein, P. I., in *14th International Conference on Condensed Matter Nuclear Science*, (ed. Nagel, D.) (Washington, DC, 2008).
[85] Sinha, K. P. , Meulenberg Jr., A., Laser stimulation of low-energy nuclear reactions in deuterated palladium, *Curr. Sci.* **91**(2006) 907 .
[86] Violante, V. et al., in *Condensed Matter Nuclear Science, ICCF-12*, (eds. Takahashi, A., Ken-ichiro, O. , Iwamura, Y.), p. 55 (World Scientific, Yokohama, Japan, 2005).
[87] Apicella, M. et al., in *Condensed Matter Nuclear Science, ICCF-12*, (eds. Takahashi, A., Ken-ichiro, O. , Iwamura, Y.), p. 117 (World Scientific, Yokohama, Japan, 2005).

[88] McKubre, M. C., in *ASTI-5*, www.iscmns.org, Asti, Italy, 2004.
[89] Letts, D. , Cravens, D., in *ASTI-5*, www.iscmns.org, Asti, Italy, 2004.
[90] Bazhutov, Y., Bazhutova, S. Y., Nekrasov, V. V., Dyad'kin, A. P. , Sharkov, V. F., in *11th International Conference on Cold Fusion*, (ed. Biberian, J.-P.), p. 374 (World Scientific, Marseilles, France, 2004).
[91] Swartz, M. R., in *10th International Conference on Cold Fusion*, (eds. Hagelstein, P. L. , Chubb, S. R.), p. 213 (World Scientific, Cambridge, MA, 2003).
[92] Storms, E. K., in *10th International Conference on Cold Fusion*, (eds. Hagelstein, P. L. , Chubb, S. R.), p. 183 (World Scientific, Cambridge, MA, 2003).
[93] Clark, E. L. et al., Energetic heavy-ion and proton generation from ultraintense laser–plasma interactions with solids, *Phys. Rev. Lett.* **85**(2000) 1654.
[94] Castellano et al., in *8th International Conference on Cold Fusion*, (ed. Scaramuzzi, F.), p. 287 (Italian Physical Society, Bologna, Italy, Lerici (La Spezia), Italy, 2000).
[95] McKubre, M. C. H. et al., (EPRI, Palo Alto, 1998).
[96] Cravens, D. , Letts, D., in *ICCF-14, International Conference on Condensed Matter Nuclear Science* (ed. Rothwell, J.), www.LENR.org, Washington, DC, 2008.
[97] Storms, E. How to produce the Pons–Fleischmann effect, *Fusion Technol.* **29**(1996) 261.
[98] Storms, E. K., in *The 7th International Conference on Cold Fusion*, ed. Jaeger, F. G., p. 356 (ENECO Inc., Salt Lake City, UT, Vancouver, Canada, 1998).
[99] Storms, E. K., Formation of b-PdD containing high deuterium concentration using electrolysis of heavy-water, *J. Alloys Comp.* **268**(1998) 89 .
[100] Storms, E. K., A study of those properties of palladium that influence excess energy production by the Pons–Fleischmann effect, *Infinite Energy* **2**(1996) 50 .
[101] Storms, E., in *American Physical Society* (Atlanta, GA, 1999).
[102] Storms, E. K., The nature of the energy-active state in Pd–D. *Infinite Energy*, 77 (1995).
[103] Lewis, N. S. et al., Searches for low-temperature nuclear fusion of deuterium in palladium, *Nature (London)* **340**(1989) 525 .
[104] Shelton, D. S., Hansen, L. D., Thorne, J. M. , Jones, S. E., An assessment of claims of 'excess heat' in 'cold fusion' calorimetry. *Thermochim. Acta* 297, 7 (1997).
[105] Hansen, L. D., Jones, S. E. , Shelton, D. S. A response to hydrogen + oxygen recombination and related heat generation in undivided electrolysis cells, *J. Electroanal. Chem.* **447**(1998) 225.
[106] Kainthla, R. C. et al., Eight chemical explanations of the Fleischmann–Pons effect, *J. Hydrogen Energy* **14**(1989) 771.
[107] Cedzynska, K., Barrowes, S. C., Bergeson, H. E., Knight, L. C. , Will, F. G., in *Anomalous Nuclear Effects in Deuterium/Solid Systems, "AIP Conference Proceedings 228"* (eds. Jones, S., Scaramuzzi, F. , Worledge, D.) 463 (American Institute of Physics, New York, Brigham Young Univ., Provo, UT, 1990).
[108] Cedzynska, K., Barrowes, S. C., Bergeson, H. E., Knight, L. C. , Will, F. G., Tritium analysis in palladium with an open system analytical procedure, *Fusion Technol.* **20**(1991) 108.
[109] Cedzynska, K. , Will, F. G. Closed-system analysis of tritium in palladium. *Fusion Technol.* 22, 156 (1992).
[110] Storms, E. K. , Talcott-Storms, C., The effect of hydriding on the physical structure of palladium and on the release of contained tritium, *Fusion Technol.* **20**(1991) 246.
[111] Claytor, T. N., Schwab, M. J., Thoma, D. J., Teter, D. F. , Tuggle, D. G., in *The 7th International Conference on Cold Fusion* (ed. Jaeger, F.), p. 88 (ENECO Inc., Salt Lake City, UT., Vancouver, Canada, 1998).
[112] Claytor, T. N., Jackson, D. D. , Tuggle, D. G., Tritium production from a low voltage deuterium discharge of palladium and other metalsm, *J. New Energy* **1**(1996) 111.
[113] Tuggle, D. G., Claytor, T. N. , Taylor, S. F., Tritium evolution from various morphologies of palladiumm, *Trans. Fusion Technol.* **26**(1994) 221 .
[114] Langmiur, I. (ed.), *Pathological science* (1989).
[115] Shermer, M., *The Borderlands of Science – Where Sense Meets Nonsense.* (Oxford Univ. Press, Oxford, UK, 2001).

J. Condensed Matter Nucl. Sci. 3 (2010) 31–34

Research Article

Simple Parameterizations of the Deuteron–Deuteron Fusion Cross Sections

Peter L. Hagelstein*

Research Laboratory of Electronics, Massachusetts Institute of Technology, Cambridge, MA 02139, USA

Abstract

Simple parameterizations of the deuteron–deuteron fusion cross sections are given in a form suitable for numerical calculations.

Keywords: dd-Fusion cross section, Fitting functions for cross section, Nuclear fusion, Numerical fits

1. Introduction

We have recently been pursuing calculations of neutron yields due to the presence of fast alphas and deuterons in PdD and D_2O, in order to better understand the relative absence of neutrons in excess heat experiments. In the course of our calculations, we needed a fit for the deuteron–deuteron fusion cross section for neutron production. The cross sections are available online in the Los Alamos ENDFB-VI nuclear data compilation. A table of them can be downloaded [1]. However, for numerical work it is useful to have a simple fitted version. After searching for a while in the literature, it seemed worthwhile to develop fits that were useful for our purposes. Perhaps these may also be useful for others as well.

We note that Li and coworkers have put forth a simple physics-based model for the deuteron–deuteron fusion cross section [2], which from our perspective represents a major step forward. The parameterizations that we present here are not intended to be physics-based fits; instead, we were interested in developing a more standard numerical type of fit.

*E-mail: plh@mit.edu

2. Parameterization of the cross section

At low energy, the asymptotic dependence of the fusion cross section in the absence of anomalous screening can be found in terms of a constant astrophysical S-factor S_0 according to

$$\sigma(E_{\rm r}) \;=\; \frac{S_0}{E_{\rm r}} \exp\left\{-\sqrt{\frac{E_{\rm G}}{E_{\rm r}}}\right\}, \tag{1}$$

where we have indicated the relative energy as $E_{\rm r}$. The relative energy for the deuteron–deuteron reaction is half of the incident deuteron energy E in the lab frame. The Gamow energy is

$$E_{\rm G} \;=\; \left(\frac{\pi}{\alpha}\right)^2 M_D c^2 \;=\; 985.8\ {\rm keV}. \tag{2}$$

To develop a parameterization, we follow the approach of Erba [3], which is based on the energy-dependent astrophysical S-factor $S(E)$

$$S(E_{\rm r}) \;=\; \sigma(E_{\rm r}) E_{\rm r} \exp\left\{\sqrt{\frac{E_{\rm G}}{E_{\rm r}}}\right\}. \tag{3}$$

It is much easier to fit this function than the cross section.

2.1. Fitting function

To proceed, we adopt a fitting function of the form

$$\ln S(E_{\rm r}) \;=\; \left\{\frac{a + bE_{\rm r} + cE_{\rm r}^2}{1 + {\rm d}E_{\rm r}}\right\}. \tag{4}$$

2.2. Fitting parameters for the ^{2}H(^{2}H,n)^{3}He reaction

In the case of the ^{2}H(^{2}H,n)^{3}He reaction, we have obtained fitting parameters given by

$$a \;=\; 10.8947, \qquad b \;=\; 34.5732\ {\rm MeV}^{-1},$$

$$c \;=\; 0.254611\ {\rm MeV}^{-2}, \qquad d \;=\; 2.6419\ {\rm MeV}^{-1}. \tag{5}$$

The $S(E)$ function derived from the ENDFB-VI data set is shown along with the fitted version of the function in Fig. 1. The units of S associated with the fit are barns eV.

2.3. Fitting parameters for the ^{2}H(^{2}H,p)^{3}H reaction

For the ^{2}H(^{2}H,p)^{3}H reaction, the fitting parameters that we found are

$$a \;=\; 10.921, \qquad b \;=\; 22.5417\ {\rm MeV}^{-1},$$

$$c \;=\; 0.150056\ {\rm MeV}^{-2}, \qquad d \;=\; 1.71503\ {\rm MeV}^{-1}. \tag{6}$$

The $S(E)$ function derived from the ENDFB-VI data set is shown along with the fitted version of the function in Fig. 2

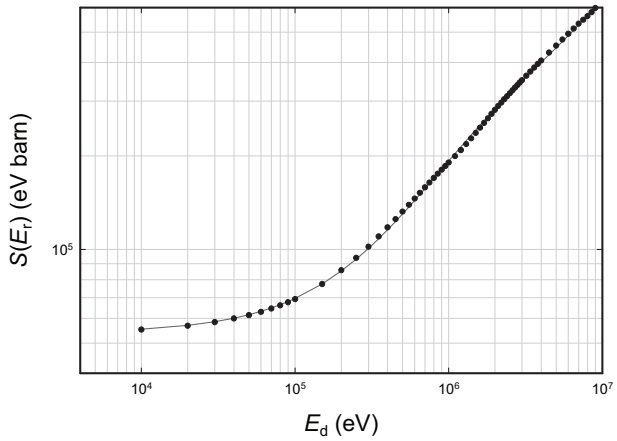

Figure 1. Astrophysical $S(E_r)$ factor for the n+^{3}He branch as a function of the deuteron energy in eV.

3. More complicated fitting function

It is possible to develop a better fit using a similar fitting function with more fitting parameters. In this case, we adopt a fitting function of the form

$$S(E_r) = \exp\left\{\frac{a + bE_r + cE_r^2 + dE_r^3}{1 + eE_r + fE_r^2}\right\}. \tag{7}$$

In the case of the ^{2}H(^{2}H,n)^{3}H reaction, the fitting parameters we found are

$$a = 10.8757, \qquad b = 51.579\ \text{MeV}^{-1},$$

$$c = 24.822\ \text{MeV}^{-2}, \qquad d = 0.070247\ \text{MeV}^{-3},$$

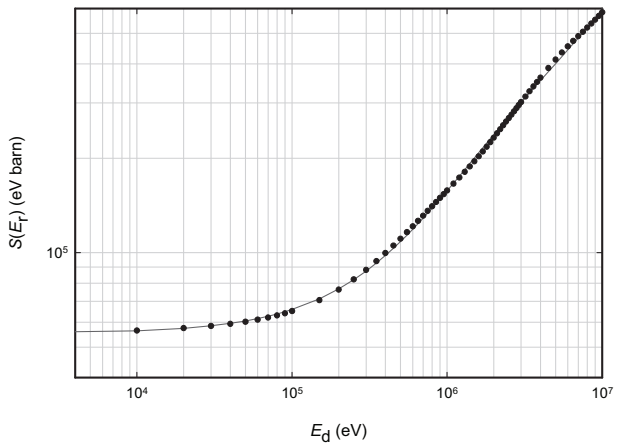

Figure 2. Astrophysical $S(E_r)$ factor for the p+^{3}H branch as a function of the deuteron energy in eV.

Table 1. Comparison of data with fits; E_r is the relative deuteron-deuteron energy; $S(n)$ is the astrophysical S-factor $S(E_r)$ for the ^{2}H(^{2}H,n)^{3}H reaction from the ENDFB-VI library; S_4(n) is the 4-parameter fitted result and S_6(n) is the 6-parameter fitted result; S(p) is the astrophysical S-factor $S(E_r)$ for the ^{2}H(^{2}H,p)^{3}H reaction from the ENDFB-VI library; S_4(p) is the 4-parameter fitted result and S_6(p) is the 6-parameter fitted result.

E_r(eV)	S(n)	S_4(n)	S_6(n)	S(p)	S_4(p)	S_6(p)
10000	56876	57019	56333	57492	57440	56911
30000	63014	63315	63205	61191	61691	61596
50000	69270	69634	69996	65132	65965	66245
100000	85718	85370	86491	76320	76700	77665
300000	145915	143856	144386	121356	118775	119873
500000	190496	192830	191405	157860	157512	156953
1000000	281353	283389	281088	232613	238054	234996
3000000	494163	487800	494855	454451	443165	454228
5000000	643531	647065	632824	583799	599158	576813

$$e = 4.1407\ \text{MeV}^{-1}, \qquad f = 1.8212\ \text{MeV}^{-2}. \tag{8}$$

For the ^{2}H(^{2}H,p)^{3}H reaction, we obtained

$$a = 10.9070, \qquad b = 32.995\ \text{MeV}^{-1},$$

$$c = 5.2903\ \text{MeV}^{-2}, \qquad d = -0.050120\ \text{MeV}^{-3},$$

$$e = 2.6291\ \text{MeV}^{-1}, \qquad f = 0.34445\ \text{MeV}^{-2}. \tag{9}$$

4. Discussion

We have developed simple fits to the deuteron–deuteron fusion cross sections which provide a reasonable match to the ENDFB-VI data set. Numerical values for the two cross sections and the different fits at selected relative energy points are given in Table 1. One can see that the fits match the data within a couple of percent. The standard error for the six parameter fits in both cases are about 60% of the standard error for the four parameter fits.

References

[1] The LANL website is: http://t2.lanl.gov/data/deuteron.html.
[2] X. Z. Li, B. Liu, S. Chen, Q. M. Wei, and H. Hora, *Laser and Particle Beams* **22** (2004) 469 .
[3] M. Erba, *J. Phys D: Appl. Phys.* **27** (1994) 1874 .

J. Condensed Matter Nucl. Sci. 3 (2010) 35–40

Research Article

Neutron Yield for Energetic Deuterons in PdD and in D_2O

Peter L. Hagelstein *

Research Laboratory of Electronics, Massachusetts Institute of Technology, Cambridge, MA 02139, USA

Abstract

To account for the excess heat in the Fleischmann–Pons experiment, it has been proposed that the reaction energy can be shared among a large number of deuterons. In order to help quantify how many deuterons are required to be consistent with experiment, we have computed the neutron yield for deuteron–deuteron fusion reactions in both PdD and in D_2O.

Keywords: Fleischmann–Pons effect, Correlation of neutrons with heat, Neutron yield for deuterons in PdD, Energy exchange with deuterons

1. Introduction

Takahashi and coworkers presented a useful assessment of the theoretical situation at ICCF5 [1], which remains relevant at the present time. Four scenarios were described, which we will outline here. In the first scenario, an aneutronic conventional fusion reaction is responsible for the excess heat, with the energetic fusion products hidden. In the second scenario, the reaction energy is communicated directly to the lattice, with no production of energetic particles. The third scenario is an exotic chemical or mechanical source for the energy, with weak associated nuclear emission. Finally, the fourth scenario is one in which the excess heat can be attributed to error.

Time and many experiments have provided ample evidence against the last of these scenarios, as there have been a great many replications of the excess heat effect. There have not appeared to the author's knowledge any credible proposal for exotic chemical or mechanical sources for the energy. To the contrary, the amount of energy produced in some experiments has been sufficiently large that there simply cannot be exotic chemical or mechanical sources. We have been interested in the second scenario since March, 1989; subsequently we reported on our progress at the ICCF conference series over the years.

However, in recent months we have developed an interest in the first scenario. Our interest has come about from a series of workshops that were held at the Naval Postgraduate School that were in part focused on the issue of mechanism.

*E-mail: plh@mit.edu

Some notable physicists were present, and after being exposed to some of the experimental results, their response was to put forth a number of proposals centered squarely within what Takahashi et al. described within their first scenario.

In these proposals, deuterons would in one fashion or another come together to produce ^{4}He, which would then carry away part of the reaction energy. The idea in these proposals was to try to have the overall mechanism remain consistent with one of the foundations of nuclear physics; that the reaction energy must be expressed as kinetic energy of the products as a consequence of energy and momentum conservation. At issue was the question of whether the reaction proceeds in a way consistent with the first scenario, or instead whether the reaction energy is communicated directly to low energy condensed matter degrees of freedom.

In the end, we were not able to come to an agreement. On the one hand, a spirited defense of the first scenario, energetic particles, and the established aforementioned foundation, was put forth; any radically new approach that would involve the direct communication of reaction energy to condensed matter modes was judged to be too farfetched to be worthy of serious consideration. On the other hand, an equally spirited argument was put forth that the proposals involving "hidden" energetic products was simply inconsistent with experiment.

So, in the months following these meetings, some effort on our part has gone into an attempt to quantify the situation with respect to the hidden particles. In the workshop discussions, the focus was on an energetic alpha as the hidden particle. However, in order to understand quantitatively the yield of observable products due to energetic alpha particles, one first has to understand the yield of energetic deuterons. The reason for this is that one important way that energetic alphas give rise to neutron emission is through energetic deuterons produced from head on collisions with the alpha particles. So, to begin the analysis, we first need to determine the yield of an energetic deuteron.

At ICCF15, Storms put forth ideas about an energy release mechanism in which MeV reaction energy would be shared among a large number of deuterons in a cluster [2]. In some ways these ideas are like proposals due to Kim [3], in which the reaction energy would be shared with a large number of deuterons which he has proposed to condense in a Bose–Einstein condensate. Our focus here is not on the issues, merits, or challenges associated with these proposals. Instead, the results that we have obtained are useful in helping to quantify how many deuterons the reaction energy

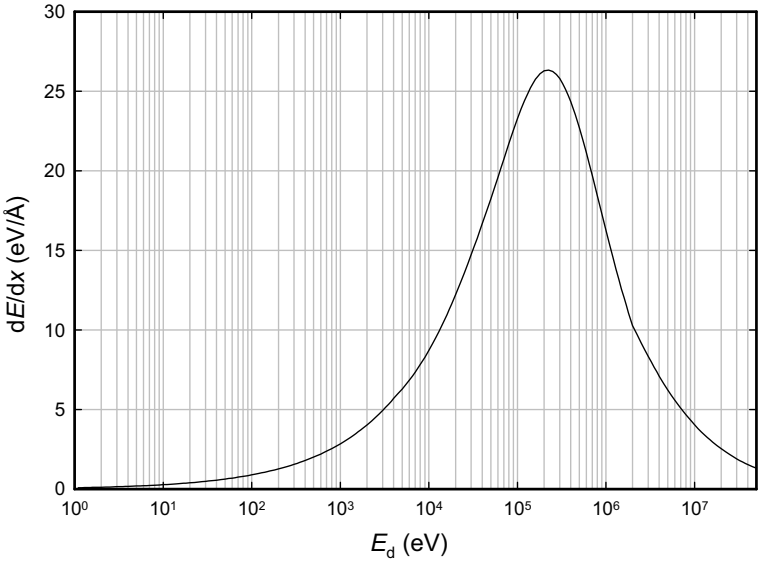

Figure 1. Stopping power for deuterons in PdD from SRIM2008.

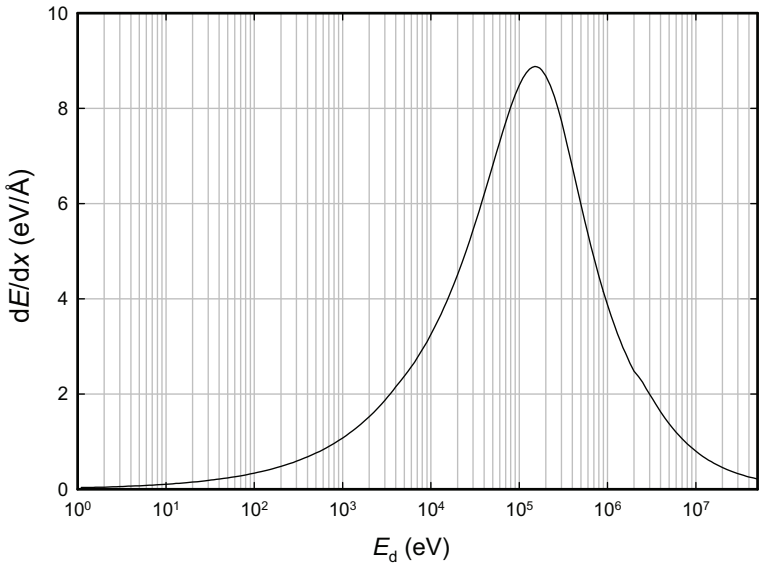

Figure 2. Stopping power for energetic deuterons in D_2O from SRIM2008.

would have to be shared with in order to be consistent with experiment.

2. Stopping power of deuterons in PdD and in D_2O

We have used the SRIM-2008 code of J. F. Ziegler, J. P. Biersack and U. Littmark to compute the stopping power of energetic deuterons in PdD and in D_2O. The stopping power for energetic deuterons in PdD is shown in Fig. 1, and the stopping power in D_2O is shown in Fig. 2. To construct these plots, we used a density of 10.921 g/cm^3 for PdD, and a density of 1.10 g/cm^3 for D_2O.

From a knowledge of the stopping power, one can compute the associated range using

$$R(E) = \int_0^E \left(\frac{\mathrm{d}E}{\mathrm{d}x}\right)^{-1} \mathrm{d}E. \tag{1}$$

Results for the range in the two cases are shown in Fig. 3.

3. Yield of neutrons from ^{2}H(^{2}H,n)^{3}He reactions

To compute the neutron yield from deuteron–deuteron fusion reactions, we need to integrate the product of the cross section and deuteron density over the deuteron trajectory as it slows down

$$Y(E) = \int_0^{R(E)} N_\mathrm{d}\sigma[E(x)]\mathrm{d}x. \tag{2}$$

Results of computations of the yield are shown in Fig. 4. For these calculations, we took the screening energy U_e to be 800 eV for PdD, and 25 eV for D_2O.

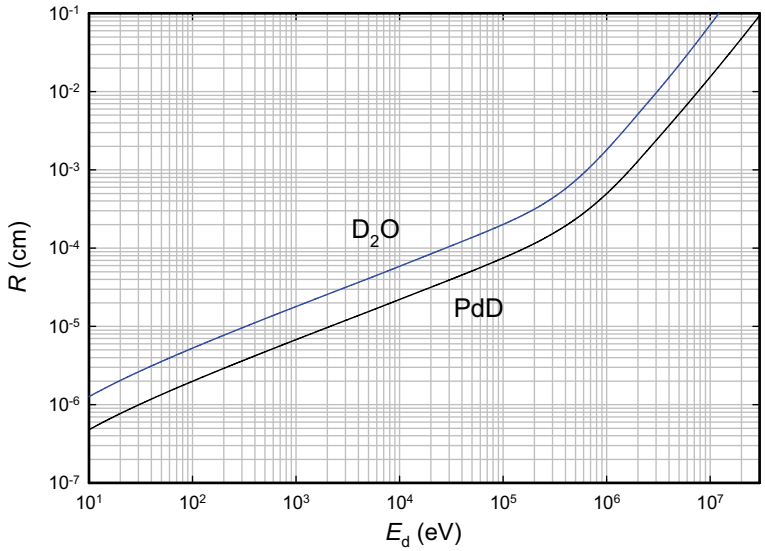

Figure 3. Range of energetic deuterons in PdD (lower curve) and in D_2O (upper curve).

4. Upper limits from experiment

The experimental data set associated with the Fleischmann–Pons experiment is often perplexing and not always consistent. With respect to the presence of low-level neutron emissions correlated with excess heat, one find mostly the absence of a correlation. In our view, there are different regimes where different effects are observed. For example in the case of a Fleischmann–Pons type rod cathode, excess heat is observed at higher current densities (several hundred mA/cm^2), while neutron emission is associated with lower current densities (tens of mA/cm^2).

If so, then of interest in the present discussion is the question of how many neutrons are seen when a system is running well, producing excess heat, and very little in the way of energetic emissions. This case presents the strictest constraints in regard to theoretical models.

Takahashi and coworkers reported on measurements of excess heat and neutron emission using Takahashi's high–low current protocol [4]. From our perspective, we would associate neutron emission with the low current part of the protocol, and excess heat with the high current part of the protocol. The data presented in this paper probably can be considered to support this notion weakly. In any event, there are numbers given both for excess power and for neutron emission above background from which we can extract a ratio. The source neutron emission rate is on the order of 1 n/s, largely uncorrelated with the presence of excess heat. The excess power is seen to reach about 100 W. Using these numbers leads to an estimate of 0.01 n/J.

Gozzi et al. reported positive measurements of excess heat run with neutron detection at ICCF4 [5]. In this case, excess power at levels on the order of 15 W, with no neutron emission above background. In the conference proceedings paper, the detector efficiency is not given. However, the detector was discussed in an earlier paper [6], and also in [7], and an efficiency of 22% is given. Using this efficiency, the background is about 35 neutrons counted in 10 min per segment, which corresponds to 12(0.265) = 3.2 source neutrons/s equivalent. We will assume that signals on the order of 10% of this number are detectable. The peak excess power in some of the bursts are in the range of 10-15 W. This leads to a limit on neutron production as low as 0.021 n/J.

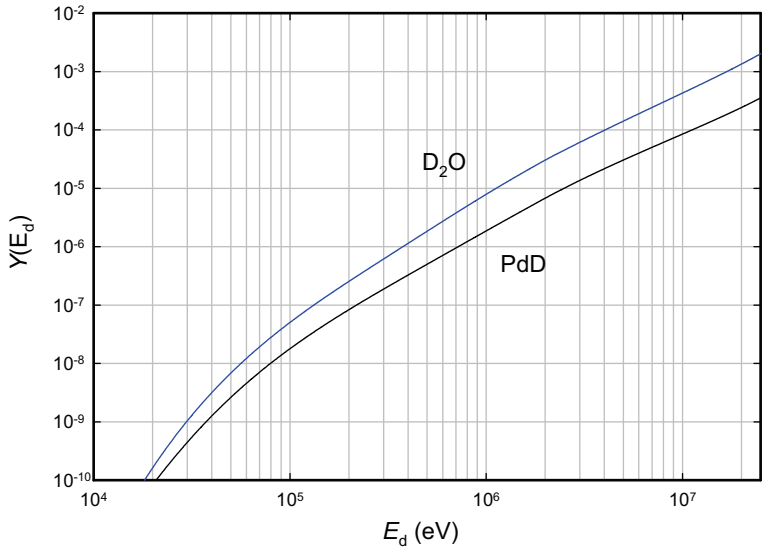

Figure 4. Yield of neutrons due to deuteron–deuteron fusion reactions in PdD (lower curve) and in D_2O (upper curve).

Scott et al. reported observations of excess heat at the same time that neutrons were detected [8]. In this case, excess heat was observed at the level of 4 W. Neutrons were monitored with an NE-213 detector with an efficiency of 0.00146, with a background of about 40 counts per day (about 0.32 n/s). If we assume that signals could be detected at the level of 10% of background, the associated upper limit is 0.008 n/J.

To compare with the calculations above, we have plotted the neutron yield divided by energy in comparable units (see Fig. 5). We see that in order to be consistent with the 0.008 n/J, that the upper limit on the deuteron energy is about 890 eV in the case of PdD. For low-energy deuterons in D_2O, the yield is less due to the weaker screening in this model.

5. Discussion

It has been suggested that the energy produced in the Fleischmann–Pons experiment is released as kinetic energy in a large number of low energy nuclei. Since most of the light nuclei in a Fleischmann–Pons experiment are deuterons, then one possibility is that the reaction energy is somehow distributed over a large number of deuterons, as has been discussed by Kim, and also by Storms. If so, then in order to be consistent with the experimental results discussed above, the average deuteron energy would have to be less than 900 eV if the deuterons remain in PdD. If the reaction energy is assumed to be 24 MeV, then this energy would need to be shared with at least 26,000 deuterons if all deuterons had the same energy. If the sharing process resulted in a thermal distribution, then probably more deuterons would be needed in order to reduce the contribution from the high energy tail of the thermal distribution. In Kim's paper [3], it is assumed that the energy is shared by on the order of 10^{10} deuterons.

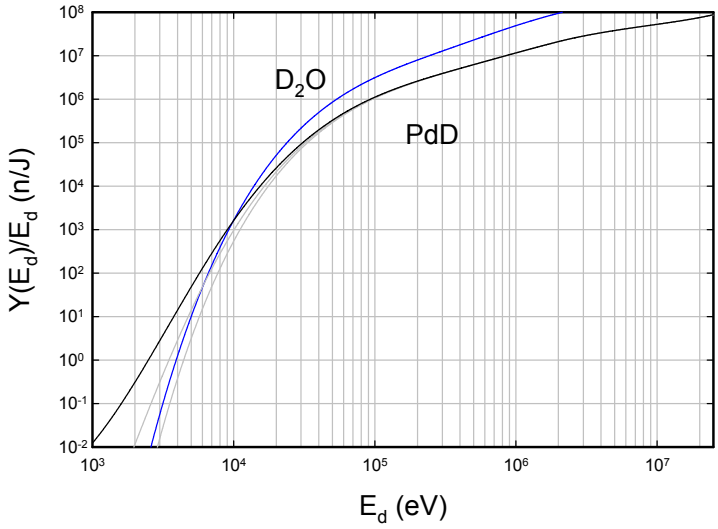

Figure 5. Yield of neutrons per unit energy due to deuteron–deuteron fusion reactions in PdD (black) and in D_2O (blue); also shown are results for PdD using 400 and 0 eV for the screening energy (gray).

References

[1] A. Takahashi, T. Inokuchi, Y. Chimi, T. Ikegawa, N. Kaji, Y. Nitta, K. Kobayashi, and M. Taniguchi, *Proc. ICCF5*, p. 69, 1995.
[2] X. Z. Li, B. Liu, S. Chen, Q. M. Wei, and H. Hora, *Laser and Particle Beams* **22** (2004) 469.
[3] Y. Kim, *Naturwissenschaften* **96** (2009) 803.
[4] A. Takahashi, A. Mega, T. Takeuchi, *Proc. ICCF3*, p.79, 1993.
[5] D. Gozzi, R. Caputo, P. L. Cignini, M. Tomellini, G. Gigli, G. Balducci, E. Cisbani, S. Frullani, F. Garibaldi, M. Jodice, G. M. Urciuoli, *Proc. ICCF4*, Vol. 1, p. 2-1, 1994.
[6] D. Gozzi, P. L. Cignini, R. Caputo, M. Tomellini, G. Balducci, G. Gigli, E. Cisbani, S. Frullani, F. Garibaldi, M. Jodice, G. M. Urciuoli, *Proc. ICCF3*, p. 155, 1993.
[7] E. Cisbani, G. M. Urciuoli, S. Frullani, F. Garibaldi, F. Giuliani, D. Gozzi, M. Gricia, M. Iodice, M. Lucentini, F. Santavenere, *Nucl. Instr. Meth.* **A 459** (2001) 247.
[8] C. D. Scott, J. E. Mrochek, T. C. Scott, G. E. Michaels, E. Newman, M. Petek M, *Fusion Technol.* **18** (1990) 103.

J. Condensed Matter Nucl. Sci. 3 (2010) 41–49

Research Article

Secondary Neutron Yield in the Presence of Energetic Alpha Particles in PdD

Peter L. Hagelstein *

Research Laboratory of Electronics, Massachusetts Institute of Technology, Cambridge, MA 02139, USA

Abstract

It has been proposed that energy can be released in the Fleischmann–Pons experiment as energetic alpha particles in aneutronic fusion reactions. In this scenario, the energetic alpha particles could be "hidden" since they have a relatively short range in PdD. We evaluate the yield of secondary neutrons which result from deuteron–deuteron fusion reactions from energetic deuterons produced in collisions with energetic alpha particles.

Keywords: Secondary neutron yield, Fleischmann–Pons effect, Aneutronic fusion, Correlation of excess power and neutrons

1. Introduction

In some recent meetings in mid-2009 on excess heat in the Fleischmann–Pons experiment, a review of experimental results was presented for scientists outside of the field. In general, the response was one of astonishment, as might have been predicted. When the discussion turned to the question of mechanism, it quickly became clear how some very good physicists from outside the field viewed the theoretical possibilities. The only possibility worthy of consideration according to them were scenarios in which two deuterons somehow managed to come together to form an alpha particle, which carried of a significant fraction of the reaction energy. If the process were assumed to happen sufficiently deep within the cathode, then they would not make it out of the cathode since the mean free path is relatively short. As a result, these energetic alpha particles would be "hidden".

The difficulty with this kind of proposal was recognized previously by Takahashi and coworkers [1], who noted that energetic alpha particles would give rise to secondary radiation such as neutrons and X-rays. As such, it becomes difficult to "hide" a large number of energetic alpha particles.

We are interested in this work in the quantification of this argument. Fast alpha particles can collide with deuterons and produce neutrons through the inelastic ^{4}He(d,np)^{4}He reaction. To be observable, the alpha energy must be above

*E-mail: plh@mit.edu

7 MeV. Much more likely is secondary neutron production which occurs after an energetic alpha particle collides with a deuteron, producing a less energetic deuteron which can then produce a neutron through the ^{2}H(^{2}H,n)^{3}He reaction. In order to understand quantitatively the yield of neutrons due to energetic alpha particles, one first has to understand the yield of energetic deuterons. Then, one needs the neutron yield as a function of energy for energetic deuterons. We describe below computations leading to the determination of the secondary neutron yield for energetic alpha particles through this mechanism.

Accurate values for the stopping power of alpha particles are readily available, and we are able to compute the energy loss over the range numerically. Given results for the incremental alpha particle energy along its trajectory, all that we need is an estimate for the scattering cross section between the alpha particle and a deuteron, from which we can estimate the yield of secondary neutrons from deuteron-deuteron fusion reactions. In a previous manuscript [2] we have computed the yield of energetic deuterons in PdD and in D_2O, which we can use for the computations discussed here.

2. Impact parameter model for scattering

To proceed, we consider the calculation of the secondary neutron production cross section in a classical impact parameter approximation. We assume that an alpha particle is incident on a deuteron with an energy E in the lab frame. The cross section in this model is expressed as

$$\sigma(E) \;=\; \int_0^\infty Y[E_{\rm d}(E,b)]\,2\pi b\;\,{\rm d}b. \tag{1}$$

Here, b is the impact parameter, which can take on all values between 0 and ∞. The contribution to the secondary neutron production cross section is weighted by the secondary neutron yield Y given the scattered deuteron energy $E_{\rm d}$. The scattered deuteron energy is a function of the initial alpha particle energy E and the impact parameter b. If we have a parameterization for the neutron yield Y, then it is possible to estimate this cross section by doing a set of classical path calculations at each alpha particle energy. This is the approach that we have used.

2.1. Potential model

For the classical path calculation, we have used a combination of a screened Coulomb potential and a hard core Woods–Saxon potential

$$V(r) \;=\; \frac{Z_\alpha Z_{\rm d} e^2}{r}{\rm e}^{-r/D_s} - V_0\frac{1}{{\rm e}^{(r-r_0)/a}+1}. \tag{2}$$

We have used one of the Woods–Saxon potentials from Kambara et al. [3], which is defined by

$$V_0 \;=\; 84.5\ {\rm MeV} \;-\; E_{\rm r}, \qquad r_0 \;=\; 1.15\ {\rm fm}, \qquad a_0 \;=\; 0.7\ {\rm fm}, \tag{3}$$

where $E_{\rm r}$ is the relative energy in MeV.

2.2. Screening

From low-energy beam experiments, we know that screening is important for deuteron–deuteron fusion reactions [4]. Consequently, we would also expect that screening should also be important for alpha–deuteron scattering. Unfortunately, we are not aware of any experimental observations that would be helpful in the selection of a screening energy

relevant for alpha–deuteron elastic scattering. There are some beam experiments for reactions with ^{3}He and deuterons [5,6] which show some increase in the screening energy, but these experiments did not make use of metal deuteride targets which show large screening effects in other experiments.

We decided to match the screening length to the deuteron–deuteron case using the screening energy ($U_e = 800$ eV) of Raiola et al. [4] (note that there is some spread in the experimental results for the screening energy for PdD samples [7]). A screening energy U_e of 1600 eV for energetic alpha particles in PdD leads to a screening length for alpha–deuteron collisions that is matched to the deuteron-deuteron experimental results in PdD.

Note also that this relatively large screening energy results for alpha–deuteron collisions results in a reduction in the in the Rutherford scattering cross section, and an increase in the deuteron–deuteron fusion yield. We were not able to find an experimental result on the screening energy for D_2O, so we used 25 eV.

2.3. Classical path calculation

The trajectories are computed in the lab frame according to

$$M_1 \frac{d^2\mathbf{r}_1}{dt^2} = -\nabla_1 V, \tag{4}$$

$$M_2 \frac{d^2\mathbf{r}_2}{dt^2} = -\nabla_2 V. \tag{5}$$

We used a simple second-order discretization (the Störmer–Verlet method [8])

$$M \frac{\mathbf{r}_{j+1} - 2\mathbf{r}_j + \mathbf{r}_{j-1}}{\Delta t^2} = -(\nabla V)_j \tag{6}$$

with a fixed (small) timestep Δt. Below 1 MeV, the computations are "easy" since the scattering is primarily Rutherford scattering with a relatively weak Coulomb potential. Above 1 MeV, the Coulomb barrier can be penetrated in the classical problem, so that the full force of the Woods–Saxon potential is felt. In this region, a shorter timestep needs to be used. Rather than put in the effort to make use of a more sophisticated numerical approach, we just used more timesteps. In all cases, energy conservation could be verified to at least six digits in the numerical solutions.

2.4. Integration over the impact parameter

We used cubic interpolation combined with local Gaussian integration to obtain a reliable numerical integration over the impact parameter. While Rutherford scattering can produce an increase in the deuteron energy at large impact parameter, the associated yield function may not be large. As a result, the contributions from large b are damped exponentially.

3. Parameterization of the yield functions

In order to compute the secondary neutron yield following elastic scattering with an alpha particle, we require a computation of the yield function for the different deuteron energies. We considered this problem previously [2]. It is convenient to fit the resulting neutron yield as a function of deuteron energy, in order to facilitate the calculation of the secondary neutron cross section.

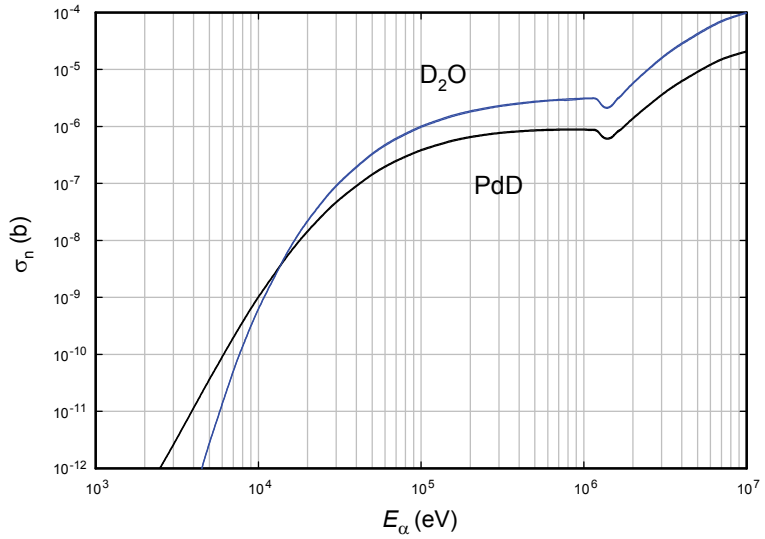

Figure 1. Secondary neutron cross section as a function of alpha particle energy (eV) for alpha particles in PdD and in D_2O.

3.1. Deuteron yield in PdD

In the case of energetic deuterons in PdD, we fit the neutron yield function according to

$$\ln Y = \frac{w}{x^3} + \frac{y}{x^2} + \frac{z}{x} + a + bx + cx^2 + dx^3 \tag{7}$$

with

$$x = \ln\left(\frac{E}{1\text{ eV}}\right) \tag{8}$$

and

$$\begin{aligned} w &= -537226.0, \qquad y = 355399.0, \qquad z = -94344.8, \\ a &= 12753.2, \qquad b = -937.761, \\ c &= 35.5573, \qquad d = -0.546338. \end{aligned} \tag{9}$$

3.2. Deuteron yield in D_2O

In the case of energetic deuterons in D_2O, we fit the neutron yield to the same function using

$$w = -117361.0, \qquad y = 88477.9, \qquad z = -28527.9,$$

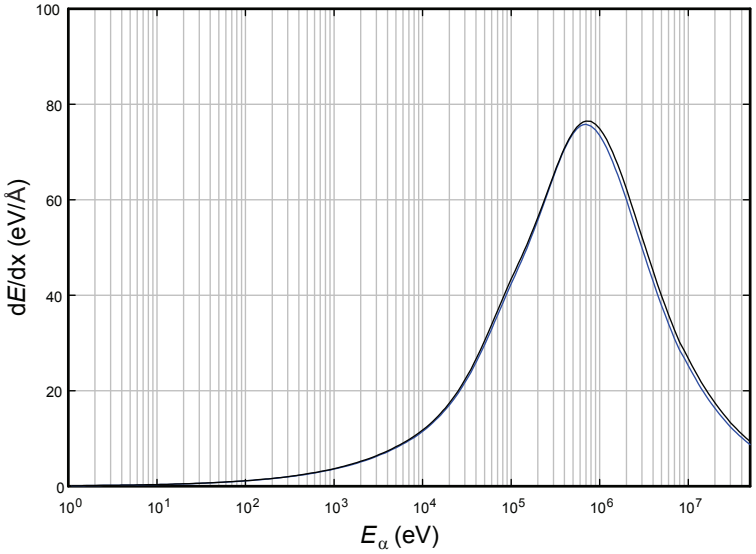

Figure 2. Stopping power for alpha particles in in Pd (black) and in PdD (blue) from SRIM2008.

$$a = 4502.29, \qquad b = -375.23,$$
$$c = 15.7547, \qquad d = -0.262152. \tag{10}$$

These fits were constructed using data between 500 eV and 10 MeV.

4. Cross section for secondary neutron emission

The cross section that results from the impact parameter calculation is shown in Fig. 1 for alpha particles in PdD and in D_2O. Three different regions are apparent in the cross section. Below about 1 MeV, Rutherford scattering is dominant, which when combined with the deuteron-deuteron fusion yield function produces a gently sloping cross section which decreases at lower energy. Above about 1.5 MeV, the alpha–deuteron scattering becomes increasingly dominated by the nuclear interaction potential at small impact parameter, which is favored in the impact parameter integration since hard core scattering produces more energetic deuterons with a higher yield function. Finally, between 1 and 1.5 MeV there is a dip in the cross section. This is a consequence of the presence of trajectories at small impact parameter where the pushing of the Coulomb potential is balanced by the pulling of the nuclear potential, which gives rise to a region where the deuteron energy is too small to cause significant fusion reactions.

The cross section for alpha particles in D_2O is larger at high alpha particle energy because the yield function for secondary neutron production is greater, due to the larger range of deuterons in heavy water as compared to PdD. The cross section for alpha particles in PdD is larger at low energy due to the much stronger screening effects in PdD as compared to D_2O.

5. Stopping power and range of alpha particles in PdD and in D_2O

We have used the SRIM-2008 code of J. F. Ziegler, J. P. Biersack and U. Littmark to compute the stopping power of energetic alpha particles in PdD and in D_2O (see Figs. 2 and 3). The stopping power can be used to compute the alpha

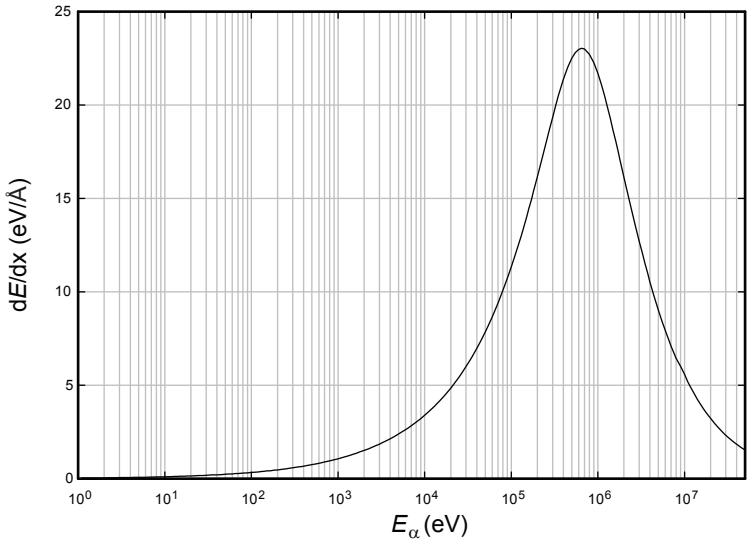

Figure 3. Stopping power for energetic alpha particles in D_2O from SRIM2008.

particle range using

$$R(E) \;=\; \int_0^E \left(\frac{\mathrm{d}E}{\mathrm{d}x}\right)^{-1} \mathrm{d}E. \tag{11}$$

We show the resulting alpha particle range in Fig. 4.

6. Yield of secondary neutrons

We can use the secondary neutron cross section and the stopping power to calculate the yield of secondary neutrons, by integrating the incremental yield over the alpha particle trajectory

$$Y(E) \;=\; \int_0^{R(E)} N_\mathrm{d}\sigma[E(x)]\;\mathrm{d}x. \tag{12}$$

The results for alpha particles in PdD and in D_2O are shown in Fig. 5. We see that the yield is higher in D_2O at high energies, due to the weaker stopping power of D_2O.

In order to compare with experiment, we require the quantity Y/E. This is shown in units of n/J in Fig. 6. At the lower energies one sees that the number of secondary neutrons per unit energy is higher in PdD due to the screening.

7. Sensitivity of yield to screening energies

Of interest in the interpretation of experimental results is the question of the sensitivity of the secondary neutron yield to the model used. In our case, we have two screening parameters with varying degrees of uncertainty. In the case of deuteron-deuteron collisions, measurements of the screening energy has yielded values between about 300 and 800 eV.

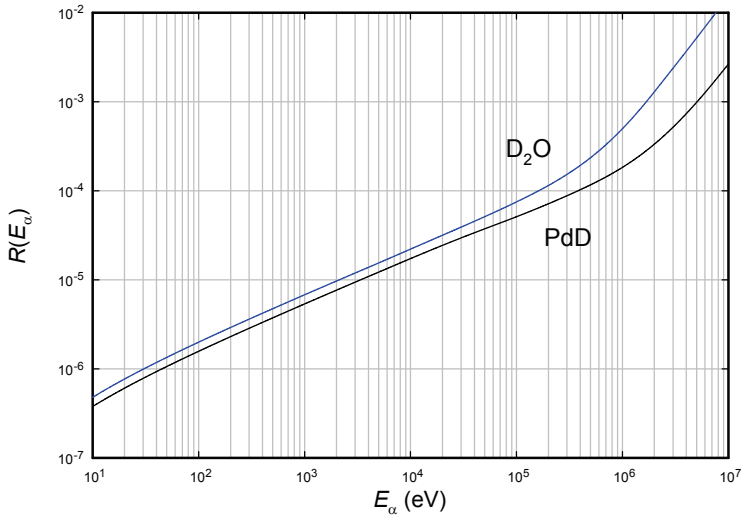

Figure 4. Range of energetic alpha particles in PdD (lower curve) and in D_2O (upper curve).

As mentioned above, we do not have results for the screening energy for alpha–deuteron collisions. As a result, it makes sense to explore the sensitivity of the secondary neutron yield to different assumptions about the two screening energies.

In Fig. 7, we show a close up of results where we have used different values for the two screening energies. In this figure, we see three bands of three curves each. The black, blue, and red curves use deuteron–deuteron screening

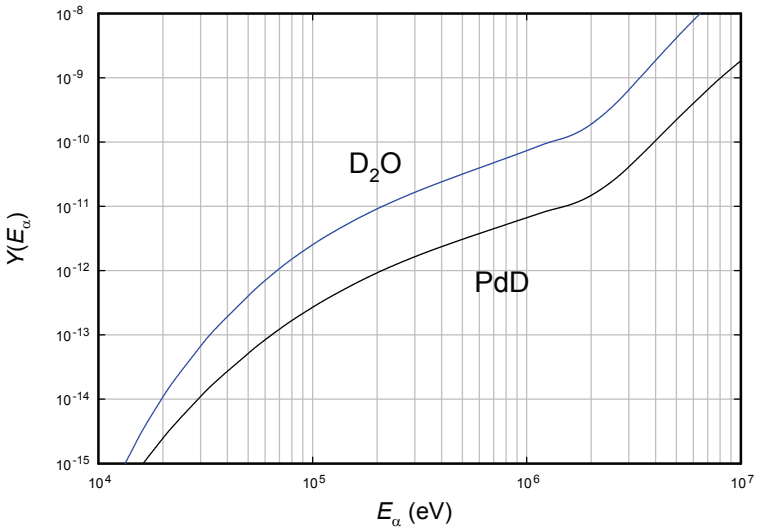

Figure 5. Yield of secondary neutrons in PdD (lower curve) and in D_2O (upper curve).

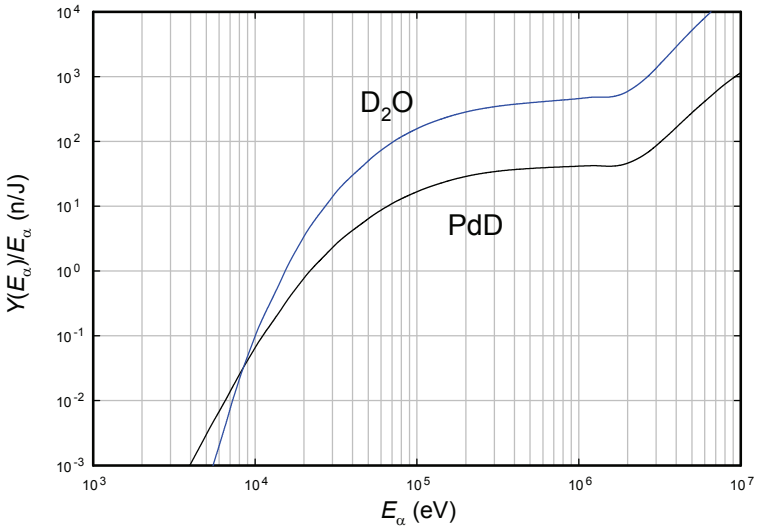

Figure 6. Number of secondary neutrons per joule in PdD (lower curve) and in D_2O (upper curve).

energies $U_e(\mathrm{dd})$ of 0, 400 and 800 eV, respectively. The three different curves within each band have alpha–deuteron screening energies $U_e(\alpha\mathrm{d})$ of 0, 800 and 1600 eV, where increasing screening energy reduces the yield. We see that the yield is most sensitive to the deuteron–deuteron screening energy, and that the spread in the experimental values

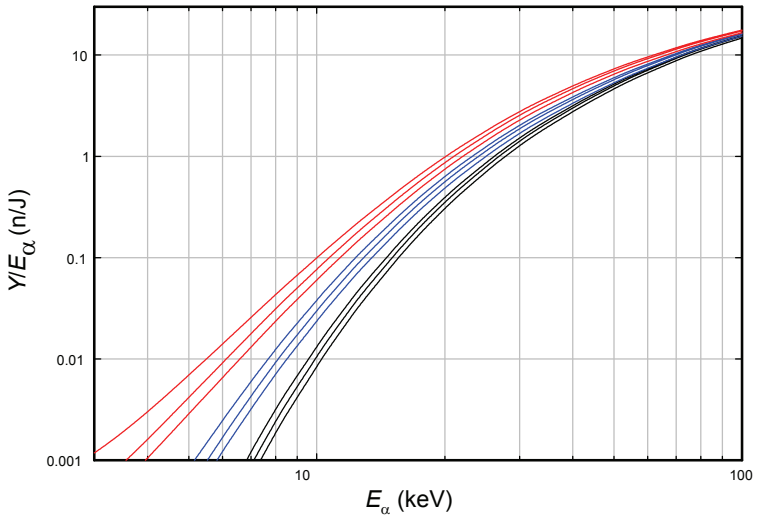

Figure 7. Secondary neutrons per alpha energy as a function of alpha energy. In the three top red curves, we have used $U_e(\mathrm{dd}) = 800$ eV; for the middle three blue curves, we have used $U_e(\mathrm{dd}) = 400$ eV; and for the bottom three black curves, we have used $U_e(\mathrm{dd}) = 0$ eV. In each case, we have run three cases with $U_e(\alpha\mathrm{d}) = 0, 800, 1600$ eV. The highest curve for each set of three corresponds to zero screening, and the lowest curve for each set corresponds to 1600 eV.

leads to about a factor of 2 difference in yield at 10 keV. The Rutherford scattering cross section is logarithmic in the alpha–deuteron screening distance, which accounts for weaker dependence on this screening parameter.

8. Discussion

As mentioned above, we were motivated to examine the secondary neutron yield due to energetic alpha particles due to the insistance of some of our colleagues, who are very good physicists, that energetic alpha particles can remain hidden in PdD. We can take advantage of the calculations presented above in order to estimate the upper limit on the alpha particle energy if it remains in PdD (or if it were to go into the D_2O electrolyte). From the experiments of Gozzi et al. [9], Takahashi et al. [10], and Scott et al. [11], we can extract upper limits on the number of neutrons per unit energy of excess heat produced to be 0.021, 0.01 and 0.008 n/J, respectively. The corresponding upper limit on the alpha particle energy is between 6200 and 7700 eV using a deuteron–deuteron screening energy of 800 eV. Assuming a deuteron–deuteron screening energy of 400 eV, the upper limit on the alpha energy is between 8200 and 9800 eV.

The experimental upper limits on the relative absence of neutrons, combined with the secondary neutron yields presented here, produces a very low upper limit on the alpha particle energy relative to the Q value from experiments (near 24 MeV). The simplistic proposals put forth by our physics colleagues are clearly inconsistent with experiment, since they would involve alpha particle energies well in excess of 1 MeV.

A preliminary version of these results and others appear in [12].

References

[1] A. Takahashi, T. Inokuchi, Y. Chimi, T. Ikegawa, N. Kaji, Y. Nitta, K. Kobayashi and M. Taniguchi, *Proc. ICCF5*, p. 69 (1995).
[2] P. L. Hagelstein, *J. Cond. Mat. Nucl. Phys.* **3** (2010) 35.
[3] T. Kambara, M. Takai, M. Nakamura and S. Kobayashi, *J. Phys. Soc. Japan* **44** (1978) 704.
[4] F. Raiola, L. Gang, C. Bonomo, G. Gyurky, M. Aliotta, H.W.Becker, R. Bonetti, C. Broggini, P. Corvisiero, A. D'Onofrio, Z. Fulop, G. Gervino, L. Gialanella, M. Junker, P. Prati, V. Roca, C. Rolfs, M. Romano, E. Somorjai, F. Streider, F. Terrasi, G. Fiorentini, K. Langanke and J. Winter, *Eur. Phys. J. A* **19** (2004) 283.
[5] F. C. Barker, *Nucl. Phys. A* **707** (2002) 277.
[6] M. La Cognata, A. Musumarra, C. Spitaleri, A. Tumino, C. Bonomo, S. Cherubini, P. Figuera, L. Lamia, M. G. Pellegriti, A. Rinolo, R. G. Pizzoni, C. Rolfs, S. Romano, D. Schürmann, F. Strieder, S. Tudisco and S. Typel, *Nucl. Phys. A* **758** (2005) 98c.
[7] K. Czerski, A. Huke, P. Heide and G. Ruprecht, *Eur. Phys. J. A* **27** (2006) 83.
[8] M. Griebel, S. Knapek and G. Zumbusch, *Numerical Simulation in Molecular Dynamics*, Springer, Berlin, 2000.
[9] D. Gozzi, R. Caputo, P. L. Cignini, M. Tomellini, G. Gigli, G. Balducci, E. Cisbani, S. Frullani, F. Garibaldi, M. Jodice and G. M. Urciuoli, *Proc. ICCF4*, Vol. 1, p. 2-1 (1994).
[10] A. Takahashi, A. Mega and T. Takeuchi, *Proc. ICCF3*, p.79 (1993).
[11] C. D. Scott, J. E. Mrochek, T. C. Scott, G. E. Michaels, E. Newman and M. Petek M, *Fusion Technol.* **18** (1990) 103.
[12] P. L. Hagelstein, *Naturwissenschaften* **97** (2010) 345.

J. Condensed Matter Nucl. Sci. 3 (2010) 50–58

Research Article

On the connection between K_α X-rays and energetic alpha particles in Fleischmann–Pons experiments

Peter L. Hagelstein *

Research Laboratory of Electronics, Massachusetts Institute of Technology, Cambridge, MA 02139, USA

Abstract

X-ray emission at K_α energies has been reported in Fleischmann–Pons experiments, and alpha particle emission has been reported in others. It is possible for energetic alpha particles to result in K_α radiation following impact ionization. As a result, one might imagine that K_α radiation is a signature of energetic ions in these experiments. We have calculated yields for K_α X-rays as a function of the energetic alpha particle energy in PdD. As a result of these calculations, we conclude that it is unlikely that these X-rays are a result of energetic alpha particles. We note that energetic alpha particles can produce excitation in lithium at 478 keV, and that the relative line strength of the Pd K_α, the Pt K_α and the Li 478 keV line can be used as a consistency check for energetic alpha particles.

Keywords: Fleischmann–Pons experiments, K-alpha emission, Gamma-emission, 478 keV line of ^{7}Li

1. Introduction

Spectroscopy is a key diagnostic in a variety of fields, including plasma physics, astrophysics, chemistry, and materials science. If a system is in thermal equilibrium, then it is may be possible to determine the plasma temperature from the relative intensity of different emission lines. At low density the atomic and ionic levels may not be in equilibrium, but in some cases it possible to determine both the temperature and electron density from the relative strengths of strong emission lines.

Spectroscopy has so far not played a particularly important role in Fleischmann–Pons experiments, which is unfortunate since it is such a powerful tool. There have been reported observations of K_α radiation from Pd [1] and from Pt [1,2] in Fleischmann–Pons experiments. Such observations are important because they give us the possibility of learning new things about the physical mechanisms behind the anomalies.

At present we do not understand why such radiation should occur. One possibility is that they are produced as a result of impact ionization from energetic particles. If so, then the X-ray emission could be considered as a secondary

*E-mail: plh@mit.edu

process which can be used as a diagnostic for the presence of energetic particles. Alternatively, it may be that X-ray emission occurs for some other reason, in which case it would be of interest to understand better what energetic process could result in the production of K_α emission.

For other reasons we have examined issues associated with nuclear radiation in general that would be expected in energetic alpha particles were present in large quantities in the Fleischmann–Pons experiment. It had been conjectured that the excess heat comes about from new reactions which result in energetic alpha particle emission in a way such that the energetic alpha particles are "hidden" deep within the PdD. We calculated the yields for a variety of reactions which would result in neutron, X-ray and γ-ray production. From a comparison with experiments in which excess heat was observed while nuclear emissions were being detected, we were able to conclude that the upper limit on the alpha particle energy must be less than 10 keV in order to be consistent with experiment.

As a result of this exercise, it became clear that spectroscopic diagnostics were available for energetic alpha particles. In particular, energetic alpha particles should produce K_α X-rays as well as the 478 keV line in ^{7}Li. Moreover, it should be possible to develop an estimate for the energy from measurements of the ratios of the different transitions. Since energetic alpha particles would also produce neutrons, one would expect a correlation between all of the different signals.

Now, there are experiments in which energetic alpha particles have been reported [3,4]. There are also experiments in which neutrons and X-rays have been reported. Previously we were interested in the correlation between excess power and nuclear radiation. Here, we are instead interested in the possible correlation between different low-level X-ray, gamma-ray and neutron emission. In what follows we will discuss results for yields of X-rays and γ-rays from energetic alpha particles. Based on these calculations, and from the few available experimental results, we conclude that the K_α radiation is not due to energetic alpha particles. Some other mechanism should be sought to account for them.

2. Impact ionization and K_α emission

X-ray emission resulting from bombardment by energetic ions is a subject that has been well studied for many years. In the case of alpha particle-induced K-shell X-ray emission, we can make use of the measurements of Wilson et al. [5], which is available in a relevant energy range for Rh and Ag (which are close to Pd).

To obtain results for Pd, we could interpolate data taken for nearby elements. There is considerable literature on the closely related problem of scaling laws for impact ionization of K-shell electrons [6]. The basic idea is that there exists an underlying scaling law that depends on a universal function, from which K-shell impact ionization cross sections for many elements can be obtained over a wide range of energies [7].

2.1. Universal function

To proceed, we would like to take advantage of ideas based on the notion that there exists a universal function for alpha particle-impact K-shell ionization. Certainly there is considerable literature both of a theoretical nature as well as experimental devoted to this problem. There are a number of specific universal functions which have been put forth based on different data sets or theoretical models.

For our computations in particular, we have the problem that the data sets which are close to Pd do not go up to high enough energy for our application. Hence our interest is in making an empirical extension of the model in which we used scaled experimental data in the higher energy regime as a way to predict what the cross section would be for Pd.

To proceed, we write

$$U\sigma_{\rm K} \;=\; \omega_{\rm K} f\left(\frac{E}{U}\right), \tag{1}$$

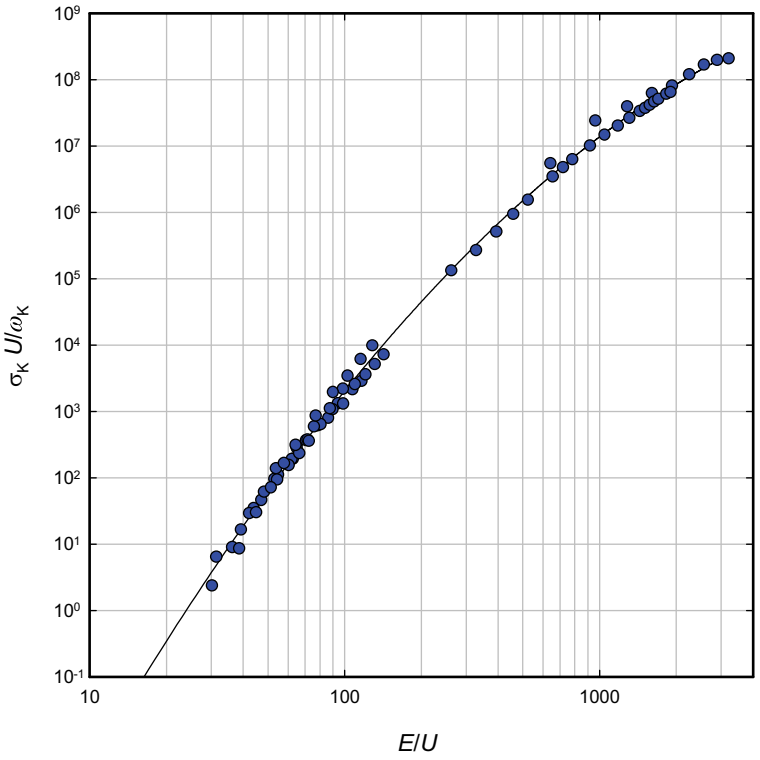

Figure 1. Universal function f (in units of barns-eV) built up from K-shell X-ray production cross sections for collisions with alpha particles.

where f is the presumed universal function, U is the K-shell binding energy and where ω_K is the fluorescence yield.

To determine whether this approach will be helpful given the data sets that we have available, we can plot the data in terms of the universal function according to

$$f\left(\frac{E}{U}\right) \;=\; \frac{U\sigma_K}{\omega_K} \tag{2}$$

as a function of E/U. The results of this are shown in Fig. 1.

2.2. Parameterization

We see that the data seems to describe a universal curve, which we have fit to

$$\ln f \;=\; a + bx + cx^2 \tag{3}$$

with

$$x \;=\; \ln\left(\frac{E}{1\ \mathrm{MeV}}\right) \tag{4}$$

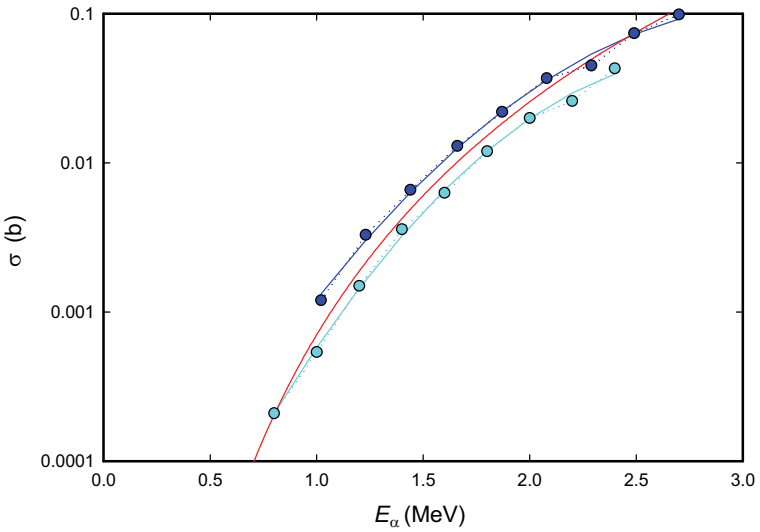

Figure 2. Comparison of the empirical X-ray cross section (red line) and data of Wilson et al. [5] for Rh (upper) and Ag (lower) data.

and

$$a = -22.7185, \qquad b = 8.4285, \qquad c = -0.3995 \tag{5}$$

for f in barns-eV.

2.3. Comparison with experimental results

We compare the empirical model with the data of Wilson et al. [5] in Fig. 2. Taking the Wilson data alone, one might think that the empirical fit was a bit off at both high and low energy. However, since there is reasonable agreement between different data sets (with data taken between Al and Gd) in the construction of the universal function, it seems that our empirical K_α cross section for Pd should be reasonable outside of the range where we have relevant data.

3. Yield of Pd K_α X-rays

We have computed the yield function for alpha particles in Pd (see Fig. 3).

3.1. Experimental result for the yield in Pd

There is an experimental data point available for the yield function of energetic alpha particles from the decay of ^{252}Cf given in a paper by Watson [8]. The yield function is given as $(0.93 \pm 0.08) \times 10^{-2}$ for the associated long range alpha particles in Pd. From the yield curve, we would compute that the associated alpha particle energy should be 15.0 MeV in order to be consistent. The long-range alpha particle energy spectrum for ^{252}Cf has been measured by Fraenkel [9], and one sees that the peak occurs roughly at 15 MeV.

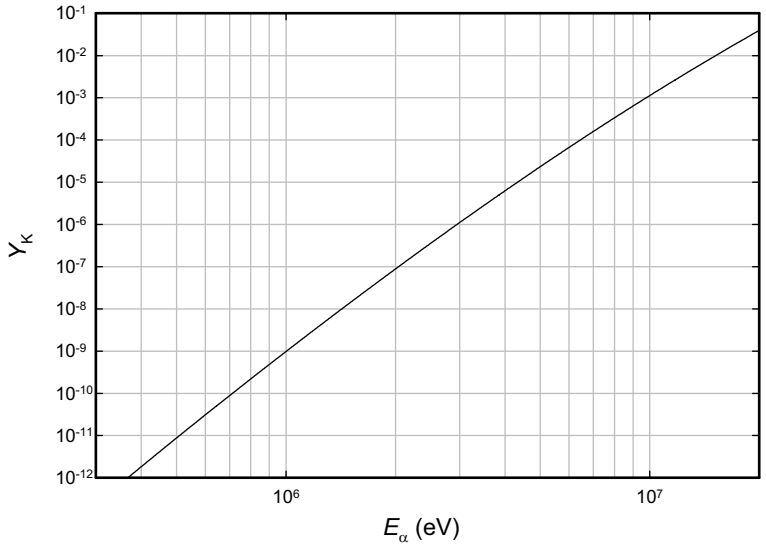

Figure 3. Yield function for Pd K-shell X-ray emission due to energetic alpha particles as a function of alpha particle energy.

3.2. K X-rays per unit energy

In order to compare with experiment, we require a computation of the yield divided by the energy, we require the K-shell X-ray yield divided by the alpha particle energy. This is shown in Fig. 4.

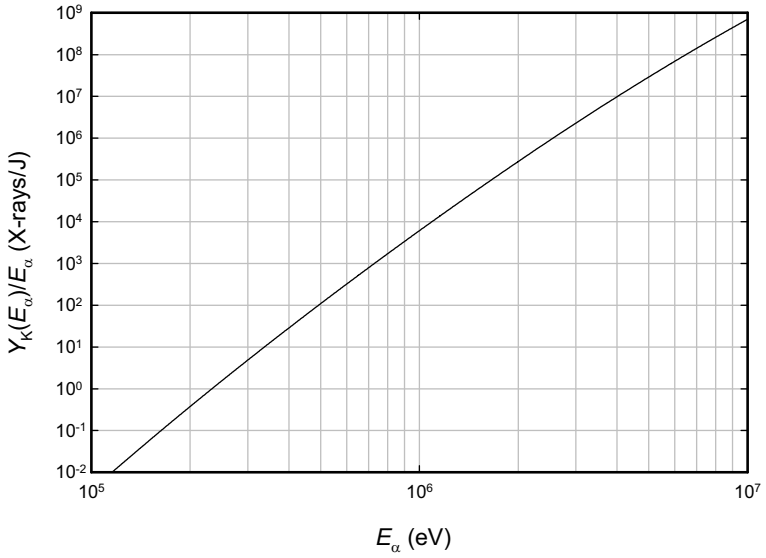

Figure 4. Yield function for K-shell X-rays in Pd produced by energetic alpha particles divided by the alpha particle energy, in X-rays/J.

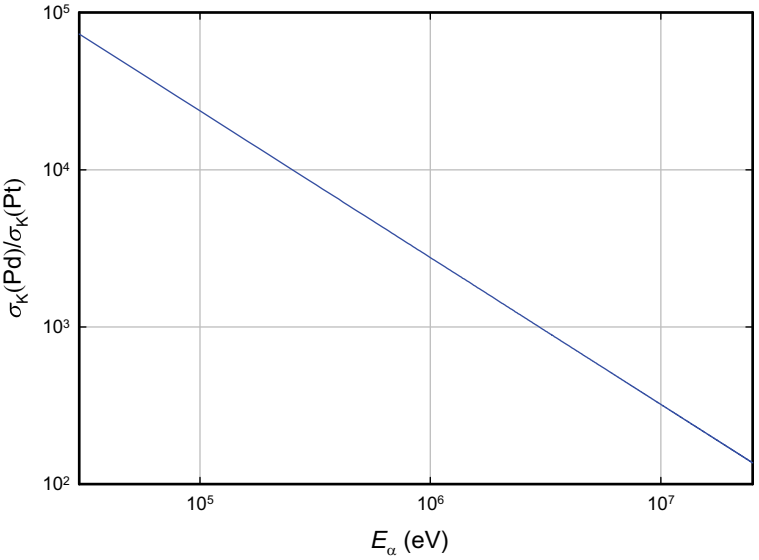

Figure 5. Ratio of K_α production cross sections for Pt relative to Pd as a function of alpha particle energy.

3.3. Ratio of Pd to Pt K_α cross sections

We mentioned above the possibility of gaining information about the alpha particle energy from the ratio of K_α emission from Pt as compared with Pd. There are few experiments where both have been measured at the same time, and the only work we could find reporting such a result was [1].

If we make use of the universal function ideas above, we can estimate the ratio of K-shell emission cross sections using

$$\frac{\sigma_K(\mathrm{Pd})}{\sigma_K(\mathrm{Pt})} = \frac{\omega_K(\mathrm{Pd})}{\omega_K(\mathrm{Pt})}\frac{U_{\mathrm{Pt}}}{U_{\mathrm{Pd}}}\frac{f(E/U_{\mathrm{Pd}})}{f(E/U_{\mathrm{Pt}})}. \tag{6}$$

This ratio is shown in Fig. 5. We see that the cross section for X-ray production is much larger for the lower energy Pd K_α X-ray than for the higher energy Pt K_α X-ray, which is as expected since it is harder to ionize a more tightly bound electron.

3.4. Surface versus bulk effects

The discussion above requires additional comment, since Pt is found only within less than a micron from the outer surface of the Pd cathode. If the alpha particles are born inside of the cathode away from the surface, then one would not expect to see any Pt K_α X-rays. If the alpha particles are born near the cathode surface, then one might expect to see excitation of the Pt K_α, but the ratio of Pd to Pt K_α emission might be expected to be even larger than the ratios found above. In the single experimental measurement that shows both, there is not a big difference in the relative strength, as discussed later on in this work. With Pt restricted to a small region near the surface, the Pd K_α should be favored even more over the Pt K_α than in Fig. 5.

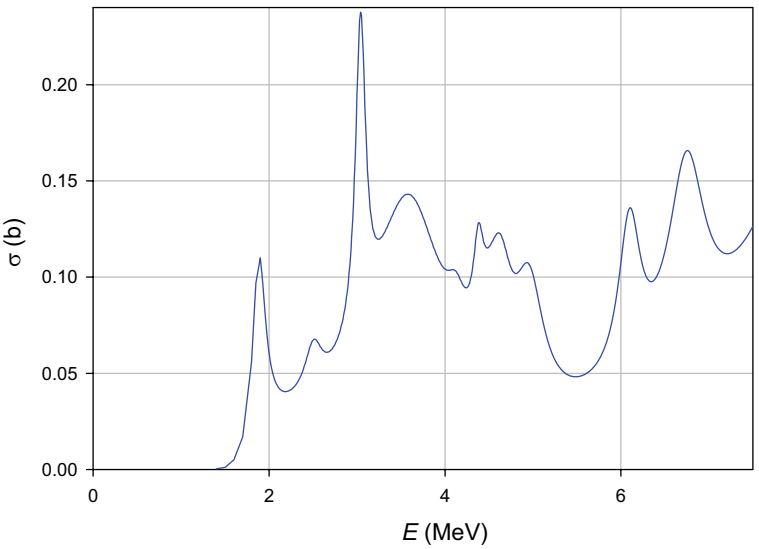

Figure 6. Cross section for ^{7}Li 478 keV gamma production as a function of alpha particle energy.

4. Excitation of the ^{7}Li nuclear state at 478 keV

If energetic alpha particles are present, one would expect to see excitation of nuclear states for low-Z nuclei that have bound excited states. In the Fleischmann–Pons experiment Li appears in the electrolyte, and presents an obvious candidate for possible nuclear excitation. In ^{7}Li the lowest excited state occurs at 478 keV, which makes it the prime candidate for nuclear excitation (other excited states in both ^{6}Li and in ^{7}Li are at significantly higher energy). This state has been the focus of numerous studies over the years precisely for this reason.

4.1. Cross section for gamma production

Because of its special status, the 478 keV gamma line has been studied experimentally in order to determine the gamma production cross section. This is somewhat different than an excitation cross section, as excitation to more highly excited states can lead to the 478 keV state as a product in a decay chain. We have made use of the measurements of Li and Sherr [10], and of Cusson [11]. The cross section is complicated, with more than a dozen resonances apparent. We have made use of the Li and Sherr data at low energy up to the first peak. Above the first peak, we have developed an approximate fit (made up of many resonance terms) to the Cusson measurements. The resulting cross section is shown in Fig. 6.

4.2. Yield function

Lithium is present in the LiOD electrolyte as mentioned above, and it also is incorporated into the outer few thousand Angstroms of the cathode surface [12,13]. We expect the alpha particles to be sourced near the surface, so that there is some possibility of interaction with the Li incorporated into the Pd. However, alpha particles born this close to the surface will also have a 50% probability of going into the electrolyte. The computation of the yield function in the electrolyte is a preferable computation for us (since we need not worry about the profile of the lithium and the trajectory of the alpha particles), and we expect that it will provide the dominant signal under most conditions.

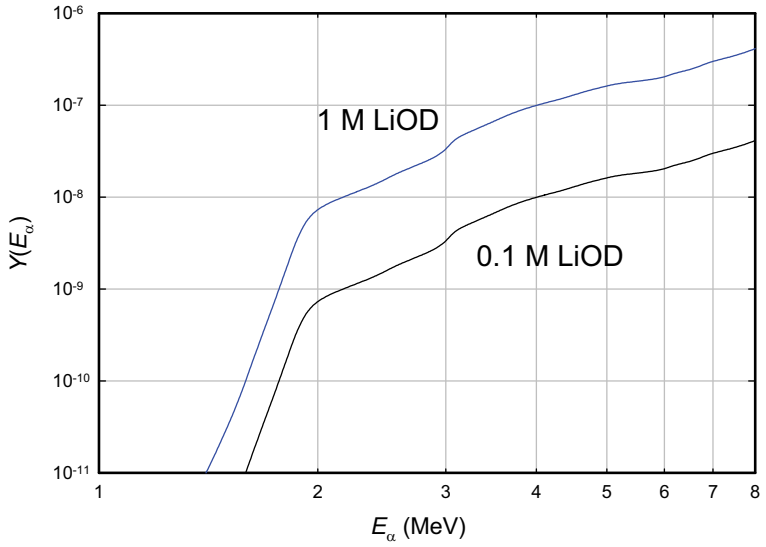

Figure 7. Yield of the ^{7}Li 478 keV gamma production as a function of alpha particle energy.

The resulting yield function for alpha particles slowing down in D_2O are shown in Fig. 7 for 0.1 M and 1.0 M LiOD. For alpha particles of energy greater than 2 MeV, we see that the yields are small, but respectable for this kind of process. Clearly a substantial flux of alpha particles would be required to observe this signal. However, large yields of alpha particles are now being claimed by Storms and Scanlan [14], and by the SPAWAR group [4]. It is probably worthwhile to look for the 478 keV line in these experiments. The associated yield per unit energy is shown in Fig. 8.

5. Discussion and conclusions

In the sections above, we have presented results for cross sections and yields of K_α X-rays and the ^{7}Li 478 keV gamma ray. Given the good accuracy of the stopping power models and cross sections, the resulting yields should be very good.

From these results, some conclusions can be drawn. In regard to ongoing experiments, it would be interesting to monitor the K_α signals and ^{7}Li signal, since they can provide independent information about the flux and energy of energetic particles. Although we have focused on energetic alpha particles here, similar yield functions for the K_α X-rays can be developed easily for other energetic ions. Excitation cross sections for the 478 keV line will be much more difficult to obtain for other light ions. These results also allow us to comment on the experiments showing K_α emission. Although important information about the Bush and Eagleton experiment [1] is not included in the write up, if we assume that the Rh, Pd and Ag K_α spectrum were taken in the same run as the Pt K_α spectrum, then we can be sure that these signals were not due to energetic alpha particle impact ionization. The reason for this is that the signal strength of the Pt appears to be comparable to that of Pd, which is inconsistent with what would be expected from alpha particle impact ionization (even if there were as much Pt as Pd available near the surface). Since the X-ray detection in this experiment has a relatively low resolution, there can be questions as to whether the signals are actually due to the K_α lines.

The presence of the Rh K_α line at similar strength to the Ag K_α line is very hard to account for in this experiment since the cathode was a PdAg alloy. In any event, we will need a confirmation of this experiment before we can be sure of our conclusions. In future investigations of K_α emission it will be important to use a high resolution detector so that

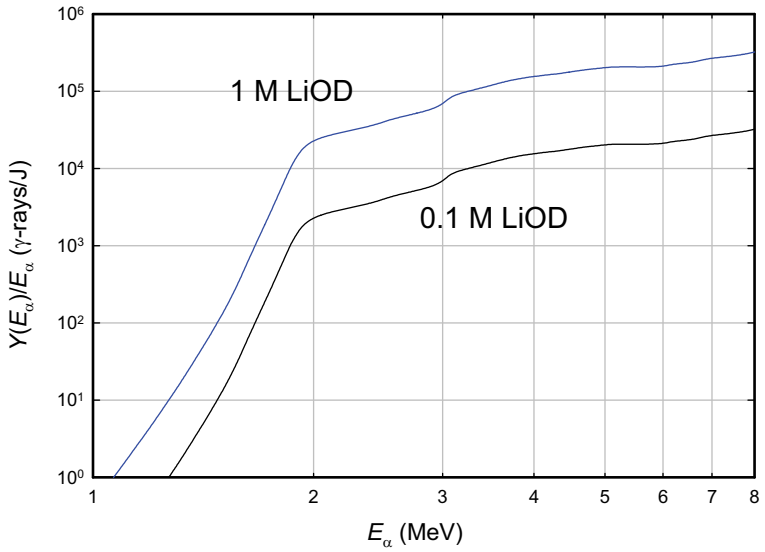

Figure 8. Yield of the ^{7}Li 478 keV gamma production divided by energy as a function of alpha particle energy.

the K_α and K_β lines can be resolved, so that we might have more confidence in the results.

Also of interest is the spectrum presented by Iwamura et al. [2], which shows clearly a dominant Pt K_α signal, but no 478 keV line. If produced by energetic alpha particles, probably the alpha particles would need to have an energy well above 2 MeV. Since there is no correlation with neutron emission, which was also measured, we are sure from other calculations that the Pt K_α signal is not associated with energetic alpha particle emission.

We draw attention to an earlier publication which contains a brief summary of these and earlier results [15].

References

[1] R. T. Bush and R. D. Eagleton, *Proc. ICCF3* 409 (1993).
[2] Y. Iwamura, N. Gotoh, T. Itoh and I. Toyoda, P̂roc. ICCF5, p. 197 (1995).
[3] A. G. Lipson, G. H. Miley, A. S. Roussetski and E. I. Saunin, *Proc. ICCF3*, p. 539 (2003).
[4] P. Mosier-Boss and L. P. G. Forsley, *Bull. APS* paper BAPS.2008.MAR.A17.10 (2008).
[5] S. R. Wilson, F. D. McDaniel, J. R. Rowe and J. L. Duggan, *Phys. Rev. A* **16** (1977) 903.
[6] J. D. Garcia, *Phys. Rev. A* **4** (1971) 955.
[7] G. Basbas, W. Brandt and R. Laubert, *Phys. Rev. A* **7** (1973) 983.
[8] R. L. Watson, *Phys. Rev.* **179** (1969) 1109.
[9] Z. Fraenkel, *Phys. Rev.* **156** (1967) 1283.
[10] C. W. Li and R. Sherr, *Phys. Rev.* **96** (1954) 389.
[11] R. Y. Cusson, *A study of the elastic and inelastic scattering of alpha particles by lithium-7*, CalTech Ph.D. Thesis (1965).
[12] O. Yamazaki, H. Yoshitake, N. Kamiya, K. Ota, *J. Electroanal. Chem.* **390** (1995) 127.
[13] H. Uchida, M. Sato, W. Cui, T. Tabata, M. Kumagai, H. Takano and T. Kondo, *J. Alloys and Compounds* **293–295** (1999) 30.
[14] E. Storms and B. Scanlan, presented at ICCF15.
[15] P. Hagelstein, *Naturwissenschaften* **97** (2010) 345.

J. Condensed Matter Nucl. Sci. 3 (2010) 59–76

Research Article

Terahertz difference frequency response of PdD in two-laser experiments

Peter L. Hagelstein*
Research Laboratory of Electronics, Massachusetts Institute of Technology, Cambridge, MA 02139, USA

D. Letts
12015 Ladrido Lane, Austin, TX 78727, USA

D. Cravens
Ambridge University, Cloudcroft, NM 88317, USA

Abstract

The cell responded to three difference frequencies in the THz range at 8.2 THz, at 15.1 THz, and at 20.8 THz. The first two of these frequencies can be associated with optical phonon frequencies of PdD with zero velocity. We examine the conjectures that the response at 20.8 THz is due to deuterium in vacancies in the gold coating, or due to hydrogen contamination.

Keywords: Fleischmann–Pons experiment, 2-Laser stimulation, Optical phonon modes, THz difference frequency

1. Introduction

It is probable that there has not been a more contentious issue in science over the last 20 years than the issue of the thermal response that has been claimed in experiments with Pd cathodes electrolyzed in heavy water. In this work, we describe results that we obtained in our experiments where we observed a version of the effect that seems to respond to the frequency difference between two weak lasers. The difference frequency in these experiments was in the terahertz regime, and the thermal response that we see appears to be correlated with characteristic frequencies associated with optical phonon modes.

*E-mail: plh@mit.edu

Before proceeding, we need to give some account of what has gone on previously (at least from our perspective) in order to place the research under discussion in context. Experiments that seemed to show a large thermal effect for Pd cathodes in D_2O:LiOD were first described by Fleischmann and Pons in 1989 [1,2]. There were many attempts to replicate the experiment that followed shortly after the announcement [3,4], with the near-uniform result that no anomalous thermal effect was observed. In addition, strong arguments were made as to the impossibility of the claimed effects. Most physicists today consider the basic experiment to be irreproducible and the claimed effect impossible, which together constitutes reason to believe that the initial experiments showing a thermal effect were in error.

Some of those continuing to work on the Fleischmann–Pons experiment have argued that these early negative results need to be reconsidered in light of subsequent experimentation. According to this point of view, the basic Fleischmann–Pons experiment was poorly understood in 1989 when many of these early experiments were done and the success rate in Fleischmann and Pons' own experiments at that time was low.

In work carried out in the early 1990s at SRI, thermal effects were observed, and an attempt was made to correlate observations of excess power with the cathode loading (D/Pd ratio), current density, and other observables. It was found in these experiments that the cathodes which showed the effect had reached a very high loading (D/Pd = 0.95) early on, and that generally no effect was observed until about a month into the experiment in the case of cathodes that had maintained a high loading [5]. Further, a correlation was noticed between the amount of excess power produced during an event and the cathode loading during the event; significant excess power was higher for higher loading, with no effects seen at a loading below about 0.83 [6].

Some effort has been devoted to understanding the early negative results in light of the criteria derived from these early SRI experiments. As an example, in very few of the early negative results was any effort reported to monitor the loading, since at that time the loading was not generally considered to be an important variable to be controlled in the experiment. In the few cases where estimates were given (such as in [3]), the loading was well below that required to see the thermal effect. From this point of view, most of these early negative results are probably not relevant to the question of the thermal effect in the Fleischmann–Pons experiment, since essentially none of them were carried out in a relevant experimental regime. This reflects the general level of understanding of the experiment in 1989 when most of these early experiments were done (which was poor), rather than on the quality of the experiments or experimentalists (many of whom were very good).

In light of these comments, the most important negative result is that of Green and Quickenden [7]. High D/Pd ratios were reported in this work, consistent with the loadings in the SRI experiments where half or more of the cathodes were seen to give a thermal effect. Why the cathodes in these experiments gave no excess heat is not immediately clear. The protocol adopted in these experiments was different than in the SRI experiments, where current steps were used (rather than current ramps in the SRI experiments), and the maximum current density used was 300 mA/cm^2 (which is on the order of the threshold current density for some of the SRI experiments). In the SRI experiments, a correlation between excess power and deuterium flux has been observed; a current ramp gives a more sustained flux, which may be important. The duration of the SRI experiments tended to be longer (two months compared to one) than those of Green and Quickenden, which may be relevant given the late onset of excess power in the SRI experiments.

From the earliest days following the Fleischmann–Pons announcement, arguments have been made that the thermal effect itself is rather small; hence, there was good reason to believe that the thermal effect could be attributed to measurement error. Once again, this perception has persisted now for more than 20 years, and is presently widely accepted within the physics community. According to Huizenga, it is the total energy which is important, rather than measurements of the excess power seen during a thermal event [4]. From this point of view, a thermal event in which excess power is observed at levels commensurate with the input power should not be considered relevant. Instead, the total energy associated with the thermal event (which might last 10 h) needs to be weighed against the total energy put into the cell since the start of the experiment (which might be 6 weeks). So, in this way an effect which was considered by the experimentalists to be significant (a 100% power excess) thermal event, could be turned into an insignificant

(1% energy excess) thermal event, which Huizenga could then argue was not within the measurement capability of the calorimeter involved.

We draw attention to the measurements described in [2] in which more than 4 MJ of energy was observed over 80 h from a Pd cathode with a volume of 0.157 cm^3. Huizenga's stated concern was that it is possible that some unknown storage mechanism might be present, so that one could not be certain that net energy was produced. Although he did not specify what storage mechanisms he had in mind, if energy storage were to occur somehow in the cathode for this example, it would need to store about 60 MJ/cm^3; in our view this would constitute a remarkable effect in its own right worthy of study. The calorimetric approach which was pioneered by Fleischmann and Pons in association with these experiments was shown to give power balance to within about 0.1 mW in the case of a Pt cathode (which shows no thermal effect) [8].

There are by now numerous publications of observations of excess power in the Fleischmann–Pons experiment in the literature [9,10]. A large number of these are discussed in the review of [11]. Although we reject Huizenga's argument that only the energy gain should be considered in regard to the thermal effect, we draw attention to the observations of the Energetics group over the past several years; large thermal events have been reported in which the energy gain computed from the start of the experiment reached 2500% [12].

We see the thermal effect in our experiments. Our protocol is different from the Fleischmann–Pons protocol, so that an experiment can be done in a week rather than in 6 weeks. In earlier related experiments, the cell was seen to respond to the illumination of the cathode surface with a single weak diode laser [13,14] . Excess power at the level of a few hundred milliwatts was seen with laser illumination with mW lasers. This effect was confirmed at other laboratories [15–18]. In the new experiments two lasers are used under conditions where a single laser is unable to produce a response, so that both together trigger a thermal response when both are p-polarized, and when the beams overlap. The response is seen to depend on the difference frequency, which is in the THz regime in these experiments.

Why there should be a thermal effect in any of these experiments is not understood at present. However, it is clear that whatever physical process is responsible is unlike other condensed matter or nuclear processes that we are familiar with. To learn about the new effect, many experiments are going to have to be done to sort out how it works one issue at a time. The results reported here should be thought of as one such step.

2. Overview of Experiment

The experiment under discussion is an electrochemical cell with a Pd cathode and Pt anode in D_2O with 0.5 M LiOD (see Fig. 1). The cathode is loaded at low current (0.050 A) for 120 h, prior to the deposition of a gold coating and commencement of the thermal experiments at higher current (1.25–1.5 A).

2.1. Outline of calorimetry

Temperature measurements from inside and outside the cell are used in connection with Fick's law in steady state to estimate the thermal output power

$$P_{\rm out} \;=\; K\,\Delta T. \tag{1}$$

The input power is taken to be the electrical power minus the contribution of the thermoneutral potential

$$P_{\rm in} \;=\; I(V - V_0). \tag{2}$$

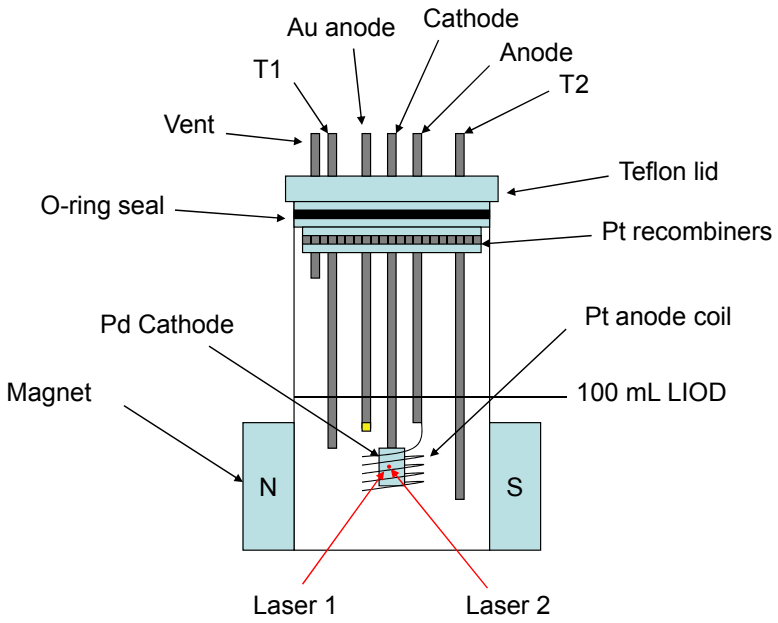

Figure 1. Schematic of the experimental set-up.

The cell is closed in the sense that the D_2 and O_2 generated by the electrochemistry are recombined at the top of the cell; however, the heat generated during the recombination is poorly coupled back to the electrolyte. The excess power is estimated from

$$P_{\rm xs} \;=\; P_{\rm out} - P_{\rm in}. \tag{3}$$

The calibration constant K is determined by running until steady state is reached prior to turning on the lasers (assuming no excess power); a check is made by running in steady state at the end of the experiment (again assuming no excess power). An example showing input and output power during a calibration run is shown in Fig. 2.

An extended discussion of related experimental issues is given in the Appendices.

2.2. Suppression of spontaneous excess power bursts

Over the years in working with these cells, we have gotten a sense of how they respond to dual laser stimulation. In previous experiments at other laboratories, it was noticed that the excess power in the Fleischmann–Pons experiment responds to current density, such that the excess power is seen to increase roughly linearly above a threshold (which occurs in the general vicinity of 200–400 mA/cm for Pd rods [6]). As a result, the current density in this experiment provides for a way to control the response of the system, much like the knob on an amplifier controls how loud music is played. Our goal was to run the system just below threshold for spontaneous bursts of excess power (in order to suppress them), so that we might be able to see more clearly the response of the system to laser stimulation. As the cathode area is about 1 cm^2 including front and back, the associated current density is about 1 A/cm^2; which is "low" for this experiment in the sense above.

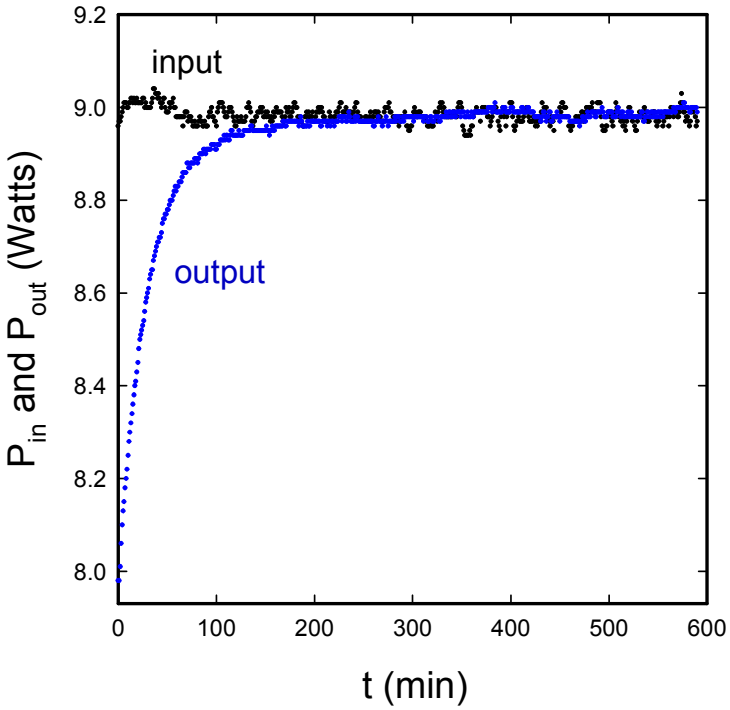

Figure 2. Measured input and output powers (W) as a function of time (min). The error in the output power points is about 10 mW; the error for the input power points is much less.

A similar control is available in the operating temperature of the cell. Once a cell produces excess heat, often more excess heat can be seen if the cell temperature is increased. Of the operating temperatures available to us, we have purposely selected a lower operating temperature, again in order to help suppress unwanted spontaneous events.

3. Results

The primary result from this set of experiments is a spectrum of the excess power response as a function of difference frequency. To understand the significance of this spectrum, we need some explanation of how individual data points were obtained.

3.1. Thermal response

The construction of an accurate spectrum requires a degree of control which is probably beyond the current capability of any laboratory currently pursuing excess power in the Fleischmann–Pons experiment. We make no such claims here for our experiments. Nevertheless, our system has responded in a very reproducible way to the difference frequency between the two lasers, and this very much seems to be a real effect. As such, the effect can be quantified. We can

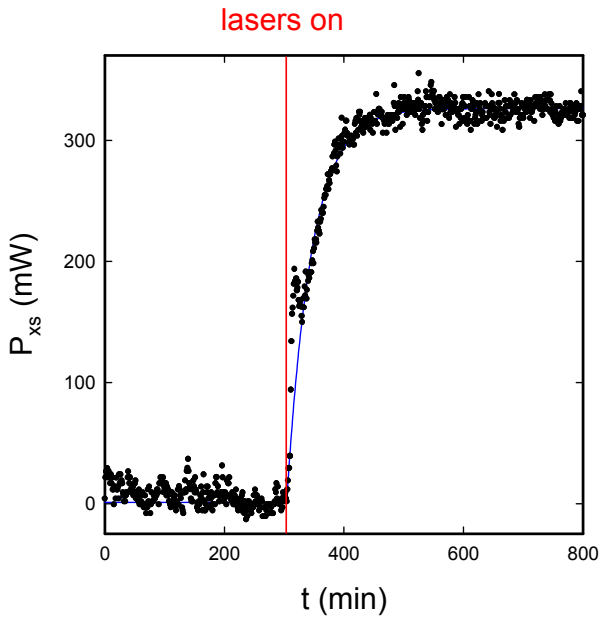

Figure 3. Excess power (mW) as a function of relative time (min) for parts of data set 662N2 and 662O2 (circles), along with a best fit relaxation model (curve). Two lasers were turned on between time 303 and 304, as indicated by the vertical line. The difference frequency is 20.66 THz.

measure the thermal response of the system in many experiments, and the difference frequency is available in these experiments. It seems clear that there is a thermal response in many of the experiments, and we have used simple relaxation models combined with a statistical analysis to quantify the excess power.

We consider in Fig. 3 one of the better examples of how this works. Before the relative $t = 0$ of this figure, the cell was charged at low current density for a great many hours; a few hours before $t = 0$, the current was run up to about 1 A/cm^2, and the cell temperature was allowed to come to a steady state. Between minute 303 and 304, the two lasers were turned on, with a difference frequency of 20.66 THz. The excess power computed using the steady state calorimetry discussed above is seen to approach a constant power by about $t = 500$ min. The apparent excess power for this run as determined from a statistical fit to a simple relaxation model

$$P_{\rm xs} \;=\; A + B\,\left(1 - {\rm e}^{-(t-t_0)/\tau}\right) \tag{4}$$

(and shown in Fig. 3) is 336 $\pm$ 8 mW. This value must be corrected to take into account the absorbed laser power (measured to be about 15 mW in other experiments), reducing it to 321 $\pm$ 8 mW.

One can see a rapid transient in the data, which peaks at $t = 320$ min. This is the response of the system to a sudden drop in cell voltage (which we have verified), which occurs in some of our experiments as a precursor to the onset of excess heat. The cell is run in a constant current mode from minute to minute, with the current set each minute to keep the power constant. When the cell voltage drops (and consequently the effective cell resistance drops), the electrical input power is a bit low, which leads to a transient difference between the output power (which changes slowly) and the input power (which is low transiently). In other experiments where excess heat is observed, such precursors are

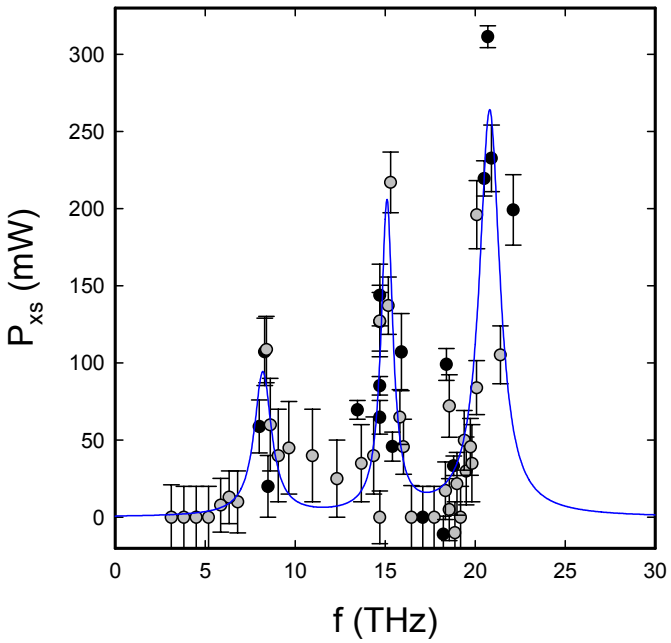

Figure 4. Excess power (mW) as a function of difference frequency (THz). Data from step results as in Fig. 3 are in black; data from scans are in grey. Best fit of three Lorentzians shown as a solid line.

sometimes seen [19]. In [20] there is an example of this where a sudden drop in the cell voltage preceeds an excess power burst. A precursor can be seen in the excess power data of McKubre et al. [21]. Why the cell voltage drops is not known. It may be due to a change in the electrolyte conductivity, to a change in the over-potential of the cathode surface, or to significant change of the cathode surface temperature. It is probably easiest to measure the electrolyte conductivity directly to help clarify this, although we have not done this yet. Of interest is the possibility that the change is a surface effect connected with low-level energetic particle emission.

In this example, the system is seen to respond to the laser stimulation, starting from an initial condition of no excess power. The excess power following laser stimulation approaches nearly a constant value which we can determine by reference to a relaxation curve. There are 18 data sets of this type from the experiments. In addition, there are experiments in which the frequency was changed several times, leading to excess power at different levels which appeared to correlate with the difference frequency. We have 37 excess power points obtained from these runs. For this data, we were able to compare the data against relaxation models in order to estimate the associated steady state excess power levels and standard deviations. In both cases the spread in excess power was similar, with values between 6 and 20 mW; in a few of the runs there are noticeable fluctuations in the excess power when high, and in some other runs the cathodes just seem to produce more noise. We note that there is a difference in the response generally observed from the different cathodes used to make up the spectrum. In some cases there is a slow drift in the calibration; consequently, we

have added 10 mW systematically to the uncertainty for the data obtained from the scans since they are more sensitive to this drift.

Given these issues, as well as others that have not been discussed here, the spectrum that results should be regarded as preliminary. Where strong responses are observed, the confidence is highest; but more work is needed in order to clarify the response away from the peaks (the region most in need of such study is the region between 10 and 13 THz). However, as these experiments take a great deal of time and effort, a decision was made to present the data that we have so far as a preliminary result.

3.2. Spectrum

The spectrum that results from using this approach in a large number of experiments is shown in Fig. 4. The spectrum appears to show three peaks near 8, 15 and 20 THz, which correspond to difference frequencies that we found in earlier experiments to give the best results. Due to constraints imposed by the lasers that we used, we were unable in these experiments to perform tests above 22.11 THz. We have constructed a least-squares fit to the the data points using a sum of three Lorentzians according to

$$P_{\rm xs}(f) \;=\; \sum_j A_j \frac{\gamma_j^2}{(f-f_j)^2+\gamma_j^2}, \tag{5}$$

where f is the difference frequency, A_j are the amplitudes, f_j the center frequencies, and γ_j are the width parameters. The fitting parameters that correspond to center frequencies and widths are given in Table 1. We have included the associated quality factor Q_j defined in terms of the fitting parameters according to

$$Q_j \;=\; \frac{f_j}{\gamma_j}. \tag{6}$$

The line width of the 8.2 THz in the excess power spectrum is comparable to the 295 K line width near 9 THz measured in the coherent neutron scattering experiment of Rowe et al. [22]. We have not found comparable results to compare with the other peaks, which have larger quality factors in the excess power spectrum.

In this analysis, we have omitted one outlier data point at 14.75 THz where a response of 521 mW was observed; inclusion of this data point results in an increase of the amplitude of the middle Lorentzian by about 70 mW, but little change of the f_j or γ_j parameters. We have some data points from a scan between 10 and 13 THz, where the excess power was close to zero, but these were not included because there was not a significant positive response at any of the scanned frequencies, which weakens the significance of the data.

We note that the fitting parameters obtained in this model-based statistical analysis are very close to the fitting parameters we obtained previously [23] based on a simple assignment of excess power numbers.

Table 1. Center frequency, width, and quality parameters for the excess power spectrum

f_j(THz)	γ_j (THz)	Q_j
8.2	0.58	14
15.1	0.39	39
20.8	0.69	30

4. Discussion

These results are interesting for a number of reasons. There are the very practical issues that allow such an experiment to be done at all, and the perhaps unexpected result that the cathode seems to be able to respond to a difference frequency, even though the laser intensity is very low. Finally, there is the important question of the interpretation of these results.

4.1. Practical issues

Before a consideration of what the spectrum means, it seems useful to consider some practical issues associated with the experiments. In earlier single laser experiments, the excess power seemed to be similar once initiated, over about a factor of 50 in incident beam power. Hence, the concept of a threshold intensity for the effect seems to be relevant, with a threshold intensity in the general vicinity of 1 mW/cm^2. In different experiments, the same cathode was observed to respond when the beam was defocused to 1 cm diameter at a power level about 50% higher than when the beam was focused to 1 mm. This suggests that when the smaller beam is used, that an area larger than the beam responds, if we assume that the power produced per unit area is similar in the two cases.

All of these seem to be helpful in a practical sense over the course of the measurements. A relative insensitivity to the laser spot size and intensity of the lasers in these experiments is likely to have contributed to the quality of the resulting spectrum.

4.2. Response to the difference frequency

Under normal conditions, we would not expect the production of difference frequencies for optical laser light at the relatively low intensity of the light in this experiment. The intensity corresponding to the initial 30 mW beam power of a single laser focused to 1 mm diameter is about 4 W/cm^2.

One plausible route for the development of a nonlinearity is to assume that the co-deposition of the gold results in irregular structures on the nano scale, so that a dramatic field enhancement occurs similar to the situation in surface enhanced Raman scattering [24–26]. In this picture, a large enhancement of the local electric fields results in strong excitation of local hybrid plasmon and optical phonon modes, allowing mixing at the difference frequency. In our experiments, we do not see a response at the difference frequency without gold co-deposition.

We know from single laser experiments that excess power is produced. If we think of a laser amplifier as an analogy, then the amplifier tends to put energy into modes that have the highest excitation. In single laser experiments with the Fleischmann–Pons effect, such an analogy would suggest that the energy produced is going into the excited hybrid plasmon and optical phonon modes stimulated by the laser. These modes are very lossy, so that when the laser is turned off, the excess power effect is not sustained. In the two-laser experiments, the excess power often remains after the lasers are turned off. The associated picture is that energy is going into these modes at a sufficient rate to sustain them, since they are at lower frequency and much less lossy.

4.3. PdD Optical phonon modes

Since the thermal signal responds to difference frequencies in the THz region, it would be natural to make a connection with the relevant phonon mode spectrum in this region. In Fig. 5, we have plotted the dispersion curves for the acoustical and optical phonon modes for the high symmetry directions in the Brillouin zone, using the Born-von Kármán fitting parameters of Rahman et al. [27] with the modification for the D–D interactions of Sansores et al. [28].

The lowest optical phonon frequency (8.57 THz) in the model occurs in the [1 1 0] direction, while the lowest points in the coherent neutron scattering experiments of Rowe et al. [22] for $PdD_{0.63}$, and Blaschko et al. [29] for $PdD_{0.78}$ are in the [1 0 0] direction, where the lowest model frequency is 8.58 THz. The loading in our experiments

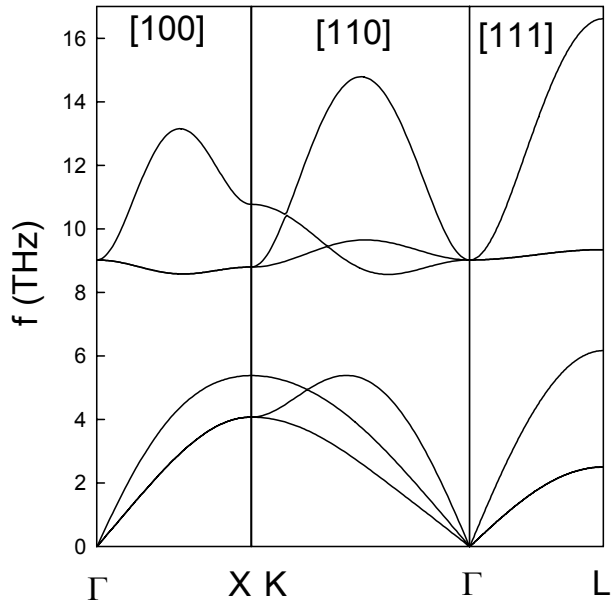

Figure 5. Phonon mode dispersion relation for PdD. Frequency in THz as a function of **k** for high symmetry directions in the Brillouin zone.

was not measured, but in other experiments where the loading was measured, excess heat usually does not appear until the loading is near 0.83 [6]. These lowest frequencies are for transverse modes; the lowest longitudinal optical phonon frequency occurs at the Γ-point, which in the model occurs at 9.02 THz. Both coherent neutron scattering experiments [22,29] agree in this case, but in [30] the Γ-point is observed in $PdD_{0.63}$ at 8.1 THz at 80 K.

The group velocity is zero at this minimum, and also at the Γ-point. In the associated microscopic picture, the energy put locally into optical phonon modes with a finite group velocity would tend to transport away, while it would remain if the group velocity is zero. Given that there are numerous modes at different frequencies, it seems noteworthy that the thermal response in these experiments seems not only connected with the optical phonon modes, but those with zero group velocity.

A similar connection seems plausible between the thermal response at 15.1 THz and the longitudinal optical phonon mode at the L-point, which in the Born-von Kármán model occurs at 16.6 THz. Note that the model seems to be high relative to the L-point experimental data; which in the experiment of Rowe et al. [22] seems to be closer to 16 THz; and in the experiment of Blaschko et al. [29] seems to be closer to 15 THz. As has been emphasized by the ENEA Frascati group [18], the coupling of p-polarized light is with longitudinal plasmon modes, which we would expect to be hybridized with the optical phonon modes. The high frequency optical phonon mode at the L-point is a longitudinal mode, and once again the group velocity is zero at this point.

4.4. Possibility of deuterium in vacancies in gold

There are no optical phonon modes in PdD near 20.8 THz, which is the difference frequency associated with the third peak in the excess power spectrum shown above. A possible explanation is that the response is due to optical phonons associated with deuterium in gold. Since the solubility of deuterium in gold is low, this perhaps would not be a first choice for an explanation. However, since the gold co-deposition may produce a large fraction of vacancies (as has been verified for Cu and Ni [31]), perhaps this is a possibility. The importance of vacancies in supporting regions of low electron density where molecular D_2 can bind has been discussed recently in [32]. Unfortunately, there there are no studies of hydrogen or deuterium in gold from which we can quantify the optical phonon spectrum.

Recent preliminary results by one of the authors (DL) with gold co-deposition on copper suggests that the co-deposited gold can produce a thermal response. If confirmed, then this would suggest that the issue of deuterium in gold should be pursued in the two-laser experiment.

4.5. Possibility of hydrogen contamination

A possible explanation for the response near 20.8 THz may be hydrogen contamination. We would expect some hydrogen contamination in the heavy water, the effect of which would be exacerbated by about an order of magnitude in palladium since the solubility of H in Pd is higher than the solubility of D (see the absorption isotherms of [33] in the beta phase region). The frequency of the longitudinal optical phonon mode at the L-point in PdH is about 20 THz, which seems encouraging.

In order to investigate further, we have run Born-von Kármán calculations for an idealized mixed crystal lattice with one deuterium atom in four replaced by a hydrogen atom (which would correspond to less than 3% contamination of light water in the electrolyte). If we make use of the force constants appropriate for PdD (since D is dominant), then we compute the frequency of the highest frequency longitudinal mode at the L-point to be 19.7 THz, which seems to compare favorably with the 20.8 THz response seen in the excess power spectrum.

It may be possible to clarify this issue in future experiments with reduced H contamination. If the thermal response is reduced or eliminated in cells that are relatively free of hydrogen, then this would support the conjecture that H is responsible for the 20.8 THz signal.

5. Conclusions

The thermal response in the Fleischmann–Pons effect has been sufficiently controversial over the years that much of the discussion has been focused on the question of whether the effect is real, or experimental error. Much less effort has been devoted to more general issues having to do with how it works; and the question of why it works has historically been relegated largely to speculation. In the experiments described here, we have found that the excess power depends on the difference between the optical frequencies of two lasers, which provides a new tool which can be used to gain information about the system that was previously unavailable. The spectrum that results suggests that optical phonon modes participate in our experiments.

Perhaps the most important feature of the excess heat in the Fleischmann–Pons experiment is that a very large amount of energy is produced (far in excess of what is possible from chemical reactions), yet no commensurate energetic particles are observed [34]. Energetic particles are observed at very low levels (more than 10 orders of magnitude below that required to be commensurate with the energy produced) under lower current density conditions where excess power would not be expected [35].

So, where does the energy go? For years it has been conjectured that the energy goes into low energy degrees of freedom associated with the solid, such as plasmon or optical phonon modes, prior to thermalization. In the experiments discussed in this work, there is indirect evidence that the energy produced is going into the optical phonon modes. The

dependence on the difference frequency signals the presence of a nonlinearity, which is not understood at present. The persistence of the the excess power after the lasers are turned off (an effect not typically associated with single laser experiments) suggests that the optical phonon modes are being sustained by the energy source.

Appendix

A.1. Electrochemical Issues

The experimental results discussed in this paper came from 20 tests conducted on three electrochemical cells using lithium deuteroxide as electrolyte and palladium cathodes. The experiments began in March 2007 and paused in May 2007, resuming in April 2008 and continue to the present. All experiments were conducted in Austin, Texas using the experimental setup shown in Fig. 1.

A.1.1 Cells

The cells used were 200 ml capacity Kimax electrochemical cells, stock number 14020 and made of borosilicate glass. The cells were approximately 11 cm tall and 6 cm in diameter. The cells were fitted with a Teflon plug which made an airtight seal, using a standard #127 Buna O-ring as shown schematically in Fig. 1. A 2 mm groove was cut below the O-ring seal to hold the recombiner catalyst (see Fig. 1).

The cells were equipped with 5 mm glass tubing that served as electrode holders and O-ring sealable pass-throughs for hook up wires and thermistors. A vent tube was open to the atmosphere and provided pressure relief in the event of recombiner failure. The cells were also equipped with a second anode, which could be connected to the positive side of the electrolysis power supply using a solid state relay. The second anode, when activated, provided for in-situ plating of gold onto the cathode during electrolysis.

The cell lid is machined Teflon, sealed using rubber O-rings. The electrode holders are 5 mm diameter soft glass tubing obtained from Richland Glass. The end of the glass tubing in the electrolyte is sealed against a platinum hook-up wire to provide mechanical stability and to keep the cell sealed. The tubing end outside of the cell is sealed with a commercial epoxy.

A.1.2. Cathode

The cathodes were all bulk palladium and were typically 5 mm $\times$ 12 mm $\times$ 0.20 mm of 0.999 purity. Our sources for the anode and cathode material vary but Alfa-Aesar and Metallium are two commonly used vendors. The cathode fabrication process is as follows: cut 10 mm $\times$ 5 mm $\times$ 0.5 mm billet from 10 mm $\times$ 10 mm $\times$ 10 mm source; polish to bright using a Dremel brush with aluminum oxide; rinse in tap water; heat in furnace to 750°C for 3 h, then cool slowly (4–8 h); etch with aqua regia for 2 min at 100°C; polish with Dremel metal brush with aluminum oxide; polish with Dremel fiber brush with aluminum oxide; ultrasonic clean for 5 min in tap water; anneal for 2.5 h at 850°C; polish with Dremel metal brush (Nicksand); ultrasonic clean for 5 min using compound remover; cold roll to about 0.25 mm, turning sample 90° on each of four passes; polish with Dremel metal brush; ultrasonic clean for 5 min using compound remover; anneal for 2.5 h at 850°C; etch with aqua regia for 2 min at 100°C; rinse in distilled water.

A.1.3. Anode

The anodes were all coils of 0.999 pure Pt wire obtained from Alfa Aesar, with a wire anode diameter of 0.5 mm, and

with four turns over the cathode.

A.1.4. Electrolyte

All experiments were conducted using 100 ml of D_2O with 0.5 M LiOD. Heavy water was obtained from Sigma Aldrich, 99.9 atom% D, stock number 151882-500g, batch 05512EE. Lithium granules were also obtained from Sigma Aldrich, 99.9+%, stock number 499811-25g, batch 02313TC.

A.1.5. Recombiner

All cells were run in a closed cell configuration. The gasses produced were recombined using small platinum coated pellets. The pellets were obtained from Alfa Aesar, 0.5% Pt on 1/8 inch Alumina, stock number 89106, lot B17Q15.

A.1.6. Loading

Cell No. 662 is typical for this series of experiments. It was loaded for 120 h at 0.05 A. The loading ratio was not measured during the experiment but our experience has shown that loading in this manner usually results in a cathode that will respond to single or dual laser stimulation. After the cathode is loaded at low current, we increase current to 1 A for 24–48 h before plating gold on the cathode.

A.1.7. Gold coating

In previous work it was observed that adding a thin layer of gold electrochemically to the surface was required in order to see a thermal response in single laser experiments [13]. To the upper left of the cathode (see Fig. 1), is an electrode holder with a small piece of 0.999 purity gold attached to a platinum hookup wire. In our experiments, the gold plating occurs following the initial 120 h charging period. This was done by adding the Au anode in parallel to the Pt anode, and running for a shorter time at a high current density (usually at 1 amp). As yet we have not determined how much gold ends up on the surface, but in our experiments we deposit gold until the cathode surface has turned dark.

What the gold coating does is not understood at present. Electrochemical deposition on a rough surface would not be expected to result in a uniform layer, and initial observations at NRL support this. Gold clusters on mica show a broad plasmon absorption feature near 2.5 eV in electron energy loss spectra [24,36], and it is possible that this helps in the absorption of the laser light. If there is separation on the nanoscale, one might expect field enhancements characteristic of surface enhanced Raman scattering [24]. The gold may also inhibit cathode deloading.

A.1.8. Power

Power to the electrolytic cell and the controlled temperature enclosure is provided by twin HP digital power supplies, model number E3632A. The power supplies can provide low ripple DC in constant current or constant voltage mode from 0 to 7 A, 0–30 V over two power ranges. Labview controls the power supplies and the electrolysis cell is run in constant power mode, with the power supply set in constant current mode. Cell power is controlled to within ± 0.01W.

A.2. Calorimetric Issues

Simple Fick's law calorimetry as described in the text was used on all tests, consistent with the set-up illustrated

in Fig. 1.

A.2.1. Temperature measurements

Two Beta Therm thermistors were used to measure cell temperature in two locations within the cell — one slightly above the cathode and one slightly below the cathode. The manufacturer provided thermistor calibration constants. The cells were not mechanically stirred; however, the mixing efficiency is reflected by the low temperature gradient between the two probes — typically 0.1°C or less. The temperature difference ΔT is taken to be the average of the internal cell temperatures minus the enclosure ambient temperature, which is a two-thermistor average also. We found that ΔT was typically 30–35°C.

A.2.2. Thermal control

Lab temperature was fairly stable at 26 ± 1°C. The cell was kept in a controlled environment where airflow was constant and ambient temperature was maintained at 25 ± 0.03°C.

A.2.3. Cell power

Cell power was provided by a digital HP E3632A DC power supply, at typically 7–10 W, with current up to 1.25 or 1.5 A. The cell power was held constant by Labview to about 10 mW.

A.2.4. Calorimetric scheme

The excess power during the live part of the experiment is estimated through

$$P_{\rm xs} \;=\; P_{\rm out} - P_{\rm in}$$

as discussed in the text. Note that the cell has a recombiner, and under normal operating conditions all of the deuterium and oxygen are recombined. When the recombiner begins to fail, then gas is lost through a vent. This gas goes through a bubbler, so that we are able to see easily when this happens. The recombiner provides a heat source with power IV_0, which in our experiments has proven to be nearly constant. Running near 1 A means that 1.54 watts is generated in the recombiner, most of which is lost. About 60 mW of this power makes it back to the cell, resulting in a constant temperature increase of about 0.25°C.

A.2.5. Calibration

A cell is run for many hours prior to turning on the lasers. We estimated the calibration constant K assuming that no excess power was present during this initial stage. The calibration constant was computed again at the end of the experiment (typically well after any thermal signals had died out), generally with good agreement between the two values. The onset of each thermal event was readily observed since transients stand out against the nearly constant zero excess power background. Variations in the excess power output during the zero excess power phase of the experiment is around 10 mW and was dominated by variations in the input power; consequently we have taken 10 mW for the error associated with the excess power measurements in steady state.

This simple method of determining excess power does not take into account the thermal relaxation time of the system; the response of the calorimeter to a constant power input is shown in Fig. 2. Constant power input is applied by measuring the current and voltage once per minute, determining the effective cell resistance, and then fixing the current

to the square root of power divided by this resistance. This results in the spread in input power seen in the figure.

A.2.6. Data collection

An Agilent 34970A and takes measurements every minute; the cell and box temperature measurements are made with the Agilent. The Agilent also provides voltage to control solid state relays used to start and stop in-situ gold plating.

A.3. Lasers

Dual tunable lasers were used to provide beat frequencies in the 3–24 THz range. The laser diodes are off-the-shelf red diodes from various manufacturers such as Sony, Hitachi and Panasonic. One laser is controlled using an Optima LDC202 with a laser mount that accepts 5.6 mm laser diodes. The LDC202 is controlled by providing DC voltage from the Agilent to set laser current and temperature. Our laser diodes typically operate at 70 mA and tune over a temperature range of 15–40°C. The second laser control system is an ILX3722B laser controller and laser mount. It operates by GPIB and can handle 5.6 mm or 9 mm laser diodes. It can tune over 0–60°C, producing a typical tuning range of 4–6 nm.

Both instruments were controlled by Labview to drive the lasers at the desired wavelengths. The output power of the diode lasers was about 20-30 mW each when new before 2002, and both combined produced close to 25 mW at the end of the experimental campaign. The linewidth was 1 nm.

A.3.1. Difference frequency

For difference frequencies in the range of 15–20 THz, we used one laser typically centered near 685 nm, and another laser centered near 658 nm; both lasers could be tuned over 4–6 nm. For observations near 8 THz, we used a third laser centered at 664 nm.

A.3.2. Laser diagnostics

The output power of the laser diodes was measured using an Ophir power meter. The wavelengths were determined using a Stellarnet optical spectrometer, which has a resolution of about 0.25 nm.

A.3.3. Beam overlap

The second beam was aligned to overlap with the first on a single spot on the cathode surface roughly 1 mm in diameter.

A.3.4. Polarization

As noted above, we needed to have both laser beams incident with p-polarization relative to the surface. This was accomplished using a half-wave filter. The lasers were oriented at wide angles to the cell so that the incident angle was greater than 45° relative to the cathode surface. The effect of laser polarization can be seen in Fig. 6. At 64 min (when two overlapping laser beams with mismatched polarization and a difference frequency of 14.88 THz) one can see a minor increase of the P_{xs} signal, which is on the order of the absorption of the laser power in the cell. At 202 min the polarization of one of the lasers was rotated by 90°, at which point both laser beams were overlapped on the surface with p-polarization. The system responds slowly, reaching an excess power of about 140 mW by about 400 min (which is significantly longer than the response time of the calorimeter). This data supports the notion that the polarization of both lasers is important in producing an excess power response. Between 64 and 202 min both lasers were on and tuned to produce a difference frequency near the middle resonance, yet there was no strong response. The system only

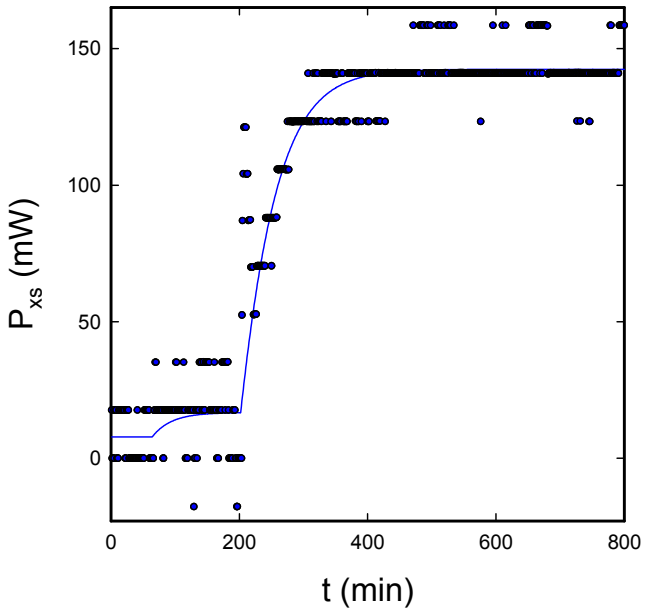

Figure 6. Excess power (mW) as a function of time (min) for parts of data set 662 J-K. The lasers were turned on at minute 64 with mismatched polarization, indicated by the first step. The polarization of one of the lasers was rotated at minute 202, indicated by the onset of a major increase in the relaxation model fit. This gave rise to a prompt (artifact) apparent increase with excess power, which can be attributed to a sustained reduction in cell resistance; and then a subsequent increase in excess power. The spread in the excess power around the model is 9 mW. Data was saved with too few digits when this experiment was run, resulting in the discretization of the points that can be seen in the figure.

responded strongly when both lasers have p-polarization, which occurred at 202 min.

A prompt apparent excess power spike can be seen in the data following the rotation of the laser polarization. This is due to a sudden drop in the cell voltage which appears sometimes as a precursor to an excess power event as discussed in the text.

A.4. Magnets

We used two permanent magnets (approximately 700 G) on either side of the cell during the thermal measurements, but these are not in place during the (preceding) loading phase. The magnets seemed to help in obtaining a thermal response, and the effect was independent of the orientation. There is some evidence that the alignment of the laser polarization with the magnetic field is important. In the present experiments the magnetic field lines are horizontal and extend along the cathode surface; the laser beams come in horizontally, at an angle of about 45° from the cathode surface; in p-polarization, the magnetic field of the light is vertical.

The magnets in this experiment are a legacy from earlier single laser experiments where, in some experiments, they

seemed to help. Magnets appear to make a difference in the Pd morphology in the co-deposition experiments described in [35]. In future work we hope to understand better how the magnetic field impacts the two-laser experiment.

References

[1] M. Fleischmann, S. Pons, M. Hawkins, *J. Electroanal. Chem.* **261** (1989) 301; errata **263** (1990) 187.

[2] M. Fleischmann, S. Pons, M.W. Anderson, L. J. Li, M. Hawkins, *J. Electroanal. Chem.* **287** (1990) 293.

[3] N.S. Lewis, C.A. Barnes, M.J. Heben, A. Kumar, S.R. Lunt, G.E. McManis, G.M. Miskelly, R.M. Penner, M.J. Sailor, P. G. Santangelo, G.A. Shreve, B.J. Tufts, M.J. Youngquist, R.W. Kavanagh, S.E. Kellogg, R.B. Vogelaar, T.R. Wang, R. Kondrat, R. New, *Nature* **340** (1989) 525.

[4] J.R. Huizenga, *Cold Fusion, the Scientific Fiasco of the Century*, (University of Rochester Press, Rochester, 1992).

[5] M.C.H. McKubre, F.L. Tanzella, Using Resistivity to Measure H/Pd and D/Pd Loading: Method and Significance, *Twelfth International Conference on Cold Fusion, Condensed Matter Nuclear Science, Yokohama*, edited by A. Takahashi, K.-I. Ota, and Y. Iwamura (World Scientific, Singapore, 2005), p. 392.

[6] M.C.H. McKubre, S. Crouch-Baker, A.M. Riley, S.I. Smedley, F.L. Tanzella, Excess Power Observations in Electrochemical Studies of the D/Pd System; The Influence of Loading, *Third International Conference on Cold Fusion, Frontiers of Cold Fusion, Nagoya*, edited by H. Ikegami (Universal Academy Press, Tokyo, 1993) p. 5.

[7] T.A. Green, T.I. Quickenden, *J. Electroanal. Chem.* **389** (1995) 91.

[8] M.H. Miles, M. Fleischmann, Accuracy of Isoperibolic Calorimetry Used in a Cold Fusion Control Experiment, *Low-energy nuclear reactions sourcebook, ACS Symposium series*, Vol. 998 (Oxford University Press, Oxford, 2008) p. 153.

[9] M.C.H. McKubre, S. Crouch-Baker, R.C. Rocha-Filho, S.I. Smedley, F.L. Tanzella, T.O. Passell, J. Santucci, *J Electroanal. Chem.* **368** (1994) 55.

[10] D. Gozzi, F. Celluchi, P.L. Cignini, G. Gigli, M. Tomellini, E. Cisbani, S. Frullani, G.M. Urciuoli, *J Electroanal. Chem.* **452** (1998) 251.

[11] E. Storms, *Science of Low Energy Nuclear Reaction: A comprehensive compilation of evidence and explanations about cold fusion* (World Scientific, Singapore, 2007).

[12] I. Dardik, T. Zilov, H. Branover, A. El-Boher, E. Greenspan, B. Khachaturov, V. Krakov, S. Lesin, M. Tsirlin, Excess heat in electrolysis experiments at energetics technologies, *Eleventh International Conference on Cold Fusion, Condensed Matter Nuclear Science, Marseilles*, edited by J.P. Biberian (World Scientific, Singapore, 2004), p. 84.

[13] D. Letts, D. Cravens, Laser stimulation of deuterated palladium: past and present, *Tenth International Conference on Cold Fusion, Condensed Matter Nuclear Science, Cambridge, MA*, edited by P.L. Hagelstein and S.R. Chubb (World Scientific, Singapore, 2003), p. 159.

[14] D. Cravens, D. Letts, Practical techniques in CF research: triggering methods, *Tenth International Conference on Cold Fusion, Condensed Matter Nuclear Science, Cambridge, MA*, edited by P.L. Hagelstein and S.R. Chubb (World Scientific, Singapore, 2003), p. 171.

[15] E. Storms, Use of a very sensitive Seebeck calorimeter to study the Pons–Fleischmann and Letts effects, *Tenth International Conference on Cold Fusion, Condensed Matter Nuclear Science, Cambridge, MA*, edited by P.L. Hagelstein and S.R. Chubb (World Scientific, Singapore, 2003), p. 183.

[16] M. McKubre, F. Tanzella, P.L. Hagelstein, K. Mullican, M. Trevithick The need for triggering in cold fusion reactions, *Tenth International Conference on Cold Fusion, Condensed Matter Nuclear Science, Cambridge, MA*, edited by P.L. Hagelstein and S.R. Chubb (World Scientific, Singapore, 2003), p. 199.

[17] M.R. Swartz, Photo-induced excess Heat from laser-irradiated electrically polarized palladium cathodes in D_2O, *Tenth International Conference on Cold Fusion, Condensed Matter Nuclear Science, Cambridge, MA*, edited by P.L. Hagelstein and S.R. Chubb (World Scientific, Singapore, 2003), p. 213.

[18] M. Apicella, E. Castagna, L. Capobianco, L. D'Aulerio, G. Mazzitelli, F. Sarto, A. Rosada, E. Santoro, V. Violante, M. McKubre, F. Tanzella, C. Sibilia, Some recent results and ENEA, *Twelfth International Conference on Cold Fusion, Condensed Matter Nuclear Science, Yokohama*, edited by A. Takahashi, K.-I. Ota, and Y. Iwamura (World Scientific, Singapore, 2005), p. 117.

[19] D. Cravens, D. Letts, The enabling criteria of electrochemical heat: beyond reasonable doubt, *Fourteenth International Conference on Cold Fusion* (in press).

[20] S. Guruswamy, M.E. Wadsworth, Metallurgical aspects in cold fusion experiments, *First Annual Conference on Cold Fusion, Salt Lake City*, edited by F. Will (National Cold Fusion Institute, 1990), p. 314; see Figure 2(c).
[21] M.C.H. McKubre, R.C. Rocha-Filho,S. Smedley, F. Tanzella, J. Chao, B. Chexal, T. Passell, J. Santucci, Calorimetry and electrochemistry in the D/Pd system, *First Annual Conference on Cold Fusion, Salt Lake City*, edited by F. Will (National Cold Fusion Institute, 1990), p. 20; see Figure 5.
[22] J.M. Rowe, J.J. Rush, H.G. Smith, M. Mostoller, H.E. Flotow, *Phys. Rev. Lett.* **33** (1974) 1297.
[23] D. Letts, D. Cravens, and P.L. Hagelstein, Dual laser stimulation and optical phonons in palladium deuteride, in low-energy nuclear reactions and new energy technologies, *Low-Energy Nuclear Reactions Sourcebook*, Vol. 2 (American Chemical Society, Washington DC). pp. 81–93 (2009).
[24] K.-H. Su, Q.-H. Wei, X. Zhang, J.J. Mock, D.R. Smith, S. Schulz, *Nano Letters* **3** (2003) 1087.
[25] D.A. Genov, A.K. Sarychev, V.M. Shalaev, A. Wei, *Nano Letters* **4** (2002) 153.
[26] X.-M. Qian, S.M. Nie, *Chem. Soc. Rev.* **37** (2008) 912.
[27] A. Rahman, K. Sköld, C. Pelizzari, S.K. Sinha, H. Flotow, *Phys. Rev. B* **14** (1976) 3630.
[28] L.E. Sansores, J. Tagüeña-Martinez, R.A. Tahir-Kheli, *J. Phys. C: Solid State Phys.* **15** (1982) 6907.
[29] O. Blaschko, R. Klemencic, P. Weinzierl, L. Pintschovius, *Phys. Rev. B* **24** (1981) 1552.
[30] J.M. Rowe, J.J. Rush, J.E. Schirber, J.M. Mintz, *Phys. Rev. Lett.* **57** (1986) 2955.
[31] Y. Fukai, M. Mizutani, S. Yokota, M. Kanazawa, Y. Miura, T. Watanabe, *J. Alloys and Compounds* **356–357** (2003) 270.
[32] P.L. Hagelstein, I.U. Chaudhary, Arguments for dideuterium near monovacancies in PdD, *Proc. 15th International Conference on Cold Fusion* (in press).
[33] R. Lässer, K.-H. Klatt, *Phys. Rev. B* **28** (1983) 748.
[34] P.L. Hagelstein, *Naturwissenschaften* **97** (2010) 345.
[35] P.A. Mosier-Boss, S. Szpak, F.E. Gordon, L.P.G. Forsley, *Eur. Phys. J.: Appl. Phys.* **40** (2007) 293.
[36] S. Holst, W. Legler, *Z. Phys. D* **25** (1993) 261.

J. Condensed Matter Nucl. Sci. 3 (2010) 77–92

Research Article

Analysis of some experimental data from the two-laser experiment

Peter L. Hagelstein*
Research Laboratory of Electronics, Massachusetts Institute of Technology, Cambridge, MA 02139, USA

Dennis G. Letts
12015 Ladrido Lane, Austin, TX 78727, USA

Abstract

We consider simple relaxation models for fitting data from two-laser experiments. The approach has been used to analyze the data systematically from many data sets. A result of the fitting is that we find that the excess power responds quickly near 8 THz, and slowly near 15 and 21 THz.

Keywords: Data analysis, Excess heat, Fleischmann–Pons experiment, Optical phonons, Two-laser experiment

1. Introduction

In a recent set of experiments where two lasers were used to stimulate excess power in Pd cathodes, the response was observed to depend on the difference frequency between the two lasers which was at THz frequencies [1]. The response was found to be largest at three different "sweet spots", corresponding to 8.2, 15.1, and 20.8 THz. The first two frequencies appear to be connected to low group velocity compressional modes in PdD. The origin of the third frequency is less clear. Possible explanations include H contamination in PdD, and optical phonon modes associated with D in vacancies in Au [2].

In this work, we are concerned with the issue of data analysis. In previous work, we reported results for the excess power increase by first determining the excess power before the lasers turned on (or changed difference frequency), and then estimating the increase in the excess power after about 3 h [1]. A weakness of this approach is that the different estimates are subjective, and it is not so easy to determine the associated error bars. This issue was raised recently by a reviewer when we submitted a paper for publication.

*E-mail: plh@mit.edu

The application of statistical methods systematically to the experimental data is in principle straightforward. However, there are issues, some of which are interesting. One approach might be to develop statistical estimates for the excess power before the stimulation, then wait for a steady state to be attained, and then do a second statistical estimate for the excess power. In either case, we need to correct for the response of the system to the absorbed laser power.

However, there is much more information that is potentially present in the data. For example, how long does it take to reach a steady state, and what kind of function [2] describes the dynamics? Are the dynamics the same in the different experiments, or does the system respond faster in some cases than in others? Then, if we understood the dynamics, would it change our picture the system? Interesting questions, but whether we are able to answer them or not depends on the degree to which the data differentiates between different models.

In what follows, we consider two different models that we have used to fit the data. We also consider two different data sets where excess power was observed.

2. Calorimeter Response

The calorimetry used in the experiments is simple Fick's law calorimetry with no dynamical correction (these and other issues are discussed in [2]). The output power is computed from measurements of the temperature difference inside and outside of the cell

$$P_{\rm out} \;=\; K\,\Delta T. \tag{1}$$

The input power for the present discussion is a combination of the electrical input power minus the contribution due to splitting of heavy water into deuterium and oxygen

$$P_{\rm in} \;=\; I\,(V - V_0), \tag{2}$$

where V_0 is the thermoneutral potential.

The cell is run in a constant current mode from minute to minute, and an approximate constant power condition is obtained by updating the current each minute so that the product of the new current times the old voltage will be matched to the desired electrical input power. As a result, there are minor fluctuations in the input power.

Of course, the calorimeter will respond to changes in the input with a delay since there is a significant heat capacity. Since this is not taken into account by the simple Fick's law calorimetry, we would expect that the Fick's law output power will relax to the input, as in the example of Fig. 1. We could take this into account by using an improved model for the calorimeter that is more complete, and make use of the sophisticated method presented by Miles and Fleischmann [3]. However, the goal of this present work is to bring out some interesting features of the experimental results, rather than to develop a better model for the calorimeter.

2.1. Fitting the output power

In the most simplistic point of view, the model output power should have the form

$$P_{\rm out} \;=\; P_{\rm in}\,\left(1 - {\rm e}^{-t/\tau}\right), \tag{3}$$

where τ is the associated relaxation time. This suggests that we should use a fitting function of the form

$$P_{\rm out} \;=\; A + B\,{\rm e}^{-t/\tau}. \tag{4}$$

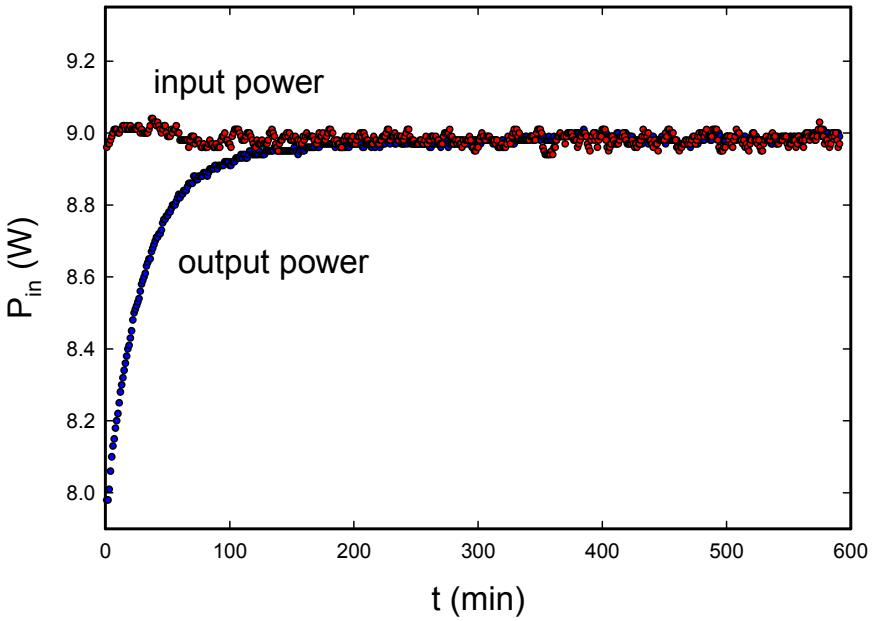

Figure 1. Input and output power points from DGL662v2.

The results from the fitting are

$$A = 8.98\ \text{W}, \qquad B = -1.06\ \text{W}, \qquad \tau = 31.9\ \text{min}. \tag{5}$$

The experimental points and the associated fit are shown in Fig. 2. We computed the variance according to

$$\text{var} = \frac{1}{N}\sum_i [P_i - P_{\text{fit}}(t_i)]^2. \tag{6}$$

The square root of the variance for this fit is

$$\Delta P = \sqrt{\text{var}} = 11.3\ \text{mW}. \tag{7}$$

2.2. Drift

There is a drift evident in the calibration data. We can fit the drift according to

$$P_{\text{out}} = A + B\, \text{e}^{-t/\tau} + Ct. \tag{8}$$

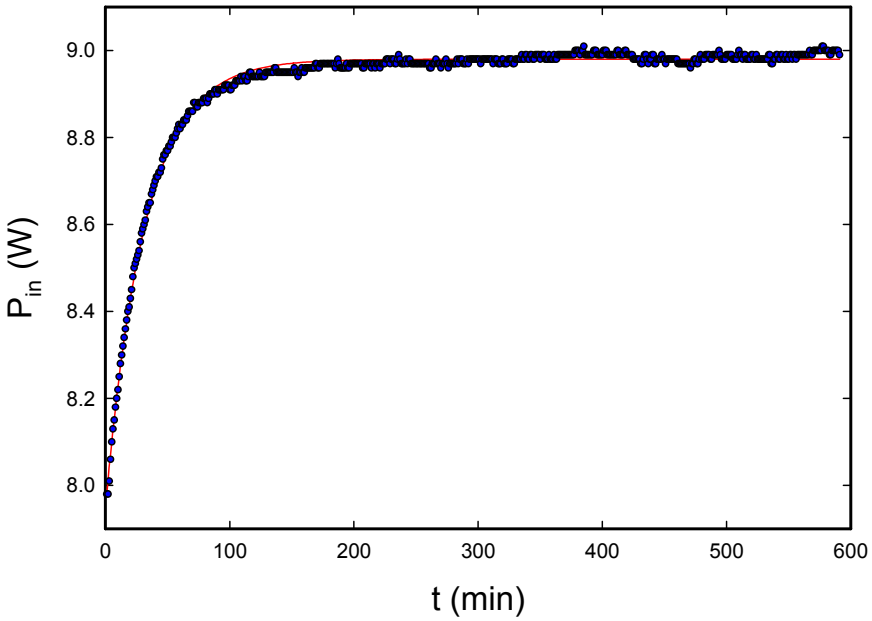

Figure 2. Output power points and fit for DGL662v2.

The fitting parameters that result are

$$A = 8.95\ \text{W}, \qquad B = -1.02\ \text{W}, \qquad C = 7.9 \times 10^{-5}\ \text{W/min}, \qquad \tau = 29.2\ \text{min}. \tag{9}$$

The associated spread in the excess power is

$$\Delta P = \sqrt{\text{var}} = 8.17\ \text{mW}. \tag{10}$$

A relevant question here is why there should be a drift in the data. One possibility is that perhaps a drift is present in the input power. To test this we show the input power in Fig. 3. Inspection of this figure indicates that there is no significant drift at late times, so that the origin of the drift lies elsewhere.

3. Absorbed Laser Power

In the calorimetric approach used, most of the excess power that is seen appears to be due to anomalous power production by the cathode. We need to correct for the absorbed laser power, since it results in a temperature increase on a similar footing to the excess power production. The amount of laser power absorbed is small in comparison to the excess power production generally near resonance. In earlier work, we neglected the absorbed laser power. In response to comments from a reviewer we expand our discussion here to include the effect.

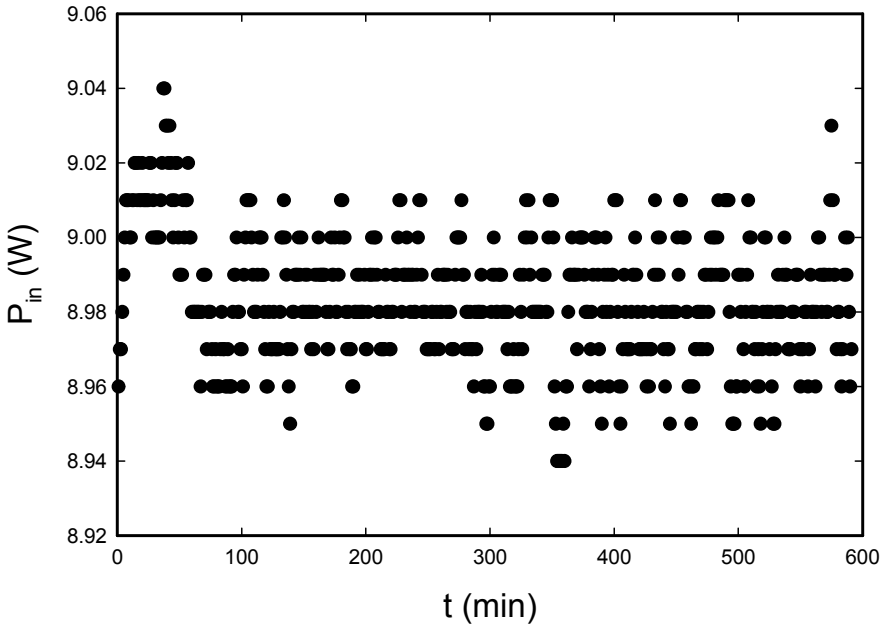

Figure 3. Input power points from DGL662v2.

In the set of experiments for which we have excess power data, the amount of laser light absorbed was not measured separately in each case. From a theoretical viewpoint, we expect the absorption of the cathode to be dominant. Hence, all that we need to do is to first estimate what fraction of the laser light makes it to the cathode, and then determine the fraction absorbed. When new (before 2002), each laser could produce up to 30 mW, but recent measurements indicate that the laser power has degraded so that the total incident power from both is about 25 mW. The incident light passes through a double-pane glass window, then air, then the borosilicate glass of the cell, and finally the electrolyte prior to reaching the cell. We would expect roughly 90% of the incident light to reach the cathode surface.

The fraction of the incident light absorbed is then dominated by the absorption at the cathode, which we discuss next. To get some intuition, we can use the Fresnel reflection coefficient appropriate for light incident on a metal in water, which we develop in the Appendix. If the cathode surface were pure Pd, then we could take the optical data from clean Pd in vacuum to arrive at an absorption coefficient of about 43% at 45^o (or about 39% of the laser radiation) for TM polarized light. In experiments in vacuum, the reflection is seen to be changed significantly due to the presence of an oxide layer. We would expect the cathode surface in the electrolyte to have a surface coating due to the electrolyte and electrochemistry, so that we would not be surprised if the measured number were different.

In the two-laser experiments we can look at the calorimetric results from experiments in which the lasers were turned on off of resonance, where the cell response is the smallest. An example of this is experiment 662I2, where data near the time when the lasers first turned on is shown in Fig. 4. The beat frequency in this case is 18.23 THz, which is in the dead region of the spectrum between the resonances at 15 and 21 THz. We see in this case a noisy calorimetric response with a relaxation time close to that of the calorimeter. This result is consistent with an absorption of 15 mW

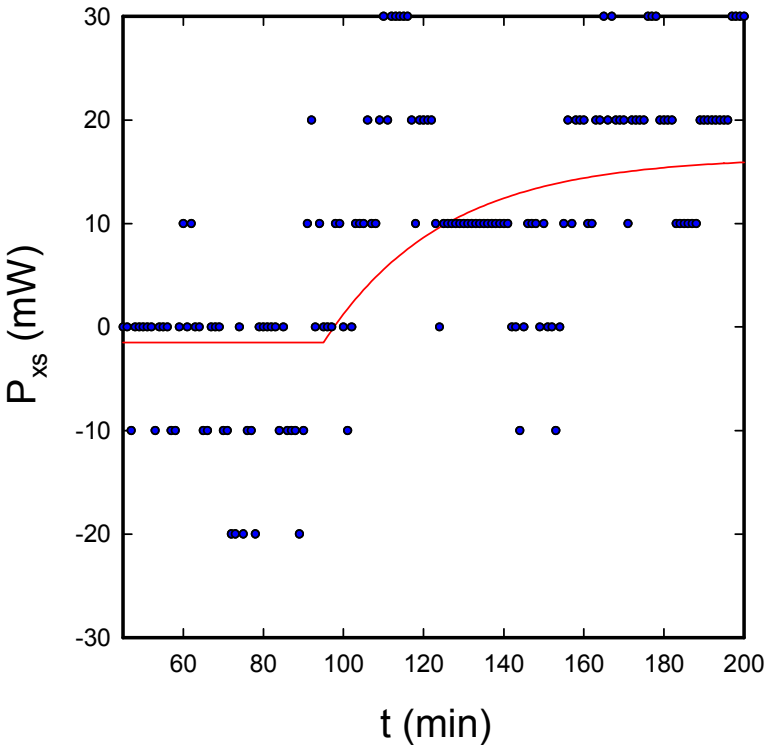

Figure 4. Data from experiment 662I2 around the laser turn on time.

of laser power. This is the number that we have adopted for the analysis of [2].

Subsequently, a calorimetric experiment in light water was run using one of the cathodes from the campaign in order to verify the absorbed power. In this experiment, one laser set at 659 nm was measured at 14.8 mW, the other set at 689 nm was measured at 11.5 mW, and the calorimeter (with no electrochemical input power) registered 15 mW of absorbed power (57% of the laser power was absorbed). In this case the lasers were both polarized in p-polarization. Changing to s-polarization was found not to impact the absorbed power. In the remainder of this paper we will neglect the absorbed laser power, since it provides a relatively small correction for the examples considered below.

4. Excess Power Event

We have focused on data from DGL662n and DGL662o combined since it provides one of the cleanest examples of excess power in the two-laser experiments. In this experiment, the cell was run for an extended period prior to turning on the two lasers, and a reasonably large excess power event was stimulated.

In the two-laser experiments, there sometimes appears an artifact shortly after the lasers turn on as a precursor to an excess power event. We know that it is an artifact since it is much shorter than the response time of the calorimeter.

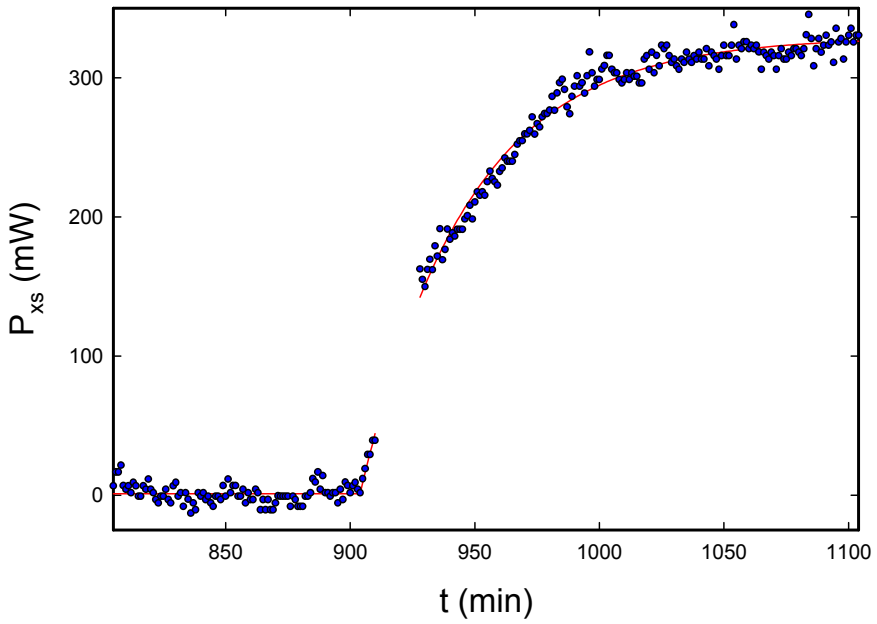

Figure 5. Excess power and fit for DGL662n and DGL662o, with the points removed around the artifact.

Measurements of the cell parameters indicates that this artifact is due to a sudden and sustained drop in the cell voltage, which leads to a temporary drop in the cell input power that is largely corrected within 10–15 min. Why the cell voltage drops is at present unknown.

4.1. Simple relaxation model

The simplest possible model that we might use is one that assumes relaxation for a step input. The excess power in such a model might look like

$$P_{\rm xs} \;=\; P_0 \left(1 - {\rm e}^{-(t-T_0)/\tau}\right) u(t - T_0), \tag{11}$$

where T_0 is the initiation time, P_0 the constant excess power source in the model, and $u(t)$ is the unit step function. This suggests that we try a fit of the form

$$P_{\rm fit} \;=\; A + B \,\left(1 - {\rm e}^{-(t-T_0)/\tau}\right) u(t - T_0). \tag{12}$$

We have removed some data around the artifact in order to obtain a fit that is less biased. The resulting fit is shown in Fig. 5, and the associated fitting parameters are

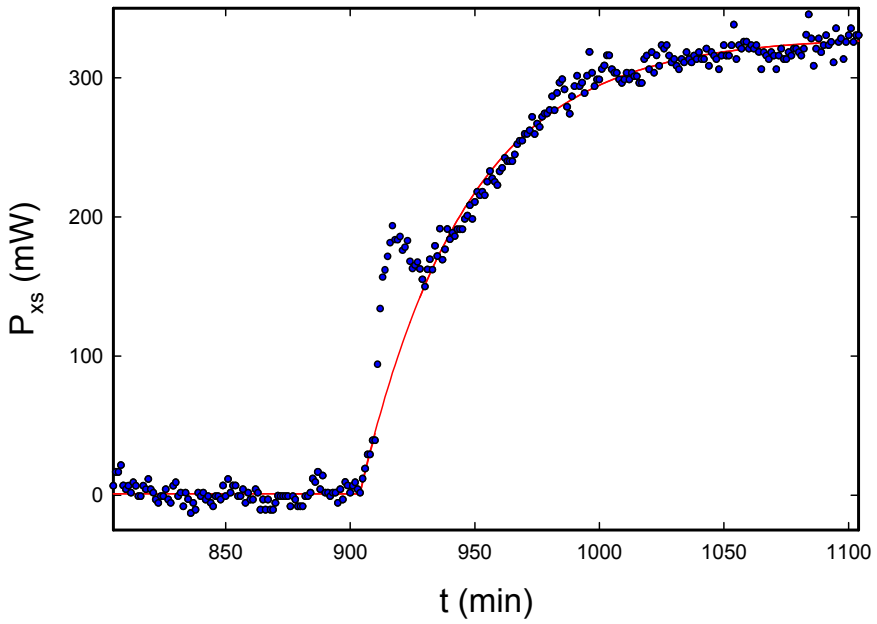

Figure 6. Excess power and fit for DGL662n and DGL662o including drift, shown with all experimental points in the time segment used.

$$A = 1.20\,\text{mW}, \qquad B = 328.24\,\text{mW}, \qquad T_0 = 904.0\,\text{min}, \qquad \tau = 42.71\,\text{min}. \tag{13}$$

Note that the relaxation time here is significantly longer than the calorimeter relaxation time. The spread in excess power as computed above is

$$\Delta P = 7.54\,\text{mW}. \tag{14}$$

4.2. Drift

We know that the calorimeter drifts from our experience with the calibration data. It is reasonable to redo the calculation assuming that there is a linear drift for this data set. To include a linear drift, we fit according to

$$P_{\text{fit}} = A + B\left(1 - \text{e}^{-(t-T_0)/\tau}\right)u(t-T_0) + C(t-T_0). \tag{15}$$

The resulting fitting parameters are

$$A = 3.58\,\text{mW}, \qquad B = 326.58\,\text{mW}, \qquad C = -2.91 \times 10^{-3}\,\text{mW/min},$$

$$T_0 \;=\; 904.1 \text{ min}, \qquad \tau \;=\; 43.04 \text{ min}. \tag{16}$$

This fit is shown compared with the data sets (including artifact) in Fig. 6. The associated spread in excess power is

$$\Delta P \;=\; 7.53 \text{ mW}. \tag{17}$$

We find that including the spread in this case changes the results at the per cent level.

4.3. Fewer points

In the computations above, we took points to 100 min before, and 200 min after. If we shorten these numbers to 70 min before and 150 min after, then we obtain

$$A \;=\; 4.12 \text{ mW}, \qquad B \;=\; 329.80 \text{ mW}, \qquad C \;=\; -4.83 \times 10^{-3} \text{ mW/min},$$
$$T_0 \;=\; 903.9 \text{ min}, \qquad \tau \;=\; 44.43 \text{ min} \tag{18}$$

with a smaller associated spread

$$\Delta P \;=\; 7.36 \text{ mW}. \tag{19}$$

5. Three-parameter Model

At this point, we have had an opportunity to apply the model and ideas above to many data sets, with the result that largely things work reasonably well. However, there remains an issue that we are motivated to address. We know that there is a characteristic response of the calorimeter to excess power sourced within the calorimeter. Yet in the model fit that we used above, we find that the relaxation time is often longer than the relaxation time of the calorimeter. If we de-convolve the associated signal, we end up with a source history that is highly constrained. It is possible to develop a more sophisticated three-parameter fit which relaxes the associated constraint.

5.1. Relaxation model

This motivates us to revise our model so as to include the basic calorimeter response, and then parameterize whatever is left over in terms of the underlying excess power signal. We consider the simplest relaxation model described by

$$\frac{\mathrm{d}}{\mathrm{d}t}P + \frac{P}{\tau_0} \;=\; \frac{P_\mathrm{s}}{\tau_0}. \tag{20}$$

Here P_s is the source excess power, and P is the excess power signal reported by the model calorimeter. We can express the calorimeter version of the power P in terms of the source version of the power P_s according to

$$P(t) \;=\; \int_{-\infty}^{\infty} P_\mathrm{s}(t')h(t-t')\mathrm{d}t', \tag{21}$$

where $h(t)$ is the impulse response

$$h(t) \;=\; \frac{\mathrm{e}^{-t/\tau_0}}{\tau_0}u(t). \tag{22}$$

5.2. Simple model based on a step

Now we are free to develop a model calorimeter power response based on a source power model. For example, if we chose a step

$$P_{\rm s}(t) \;=\; P_0 u(t). \tag{23}$$

Then we would obtain a calorimeter power given by

$$\begin{aligned} P(t) \;&=\; \int_{-\infty}^{\infty} P_0 u(t') \, \frac{{\rm e}^{-(t-t')/\tau_0}}{\tau_0} u(t-t') \, {\rm d}t' \\ &=\; u(t) P_0 {\rm e}^{-t/\tau_0} \int_0^t \frac{{\rm e}^{t'/\tau_0}}{\tau_0} {\rm d}t' \;=\; u(t) P_0 (1 - {\rm e}^{-t/\tau_0}). \end{aligned} \tag{24}$$

This is closely related to the fitting function that we selected, but in this version the τ_0 parameter is fixed by the calorimeter response rather than being determined by the data.

5.3. Source power for the model above

The natural question occurs as to what is the source assumed with the model that we discussed above. For this model, if we neglect the constant or linear offset, we might write

$$P(t) \;=\; B u(t) \left(1 - {\rm e}^{-t/\tau}\right). \tag{25}$$

The associated source power that would correspond to this is

$$P_{\rm s}(t) \;=\; P(t) + \tau_0 \frac{{\rm d}P}{{\rm d}t} \;=\; u(t) B \left[1 - \left(1 - \frac{\tau_0}{\tau}\right) {\rm e}^{-t/\tau}\right]. \tag{26}$$

We can recast this as

$$P_{\rm s}(t) \;=\; u(t) B \left(1 - \frac{\tau_0}{\tau}\right) \left(1 - {\rm e}^{-t/\tau}\right) + u(t) B \frac{\tau_0}{\tau}. \tag{27}$$

There is an initial step along with a relaxation curve. The amplitude of the step in this model is fixed by the ratio of the relaxation times.

5.4. More general model

Based on the argument above, it seems that we should be able to put together a better model based on separate parameters for the step and relaxation terms. For example, we might adopt a source power model of the form

$$P_s(t) \;=\; u(t) B \left(1 - {\rm e}^{-t/\tau}\right) + u(t) D. \tag{28}$$

The corresponding calorimeter power is

$$P(t) = \int_{\infty}^{\infty} P_s(t')h(t-t')\mathrm{d}t'$$

$$= u(t)(B+D)\left(1-\mathrm{e}^{-t/\tau_0}\right) - u(t)B\frac{(\mathrm{e}^{-t/\tau}-\mathrm{e}^{-t/\tau_0})}{\left(1-\frac{\tau_0}{\tau}\right)}. \quad (29)$$

6. Fitting Data with the Three-parameter Model

In order to tell whether the revised model helps, we need to try it on some data sets. The reference data set is a good data set generally, but in order to develop a useful fit, we need to remove some of the points around the artifact. As such, we would not expect to see much difference between the different models since the points where the models would show the difference is in the excluded region. Better is to test a different data set that is free of the artifact.

6.1. Reference data set

We begin by considering the reference data set. We have fit the data (with no drift), and we have obtained the following fit parameters

$$A = 1.57\,\mathrm{mW}, \qquad B = 110.67\,\mathrm{mW}, \qquad D = 214.33\,\mathrm{mW},$$

$$\tau_0 = 30.0\,\mathrm{min}, \qquad \tau = 33.45\,\mathrm{min} \quad (30)$$

with T_0 fixed at 904. The associated spread in excess power is

$$\Delta P = 7.52\,\mathrm{mW}. \quad (31)$$

This model gives results that are pretty similar to what we found previously.

6.2. Example without an artifact

In the different data sets, there occur examples that are fit well by a step function source model, and also examples that are fit by a dynamic source function. One example of a data set with a dynamic source function is DGL670a, which was listed as point 42 on the earlier table at 19.28 THz, but which was subsequently corrected to 13.45 THz. The fitting parameters in this case are

$$A = 6.49\,\mathrm{mW}, \qquad B = 66.15\,\mathrm{mW}, \qquad D = 18.52\,\mathrm{mW},$$

$$\tau_0 = 30.0\,\mathrm{min}, \qquad \tau = 54.69\,\mathrm{min} \quad (32)$$

with T_0 taken to be 8266. The associated spread in excess power is

$$\Delta P = 6.16\,\mathrm{mW}. \quad (33)$$

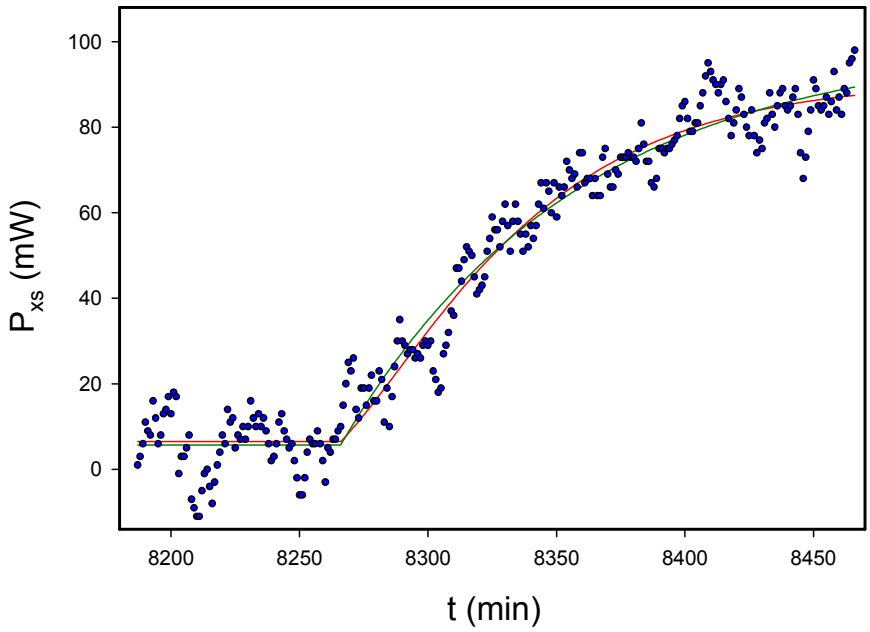

Figure 7. Excess power and fit for DGL670a using the three-parameter model (*red*) compared with the optimized simple model (*green*).

However, having made arguments in favor of a slowed onset, in fairness we need to also argue the other side as well. In this case, the simpler model also gives reasonable results, as shown in Fig. 7. In this case the fitting parameters are

$$A = 5.78\ \text{mW}, \qquad B = 0\ \text{mW}, \qquad D = 94.84\ \text{mW},$$

$$\tau = 92.97\ \text{min} \tag{34}$$

with

$$\Delta P = 6.30\ \text{mW}. \tag{35}$$

This model gives a higher estimate for the source power, and a poorer fit to the data.

Results for both models are shown in Fig. 7. It is possible to see the effect of the slower rise in the associated curve for the three-parameter model relative to the simpler model. Unfortunately, since the two different models lead to curves that are close together, it is unlikely that one could make a compelling case that the data requires the more sophisticated model. If one uses the more sophisticated model, it seems unlikely that we would be sure that the parameters that provide an optimum fit tell us much about the source history, since we can obtain very similar curves with other parameters.

7. Discussion and Conclusions

There are a number of conclusions which might be drawn from the discussion of the previous sections. Perhaps the most notable conclusion is that in the two-laser experiments, the excess power appears to relax to a constant value (which depends on the difference frequency between the two lasers). This is different qualitatively from some of the early Fleischmann–Pons experiments in which the excess power often would occur in bursts with sometimes complicated histories. For the data sets considered here, a simple relaxation model can provide a good fit for the experimental data. We found this to be the case for the majority of the 18 data sets of this type that we analyzed.

A second important conclusion is that the relaxation time associated with the excess power response is usually longer than the calorimeter response time. We can conclude that the source excess power itself relaxes to a reasonably constant level over times ranging between a few minutes and 4 h. There does not seem to be a clear correlation between the relaxation time and the excess power level. There does seem to be a correlation between the relaxation time and the difference frequency (see Fig. 8). The three data sets near 8 THz show short relaxation times, where the source τ of the three-parameter model is less than 13 min. All but one of the other data sets associated with the 15 and 20 THz resonances have longer relaxation times, most above 30 min.

What this source relaxation time is due to is not known. There are two plausible scenarios that suggest themselves as possibilities. In one scenario, the two lasers are focused to a small spot on the cathode, and the lag time is associated with the spreading of the source from initially being localized to extending over a large fraction of the cathode surface

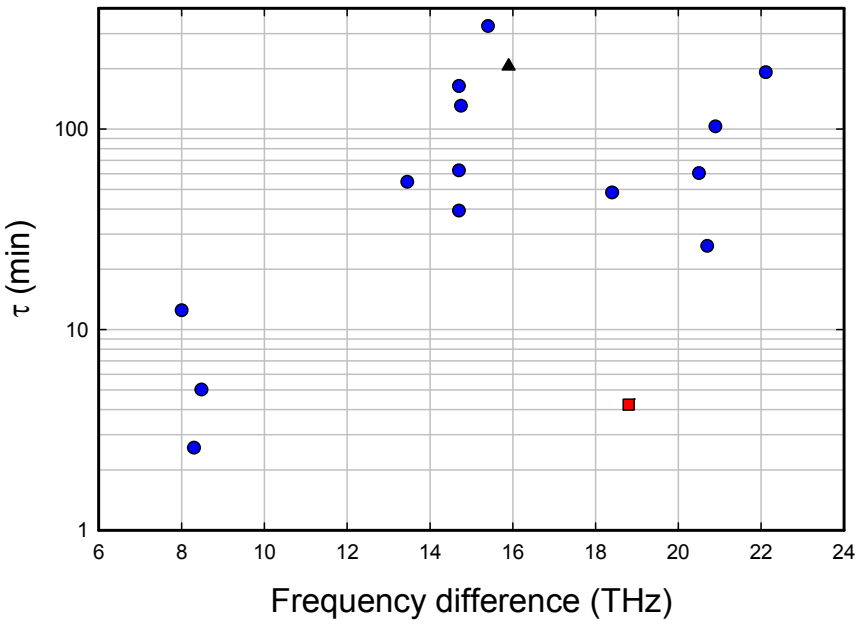

Figure 8. Source relaxation time parameter τ from three-parameter model fits of two-laser experiments. The data in blue circles are for the "normal" runs; the excess power was interrupted for the red square at 18.8 THz, so that the τ of 4.2 min is inaccurate; the data set is incomplete for the black triangle at 15.9 THz, so that the estimate of 206 min has a large uncertainty.

at late time. In another scenario, the response is delocalized in space from early time, but it is the amplitude that builds up. Simple calorimetric experiments cannot resolve between these scenarios. If the cathodes showed a response in the IR, as was the case in the Swartz experiments [4], then perhaps we would be able to see the surface area response change in time, and perhaps correlate with the excess power production.

If a faster calorimeter were used, then it would be possible to measure the excess power history and dynamics with more resolution. This would seem to be a good thing. If the short time response for the 8 THz frequency points is a real effect, and if the longer response for the 15 and 21 THz points is also real, then this might be useful to confirm and to study. Perhaps the system is telling us something helpful in this data.

Appendix A. Idealized Absorption Model

We are interested in developing a simple theoretical model for laser light absorption from a a model metal surface in the electrolyte. Our motivation for this is that such a model can shed light on how much absorption might be expected under conditions that are better understood than those of the experiment.

The light initially comes through air, then hits the outer glass cell, passes into the electrolyte, and then is absorbed and reflected at the cathode surface. We can analyze a simplified version of the problem using four homogeneous regions. Good optical data is available for palladium and for gold in vacuum, but the observed reflection or absorption depends also on surface contaminants and morphology. We estimate a relatively high absorption fraction from the optical data for a clean Pd surface.

Appendix A.1. TM absorption at a metal surface

In what follows we are interested in obtaining the relevant Fresnel equations to determine the absorption of a beam in heavy water on a metal surface, and separately the reflection associated with going from air through glass into heavy water. For TM light (which corresponds to p-polarization), we focus on the magnetic field. In the electrolyte we write

$$\mathbf{H} \;=\; \hat{y}\left[H_{\rm i}{\rm e}^{i(k_x x+k_z z)} + H_{\rm r}{\rm e}^{i(k_x x-k_z z)}\right]. \tag{A.1}$$

In the metal the electromagnetic field does not propagate because the laser frequency is below the plasma frequency. In this case we may write

$$\mathbf{H} \;=\; \hat{y}H_{\rm t}{\rm e}^{ik_x x}{\rm e}^{-\alpha z}. \tag{A.2}$$

In the absence of a surface current the (transverse) magnetic field is continuous across the boundary, so that

$$H_{\rm i} + H_{\rm r} \;=\; H_{\rm t}. \tag{A.3}$$

The transverse component of the electric field must also be continuous across the boundary, which leads to

$$\frac{k_z}{\omega\epsilon[{\rm D_2O}]}(H_{\rm i} - H_{\rm r}) \;=\; i\frac{\alpha}{\omega\epsilon[{\rm Pd}]}H_{\rm t}. \tag{A.4}$$

We can solve these simultaneously to obtain

$$r_{\rm TM}(\theta) \;=\; \frac{H_{\rm r}}{H_{\rm i}} \;=\; -\frac{\alpha\epsilon[{\rm D_2O}] + ik_z\epsilon[{\rm Pd}]}{\alpha\epsilon[{\rm D_2O}] - ik_z\epsilon[{\rm Pd}]}, \tag{A.5}$$

where $r_{\rm TM}$ is the reflection coefficient.

We can make use of the relations

$$\epsilon[{\rm D_2O}]\mu_0\omega^2 \;=\; k^2, \tag{A.6}$$

$$k_z \;=\; k\cos\theta, \qquad k_x \;=\; k\sin\theta, \tag{A.7}$$

$$-\epsilon[{\rm Pd}]\mu_0\omega^2 \;=\; \alpha^2 - k_x^2 \tag{A.8}$$

in order to rewrite $r_{\rm TM}$ as

$$r_{\rm TM}(\theta) \;=\; \frac{H_{\rm r}}{H_{\rm i}} \;=\; -\,\frac{\sqrt{\epsilon[{\rm D_2O}]\sin^2\theta - \epsilon[{\rm Pd}]}\epsilon[{\rm D_2O}] + i\sqrt{\epsilon[{\rm D_2O}]}\epsilon[{\rm Pd}]\cos\theta}{\sqrt{\epsilon[{\rm D_2O}]\sin^2\theta - \epsilon[{\rm Pd}]}\epsilon[{\rm D_2O}] - i\sqrt{\epsilon[{\rm D_2O}]}\epsilon[{\rm Pd}]\cos\theta}. \tag{A.9}$$

Since there is very little loss in the electrolye, the associated dielectric constant $\epsilon[{\rm D_2O}]$ is real to within an excellent approximation and positive. Since the laser light is below the plasma frequency of the cathode, the real part of the dielectric constant $\epsilon[{\rm Pd}]$ is negative. Since the metal is lossy, there will be a nonzero imaginary part of this dielectric constant.

A similar analysis for TE polarization leads to

$$r_{\rm TE}(\theta) \;=\; \frac{E_{\rm r}}{E_{\rm i}} \;=\; -\,\frac{\sqrt{\epsilon[{\rm D_2O}]\sin^2\theta - \epsilon[{\rm Pd}]} + i\sqrt{\epsilon[{\rm D_2O}]}\cos\theta}{\sqrt{\epsilon[{\rm D_2O}]\sin^2\theta - \epsilon[{\rm Pd}]} - i\sqrt{\epsilon[{\rm D_2O}]}\cos\theta}. \tag{A.10}$$

The fraction of the light absorbed in this part of the model is

$$f_{\rm abs}(\theta) \;=\; 1 - |r(\theta)|^2, \tag{A.11}$$

where r is taken to be one of the two expressions above depending on the polarization.

Appendix A.2. Optical constants and absorption

To proceed we require estimates for the dielectric constant of heavy water and for the cathode. We will adopt 665 nm as a reference laser wavelength for our estimates. The optical constant for light water is n is 1.331 [5] (we do not have data at present for heavy water in this spectral range), so that we will use for $\epsilon[{\rm D_2O}]$

$$\epsilon[{\rm D_2O}] \;=\; 1.77\,\epsilon_0, \tag{A.12}$$

The optical constants for Pd at 665 nm are $n = 1.81$ and $k = 4.38$ [6], so that for this calculation we can use

$$\epsilon[{\rm Pd}] \;=\; -\,15.9(1+i)\,\epsilon_0. \tag{A.13}$$

These optical data can be used to construct the absorption curve shown in Fig. 9. The absorption fraction at an incident angle of $45^{\rm o}$ is calculated to be 0.43.

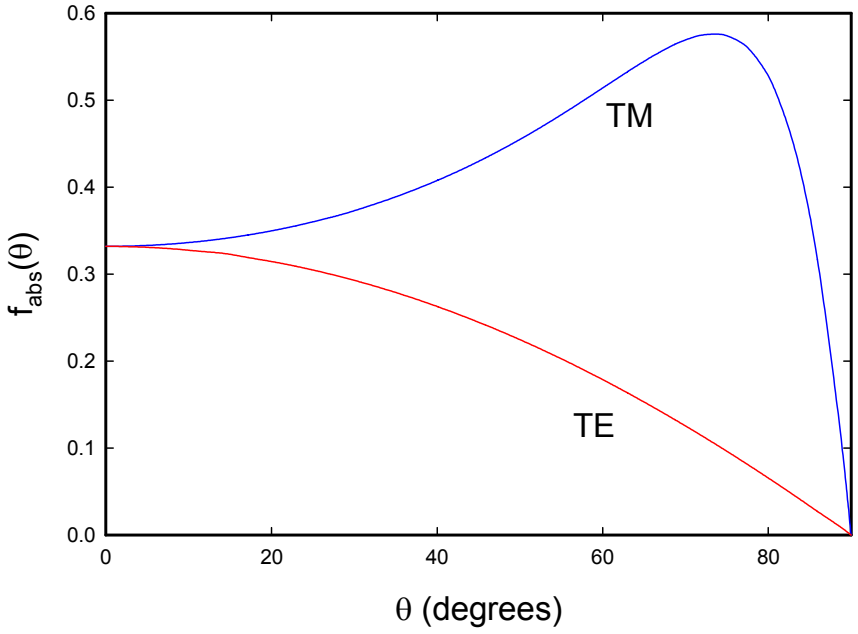

Figure 9. Absorbed TM and TE fraction of 685 nm light in water on Pd as a function of angle θ relative to normal.

We note that the absorption fraction shown in Fig. 9 is high, and that very clean surfaces in vacuum were used for the measurements of the optical constants that we used. It was noted in [6] that if the surface is oxidized, then a different amount of light is reflected (an oxide layer in vacuum decreases the reflection).

There is gold electroplated on the surface in the two-laser experiment. From the optical constants of metallic gold near 685 nm ($n = 0.14$ and $k = 3.76$ [7]), we would find an absorption fraction of about 0.025 for a planar gold surface.

References

[1] D. Letts, D. Cravens, and P.L. Hagelstein, Dual laser stimulation and optical phonons in palladium deuteride, in low-energy nuclear reactions and new energy technologies, *Low-Energy Nuclear Reactions Sourcebook*, Vol. 2, American Chemical Society: Washington DC, 2009, pp. 81–93.

[2] P.L. Hagelstein, D.G. Letts and D. Cravens, *J. Cond. Mat. Nucl. Sci.* **3** (2010) 59.

[3] M.H. Miles and M. Fleischmann, Accuracy of isoperibolic calorimetry used in a cold fusion control experiment, *Low-Energy Nuclear Reactions Sourcebook*, edited by J. Marwan and S. Krivit, 2009, p. 153.

[4] M.R. Swartz, G. Verner, A. Weinberg, Non-thermal near-IR emission linked with excess power gain in high impedance and codeposition phusor-LANR devices, *Proc. 14th International Conference on Condensed Matter Nuclear Science*, Washington, DC (in press).

[5] G.M. Hale and M.R. Querry, *Appl. Optics* **12** (1973) 553.

[6] P.B. Johnson and R.W. Christy, *Phys. Rev.* B **9** (1974) 5056.

[7] P.B. Johnson and R.W. Christy, *Phys. Rev.* B **6** (1972) 4370.